TABLE OF CONTENTS

NASA Contractor Report 3140

Minimization Theory of Induced Drag Subject to Constraint Conditions

John DeYoung

CONTRACT NAS1-13500
JUNE 1979

NASA Contractor Report 3140

Minimization Theory of Induced Drag Subject to Constraint Conditions

John DeYoung
Vought Corporation Hampton Technical Center
Hampton, Virginia

Prepared for
Langley Research Center
under Contract NAS1-13500

National Aeronautics
and Space Administration

Scientific and Technical
Information Office

1979

Blanche Page

TABLE OF CONTENTS

SUMMARY

The method treats wing configurations with trailing vorticity sheets of arbitrary shape. Induced angles normal to the wake are analytically formulated. These, factored by the vorticity in the sheet, form the induced drag integral. The vorticity is represented as a Fourier series in loading, then the unknown Fourier coefficients can be determined after specifying the constraint conditions then minimizing with respect to the loading Fourier coefficients. Exact analytical solutions in terms of induced drag influence coefficients can be attained which define the spanwise loading with minimized induced drag, subject to specified constraint conditions, for any nonplanar wing shape or number of wings. Closed exact solutions have been obtained for the planar wing with the constraints of lift plus wing bending moment about a given wing span station. Compared with a wing with elliptic loading having the same lift and same wing bending moment about a span station, the induced drag can be of the order 15 percent less for the wing with the inboard minimized-solution loading. Example applications of the theory are made to a biplane, a wing in ground effect, a cruciform wing, a V-wing, and a planar-wing winglet. For minimal induced drag the spanwise loading, relative to elliptic, is outboard for the biplane and is inboard for the wing in ground effect and for the planar-wing winglet. The theory can be applied to determine the loading for minimal induced drag of wings in formation flying, banked wings, flying in or near wake, and linked wingtips. No-roll can be an additional constraint. A spinoff of the biplane solution provides mathematically exact equations for downwash and sidewash about a planar vorticity sheet having an arbitrary loading distribution.

INTRODUCTION

Induced drag minimization theory is in a rapid development and use phase. This is because of widespread interest in performance and structural advances that possibly may be realized with unconventional aircraft configurations, or by imposing structural and/or performance constraint conditions. Numerical solutions of minimization theory have been programmed for computers, which extends the application range of the theory. Unconventional aircraft include such configurations as a wing with winglets; a biplane; a tandem wing; a cruciform; a V-wing, swept box wing; a strutted wing; a skewed wing; and a nonplanar wing designed to lessen wing and fuselage bending moments. A structural constraint condition can be that the wing bending moment about a given span station be minimum. A performance constraint condition can be an aircraft flying near ground, a surface flying vehicle, or an aircraft in a flying formation.

Minimum induced drag solutions for planar wings with different structural constraint conditions have been developed by several investigators. Dr. L. Prandtl (ref. 1) in 1933 obtained a solution using the constraint that the integral of the local bending moment be specified. Compared with an 18.1 percent smaller span wing with elliptic loading, and the same lift and constraint magnitude, the induced drag is 11.1 percent less. In reference 2, the constraint condition is the wing-root bending moment. The solution for spanwise loading is obtained after the induced angle function is determined. Compared with a 25 percent smaller span wing with elliptic loading, and same lift and wing-root bending moment, the induced drag can be 15.6 percent less. In reference 3 the constraint condition also is the wing-root bending moment and the solution is somewhat similar to that of reference 2. For approximating wing structural weight, the integrals of wing shear force and of wing local bending moment are used as constraint conditions in reference 4. With these two constraints, the induced drag can be 7.1 percent less when compared to the 13.8 percent smaller span wing with elliptic loading and same lift and constraint magnitude.

Numerical solution vortex-lattice methods for computing the optimum spanwise loading which results in minimum induced drag, have been developed in references 5 and 6. These are quite adaptable to complicated nonplanar

configurations. In reference 5, the optimum loading calculation is based on Munk's theorem III in which conditions are defined on the induced velocity. In reference 6, the numerical procedure is generalized in terms of constraint conditions. An application of a nonplanar wing numerical method is made in reference 7 to the investigation of wing-winglet characteristics. Examples of nonplanar wing analytical or classical theory solutions for loading are given in references 8 and 9.

The principal objective of the present study is to develop a generalized analytical induced drag minimization theory to which aerodynamic and configuration constraint conditions can be imposed. The term generalized implies direct solutions are possible for arbitrary configurations without having to resort to complex conformal transformations. Here generalized also means that minimization is done without resort to other induced drag theorems such as Munk's. Aerodynamic constraint condition examples are, for a given lift, for a given rolling moment, and/or for a given wing bending moment about an arbitrary span station. Configuration constraints include, multi-wing, wing-winglet, or flying near wake of other aircraft. It was found that a generalized theory could be formulated by expressing the spanwise loading distribution as a Fourier series in which the Fourier loading coefficients are unknowns. With constraints imposed and minimization, equations are evolved in terms of the unknown loading coefficients and induced drag influence coefficients. Solutions of these equations leads to an analytically exact evaluation of the loading coefficients. In an age of numerical solutions, available exact solutions provide an accuracy check. The present theory also serves as such a check for the evolving numerical minimization methods.

SYMBOLS

A	aspect ratio, b^2/S
a_n, a_{n^*}	Fourier coefficient of spanwise loading, equation (1)
b	wing span
C_b	ratio of wing bending moment coefficient to lift coefficient, C_{mbb}/C_L, equation (11)

C_{bc}	C_b of wing with elliptic loading, $f_1/4\pi$
C_{D_i}	induced drag coefficient, D_i/qS, equation (13)
C_L	lift coefficient, L/qS, equation (3)
C_ℓ	rolling moment coefficient, L/qSb, equation (78)
C_{mbb}	wing bending moment coefficient about lateral point η_b, M_{bb}/qSb, equation (7)
c	wing chord
c_{av}	average or mean wing chord, S/b
c_ℓ	section lift coefficient, equation (5)
D_i	induced drag
D_{nn^*}	induced drag influence coefficient for planar-wing winglet, equation (164)
e	induced drag efficiency factor, equation (15)
e_r	induced drag efficiency factor of rolling wing, equation (79)
f_1, f_n	wing bending moment influence coefficients for planar wing, equations (9) and (10)
G	dimensionless circulation, Γ/bV, equation (1)
I_n	downwash influence coefficient for biplane, equations (67) and (118)
I_{nn^*}	induced drag influence coefficient for biplane, equation (70)
J_n	sidewash influence coefficient for biplane, equations (119) and (B12)
k	planar wing bending moment constraint parameter of C_b and e, equations (26) and (37)
k_o	planar wing bending moment constraint spanwise loading function, equation (31)
k_1	planar wing bending moment constraint parameter of η_{cp}, equation (33)
L	wing lift, also, rolling moment
L_{n^*w}	induced normal velocity influence coefficient for wing winglet, equations (165) and (166)
M_{bb}	wing bending moment about span station η_b
m,n,n^*,N	integers in Fourier series for loading and in influence coefficients, odd only for symmetric loading

P_n	induced velocity influence coefficient for cruciform wing, equation (125)
P_{nn^*}	induced drag influence coefficient for cruciform wing, equation (128)
Q_n	induced velocity influence coefficient for V-wing, equation (141)
Q_{nn^*}	induced drag influence coefficient for V-wing, equation (143)
q	dynamic pressure, $\frac{1}{2}\rho V^2$
S	wing area
s	spanwise coordinate along nonplanar wing surface
s_e	spanwise semispan along nonplanar wing surface
T_n	wing bending moment constants, equation (171)
t	arbitrary constant, proportional to how much wing bending moment constraint is imposed
t_1	limit condition for t, equation (29)
V	free stream velocity
v_s	induced sidewash, tangent to surface
w	induced downwash, normal to surface
y	lateral coordinate, from midspan station
z	vertical coordinate
α_w	induced angle normal to the wake
Γ	circulation, also dihedral angle
γ	angle between wings in cruciform, also, dihedral cant angle of winglet
ζ_r	influence coefficient constants used for evaluating I_{n0} and I_{n1}, equations (B39) and (B40)
ζ	dimensionless vertical coordinate, $2Z/b$ or Z/s_e
η	dimensionless lateral coordinate, $2y/b$ or y/s_e
η_b	span station about which bending moment is taken, equation (6)
η_0	span station at which winglet starts, $\eta_0 = \cos\phi_0$
η_{cp}	semispanwise center of pressure, equals $4C_b$ when $\phi_b = \pi/2$
ρ	air density

ϕ	spanwise trigonometric coordinate, $\cos^{-1}\eta$

Subscripts

av	average
b	bending moment
c	wing with elliptic loading
m,n,n*	series integers
s	symbolizes, from vorticity sheet

MINIMIZED INDUCED DRAG OF PLANAR WINGS WITH THE CONSTRAINTS OF LIFT PLUS WING BENDING MOMENT

Relations between spanwise loading quantities can be established in the wake or Trefftz plane of the aircraft. Then solutions reduce to two-dimensional problems and are independent of the chordwise shape of the wing and of how the loading is developed. Quantities dependent on spanwise loading include, induced velocity normal to the wake, induced drag, spanwise center of pressure, wing bending moment, and rolling moment when the loading is antisymmetric. When constraint conditions are imposed and induced drag is minimized, then from the relation between loading and induced drag, the optimum spanwise loading can be evaluated. A simple method for establishing the relationships between the spanwise loading quantities is by expressing the spanwise loading as a Fourier series in which the Fourier loading coefficients are unknowns (see eq. 1). This method permits a manageable, viable, analytical solution, regardless of the complexity of the configuration or of the constraint conditions. The method can be demonstrated by showing the solution for a planar wing with simple constraints. With the constraint that lift is specified, then (by eq. 15)

$$C_{D_i} = \frac{\pi A}{4} \left(a_1^2 + \sum_{n=2}^{\infty} n\, a_n^2\right), \quad \frac{\partial C_{D_i}}{\partial a_m} = \frac{\pi A}{4} (2m\, a_m)_{m>1} = 0, \quad G = a_1 \sin \phi$$

that is, the loading for minimum induced drag for a given lift is elliptic loading. Also, for a planar wing with the constraint that rolling moment is specified, then

$$C_{D_i} = \frac{\pi A}{4} \left(2\, a_2^2 + \sum_{n=1\neq 2}^{\infty} n\, a_n^2\right), \quad \frac{\partial C_{D_i}}{\partial a_m} = \frac{\pi A}{4} (2\, m\, a_m)_{m\neq 2} = 0, \quad G = a_2 \sin 2\phi$$

which is the loading for minimum induced drag for a given rolling moment.

In this section solutions are developed for the constraint conditions of lift and wing bending moment about a given span station such as at a wing strut connection. It can be noted as pointed out in reference 2 that the induced drag of a wing having a given lift and a given spanwise load distribution is not affected by the compressibility of the air at subsonic speeds. At supersonic speeds an additional drag associated with the formation of waves arises.

Force and Moment Coefficients in Terms of Fourier Coefficients

The wing spanwise loading distribution expressed as a Fourier series has proven to be a versatile analytical tool (see e.g. refs. 10, 11, 12, and 13). In Fourier series

$$G(\phi) = \frac{\Gamma}{bv} = \frac{c_\ell c}{2b} = \sum_{n=1}^{\infty} a_n \sin n\phi \tag{1}$$

where for symmetric loading n is an odd integer, and ϕ is related to span station by

$$\eta = 2y/b = \cos \phi \tag{2}$$

Lift coefficient is

$$C_L = \frac{L}{qS} = \frac{1}{qS} \int_{-b/2}^{b/2} \rho V \Gamma dy = A \int_{-1}^{1} G d\eta = A \int_0^{\pi} G \sin \phi \, d\phi \tag{3}$$

then with equation (1), equation (3) becomes

$$C_L = \frac{\pi A}{2} a_1 \tag{4}$$

When C_L is known the loading distribution can be written

$$\frac{c_\ell c}{C_L c_{av}} = \frac{2A}{C_L} G = \frac{4}{\pi} \left(\sin \phi + \sum_{\substack{n=3 \\ \text{odd}}}^{\infty} \frac{a_n}{a_1} \sin n\phi \right) \tag{5}$$

Wing bending moment coefficient about the span station

$$\eta_b = 2y_b/b = \cos \phi_b \tag{6}$$

is

$$C_{mbb} = \frac{M_{bb}}{qSb} = \frac{1}{qSb} \int_{y_b}^{b/2} (y - y_b) \rho V \Gamma dy = \frac{A}{2} \int_{\eta_b}^{1} (\eta - \eta_b) G d\eta = \frac{A}{2} \int_0^{\phi_b} (\cos \phi - \cos \phi_b)$$

$$G \sin \phi \, d\phi \tag{7}$$

then inserting equation (1) and performing the integration

$$C_{mbb} = \frac{A}{8} a_1 \left(f_1 + \sum_{\substack{n=3 \\ \text{odd}}}^{\infty} n f_n \frac{a_n}{a_1}\right) \tag{8}$$

where

$$f_1 = 2(\sin \phi_b - \frac{1}{3} \sin^3 \phi_b - \phi_b \cos \phi_b) \tag{9}$$

$$f_n = \frac{1}{n} \left[\frac{\sin (n-2)\phi_b}{n-2} - \frac{\sin (n+2)\phi_b}{n+2} - \frac{2 \cos \phi_b \sin (n-1)\phi_b}{n-1} + \right.$$

$$\left. \frac{2 \cos \phi_b \sin (n+1)\phi_b}{n+1} \right] = \frac{\sin (n-2)\phi_b}{(n-2)(n-1)n} - \frac{2\sin n \phi_b}{(n-1)n(n+1)} + \frac{\sin (n+2)\phi_b}{n(n+1)(n+2)} \tag{10}$$

$$\text{At } \phi_b = \frac{\pi}{2}: \quad f_1 = \frac{4}{3} \; ; \; f_n = \frac{-4(-1)^{\frac{n-1}{2}}}{n(n^2-4)} \tag{10a}$$

An important parameter is the ratio of wing bending moment to wing lift. From the ratio of equations (8) and (4)

$$C_b = \frac{C_{mbb}}{C_L} = \frac{1}{4\pi} \left(f_1 + \sum_{\substack{n=3 \\ \text{odd}}}^{\infty} n f_n \frac{a_n}{a_1}\right) \tag{11}$$

where f_1 and f_n are given in equations (9) and (10). When the loading extends over the semispan, then $\phi_b = \pi/2$, and C_b is 1/4 of the spanwise center of pressure, η_{cp}. Then, combining equations (10a) and (11)

$$\eta_{cp} = \int_0^1 \frac{c_\ell c}{C_L c_{av}} \eta d\eta = \frac{4}{3\pi} \left[1 - 3 \sum_{\substack{n=3 \\ \text{odd}}}^{\infty} \frac{(-1)^{\frac{n-1}{2}}}{n^2-4} \frac{a_n}{a_1}\right] \tag{12}$$

Induced drag coefficient is

$$C_{D_i} = \frac{D_i}{qS} = \frac{1}{qS} \int_{-b/2}^{b/2} \rho V \Gamma \frac{\alpha_w}{2} dy = \frac{A}{2} \int_{-1}^{1} G \alpha_w d\eta = \frac{A}{2} \int_0^{\pi} G \alpha_w \sin \phi \, d\phi \tag{13}$$

where α_w is the downwash angle in the wake given by

$$\alpha_w = \frac{1}{\pi}\int_0^{\pi} \frac{\frac{dG}{d\phi^*}\, d\phi^*}{\cos\phi^* - \cos\phi} = \frac{1}{\sin\phi} \sum_{n^*=1}^{\infty} n^* a_{n^*} \sin n^*\phi \qquad (14)$$

Inserting equations (1) and (14) into equation (13) leads to

$$C_{D_i} = \frac{\pi A}{4} \sum_{n=1}^{\infty} n a_n^2 = \frac{C_L^2}{\pi A} \sum_{n=1}^{\infty} n\left(\frac{a_n}{a_1}\right)^2 = \frac{C_L^2}{\pi A e} \qquad (15)$$

where for symmetrical span loading

$$e = \frac{1}{1 + \sum_{\substack{n=3 \\ \text{odd}}}^{\infty} n\left(\frac{a_n}{a_1}\right)^2} \qquad (16)$$

Solution for a_n/a_1 Fourier Spanwise Loading Coefficients

The problem is to evaluate the infinite number of a_n/a_1 Fourier coefficients such that the spanwise loading is defined which has minimum induced drag per wing bending moment about η_b. Minimal combined induced drag and wing bending moment per unit lift can be realized by minimizing the parameter C_b/e. From maxima and minima theory for a function of many variables, the necessary conditions for an extreme value are that all the partial derivatives with respect to each variable be zero. Taking partial derivatives of C_b/e with respect to a_3/a_1, a_5/a_1, ... a_m/a_1, results in

$$\frac{\partial(C_b/e)}{\partial(a_m/a_1)} = \frac{1}{e}\frac{\partial C_b}{\partial(a_m/a_1)} - \frac{C_b}{e^2}\frac{\partial e}{\partial(a_m/a_1)} = 0 \qquad (17)$$

The partial derivatives of equations (11) and (16) are

$$\left.\begin{aligned} \frac{\partial C_b}{\partial (a_m/a_1)} &= \frac{m}{4\pi} f_m \\ \frac{\partial e}{\partial (a_m/a_1)} &= -\frac{2m(a_m/a_1)}{\left[1 + \sum_{\substack{n=3 \\ \text{odd}}}^{\infty} n \left(\frac{a_n}{a_1}\right)^2\right]^2} = -2\, e^2\, m\, \frac{a_m}{a_1} \end{aligned}\right\} \qquad (18)$$

With equation (18), equation (17) becomes

$$\frac{m}{4\pi e} f_m + 2\, m\, C_b \frac{a_m}{a_1} = 0$$

which can be solved for a_m/a_1. Then the solution for the Fourier loading coefficient, with m referred to the general n, becomes

$$\frac{a_n}{a_1} = -\frac{f_n}{8\pi e C_b} \qquad (19)$$

Equation (19) is in the form of a constant times $(-f_n)$. Let t be an arbitrary number, then the minimization condition is

$$\frac{a_n}{a_1} = -\, t\, f_n \qquad (20)$$

A better parameter for the minimization process is $C_b{}^2/e$ since it indicates induced-drag bending-moment efficiency. However, the minimization of the term $C_b{}^r/e$ where r is any constant leads to $(a_n/a_1) = -(r/8\pi e C_b) f_n$, that is, a constant times f_n and can be expressed as in equation (20).

Wing Bending Moment Minimized Solution Loading Characteristics

Solution in infinite series. - Equation (20) inserted into equations (5), (11), (12), (14), and (16) leads to the following spanwise loading characteristics:

$$\frac{c_\ell c}{C_L c_{av}} = \frac{2A}{C_L} G = \frac{4}{\pi} \left(\sin \phi - t \sum_{\substack{n = 3 \\ \text{odd}}}^{\infty} f_n \sin n\phi\right) \tag{21}$$

$$\eta_{cp} = \frac{4}{3\pi} \left[1 + 3t \sum_{\substack{n = 3 \\ \text{odd}}}^{\infty} \frac{(-1)^{\frac{n-1}{2}}}{n^2 - 4} f_n\right] \tag{22}$$

$$\frac{A}{C_L} \alpha_w = \frac{2}{\pi} \left(1 - \frac{t}{\sin\phi} \sum_{\substack{n = 3 \\ \text{odd}}}^{\infty} n f_n \sin n\phi\right) \tag{23}$$

$$C_b = \frac{C_{mbb}}{C_L} = \frac{1}{4\pi} (f_1 - kt) \tag{24}$$

$$e = \frac{C_L^2}{\pi A C_{D_i}} = \frac{1}{1 + kt^2} \tag{25}$$

where

$$k = \sum_{\substack{n = 3 \\ \text{odd}}}^{\infty} n f_n^2 \tag{26}$$

where f_n is given in equation (10) and f_1 in equation (9).

A limit on the magnitude of t. - A limit can be defined by the condition that the spanwise loading remains positive at all span stations. This condition is satisfied by requiring that the slope of the loading distribution be zero at the wingtip. Taking the derivative of equation (21) with respect to ϕ, setting to zero, and solving for t at $\phi = 0$

$$t_1 = \frac{1}{\sum_{\substack{n = 3 \\ \text{odd}}}^{\infty} n f_n} \tag{27}$$

where t_1 is the value of t at which the loading is positive at all span stations. If t exceeds t_1 the spanwise loading becomes negative in the region near the wing tip. The summation in equation (27) is readily found by expanding $n f_n$. From equation (10)

$$\sum_{\substack{n=3 \\ \text{odd}}}^{\infty} n f_n = \sin \phi_b + \frac{1}{3} \sin 3 \phi_b + \frac{1}{5} \sin 5 \phi_b + \frac{1}{7} \sin 7 \phi_b + \ldots$$

$$- \frac{1}{5} \sin 5 \phi_b - \frac{1}{7} \sin 7 \phi_b - \ldots$$

$$- 2 \cos \phi_b \left(\frac{1}{2} \sin 2 \phi_b + \frac{1}{4} \sin 4 \phi_b + \frac{1}{6} \sin 6 \phi_b + \ldots \right.$$

$$\left. - \frac{1}{4} \sin 4 \phi_b - \frac{1}{6} \sin 6 \phi_b - \ldots \right)$$

$$= \sin \phi_b + \frac{1}{3} \sin 3 \phi_b - \sin 2 \phi_b \cos \phi_b = \frac{2}{3} \sin^3 \phi_b \qquad (28)$$

then equation (27) becomes

$$t_1 = \frac{3}{2 \sin^3 \phi_b} = \frac{3}{2(1-\eta_b^2)^{3/2}} \qquad (29)$$

Solution in closed functions. - The infinite series summations of equations (22) and (26) converge quite rapidly, however, those of equations (21) and (23) do not, especially that of equation (23). Summation methods are developed and presented in appendix A which includes the functional evaluation of the summations given in equations (21), (22), (23), and (26). Using equations (A60), (A74), (A87), and (A95) the closed function form of equations (21) through (26) become

$$\frac{c_\ell c}{C_L c_{av}} = \frac{2A}{C_L} G = \frac{4}{\pi} (1 - \eta^2)^{\frac{1}{2}} (1 - k_o t) \qquad (30)$$

where

$$k_o = -\frac{1}{3}(1 + 2\eta_b^2)(1 - \eta_b^2)^{\frac{1}{2}} + \frac{(\eta_b+\eta)^2}{2(1-\eta^2)^{\frac{1}{2}}} \cdot \cosh^{-1}\frac{1+\eta_b\eta}{|\eta_b+\eta|} +$$

$$\frac{(\eta_b-\eta)^2}{2(1-\eta^2)^{\frac{1}{2}}} \cosh^{-1}\frac{1-\eta_b\eta}{|\eta_b-\eta|} \overset{\eta=1}{=} \frac{2}{3}(1 - \eta_b^2)^{3/2} \tag{31}$$

$$\eta_{cp} = \frac{4}{3\pi}(1 - k_1 t) \tag{32}$$

where

$$k_1 = \frac{1}{6}(1 - \frac{5}{2}\eta_b^2)(1 - \eta_b^2)^{\frac{1}{2}} + \frac{1}{4}\eta_b^4 \cosh^{-1}\frac{1}{\eta_b} \tag{33}$$

$$\frac{\pi A}{2C_L}\alpha_w = 1 + t\left\{f_1 - \left[\begin{matrix} 0, & |\eta| \le \eta_b \\ \pi(|\eta| - \eta_b), & |\eta| \ge \eta_b \end{matrix}\right]\right\} \tag{34}$$

$$C_b = \frac{C_{mbb}}{C_L} = \frac{1}{4\pi}(f_1 - kt) \tag{35}$$

where $f_1 = \frac{2}{3}(2 + \eta_b^2)(1 - \eta_b^2)^{\frac{1}{2}} - 2\eta_b \cos^{-1}\eta_b$ (36)

$$k = \frac{2}{9}(1 - 6\eta_b^2 + 3\eta_b^4 + 2\eta_b^6 - 6\eta_b^4 \ln \eta_b^2) \tag{37}$$

$$e = \frac{C_L^2}{\pi A C_{D_i}} = \frac{1}{1+kt^2} \tag{38}$$

The functional behavior as η_b approaches unity of the coefficients k, k_1, and f_1 can be made as done in the development of equation (A75).

For $\eta_b \to 1$:

$$\left.\begin{aligned} k &= \frac{16}{9}(1-\eta_b)^4\left[1-\frac{3}{10}(3+\eta_b)(1-\eta_b)\right] \\ k_1 &= \frac{8}{15}(1-\eta_b)^{5/2}(1+\eta_b)^{1/2}\left[1-\frac{5}{7}(1-\eta_b)\right] \\ f_1 &= \frac{16}{15}\sqrt{2}\,(1-\eta_b)^{5/2}\left[1-\frac{3}{28}(1-\eta_b)\right] \end{aligned}\right\} \tag{39}$$

Solutions in closed functions for $\eta_b = 0$. - In this case the solution simplifies. The condition that bending moment is taken about the wing root is that $\eta_b = 0$. Then the k, k_1, and f_1 factors simplify considerably. For $\eta_b = 0$; $k = 2/9$, $k_1 = 1/6$, $f_1 = 4/3$. With these values the aerodynamic characteristics are, for $\eta_b = 0$

$$\frac{c_\ell c}{C_L c_{av}} = \frac{4}{\pi}\left[\left(1+\frac{t}{3}\right)(1-\eta^2)^{1/2} - t\,\eta^2\cosh^{-1}\frac{1}{|\eta|}\right] \tag{40}$$

$$\eta_{cp} = \frac{4}{3\pi}\left(1-\frac{t}{6}\right) \tag{41}$$

$$\frac{\pi A}{2C_L}\alpha_w = 1 + t\left(\frac{4}{3} - \pi|\eta|\right) \tag{42}$$

$$C_b = \frac{1}{3\pi}\left(1-\frac{t}{6}\right) \tag{43}$$

$$e = \frac{1}{1+\frac{2}{9}t^2} \tag{44}$$

Numerical values of loading characteristics for various η_b and t. - In this wing bending moment minimized solution several generalized constants appear. These include k, k_1, and f_1. The term k_o is a generalized function of the spanwise coordinate. Values of k, k_1, f_1, and the ratio k/f_1 have been computed from equations (37), (33), and (36) for a range of η_b values. These are presented in table 1. Values of k_o determined from equation (31) appear in table 2.

The spanwise loading distribution is given in equation (21) in the form of an infinite series, and in equation (30) in the form of a closed function. It is of interest to know the magnitude of the loading harmonics, that is, the factors of sin 3ϕ, sin 5ϕ, . . . Values of f_n computed from equations (10) and (10a) are presented in table 3. These data show that the optimized loading is made up primarily of elliptic loading and the sin 3ϕ harmonic, and much less due to higher harmonics.

The value for t such that the spanwise loading gradient is zero at the wing tip is t_1 given by equation (29). For these $t = t_1$ values, the aerodynamic characteristics are listed in table 4. These are computed by use of equations (32), (34), (35), (38), and table 1. The parameter $(C_b^2/e)/(C_b^2/e)_c$, c denotes $t = 0$, is a measure of the induced drag efficiency compared to a wing with elliptic loading having the bending moment ratio C_{bc}/C_b. The optimized loading is elliptic when $t = 0$. The parameter of the induced angle in the wake has a constant value from $\eta = 0$ to η_b, then it is a straight line joining the points at η_b and at 1.

The bending moment ratio is obtained from equation (35). Then

$$\frac{C_{bc}}{C_b} = \frac{1}{1 - \frac{k}{f_1} t} \tag{45}$$

Solving for t

$$t = \frac{1}{k/f_1} \left(1 - \frac{1}{C_{bc}/C_b}\right) \tag{46}$$

For comparison of data it is convenient to keep the parameter C_{bc}/C_b constant. Then t is evaluated from equation (46). The aerodynamic characteristics for $C_{bc}/C_b = 1.1$, 1.2, and 4/3 are presented in tables 5, 6, and 7. These values are determined with the t of equation (46) and using equations (32), (34), (35), (38), and table 1.

The spanwise loading distribution due to the specified conditions on loading in tables 4 through 7 is obtained by using equation (30) with the listed k_o values in table 2, and t values of tables 4 through 7. Values of spanwise loading are presented in table 8. For positive values of t the loading is inboard of elliptic loading.

For $\eta_b \to 1$, mathematical limits need to be taken. With equations (39) and (29) the terms $k_1 t$, $f_1 t$, kt, and kt^2 can be evaluated and are all zero at $\eta_b = 1$. Then $\eta_{cp} = 4/3\pi$, and $e = 1$, that is the values for elliptic loading. However, $(kt/f_1) \to 5/8$, and $\pi(1 - \eta_b)t \to 3\pi\sqrt{2}/8(1 - \eta_b)^{\frac{1}{2}}$, as $\eta_b \to 1$. Thus for the t of equation (29) as $\eta_b \to 1$

$$\frac{\pi A}{2C_L} a_w(\eta) \to 1, \quad \frac{\pi A}{2C_L} a_w(1) \to 1 - \frac{3\pi\sqrt{2}}{8(1-\eta_b)^{\frac{1}{2}}}, \quad \frac{C_{bc}}{C_b} \to \frac{8}{3} \tag{47}$$

Since from equation (39), $(k/f_1) \to (5\sqrt{2}/6)(1 - \eta_b)^{3/2}$, then t of equation (46), as $\eta_b \to 1$, becomes

$$t \to \frac{3\sqrt{2}}{5(1-\eta_b)^{3/2}} \left(1 - \frac{C_b}{C_{bc}}\right) \tag{48}$$

where C_b/C_{bc} is a specified value. With the t of equation (48) then, as before, $\eta_{cp} \to 4/3\pi$, $e \to 1$, and $a_w(1)$ at $\eta_b = 1$ approaches minus infinity. The values for $\eta_b = 1$ are incorporated into tables 1 through 7.

Comparison with Elliptic Loading

A measure of the efficiency of a wing with inboard spanwise loading can be attained by comparing this wing with a wing having elliptic loading and the same lift and wing bending moment. Since elliptic loading is the most efficient in terms of induced drag it serves as a good standard for comparison with the inboard loading characteristics. The induced drag ratio and ratio of aspect ratios are

$$\frac{D_i}{D_{ic}} = \left(\frac{L}{L_c}\right)^2 \left(\frac{b_c}{b}\right)^2 \frac{e_c}{e}, \qquad \frac{A_c}{A} = \frac{S}{S_c}\left(\frac{b_c}{b}\right)^2 \tag{49}$$

where subscript c refers to the wing with elliptic loading. The wing bending moment coefficient ratio is

$$\frac{C_b}{C_{bc}} = \frac{C_{mb}/C_L}{(C_{mb}/C_L)_c} = \frac{M_{bb}}{M_{bbc}} \frac{L_c}{L} \frac{b_c}{b} \tag{50}$$

for the same lift and bending moment, and since for elliptic loading $e_c = 1$, then equations (49) and (50) reduce to

$$\frac{b}{b_c} = \frac{C_{pc}}{C_b} \tag{51}$$

$$\frac{D_i}{D_{ic}} = \frac{1}{e} \left(\frac{b}{b_c}\right)^{-2} \tag{52}$$

The ratio of aspect ratios depends on S/S_c. It can be noted that when these wing surfaces are the same then friction drag will remain about equal. In equations (51) and (52), C_b and e are given in equations (35) and (38), respectively. The wing bending moment parameter for elliptic loading is equation (35) with t = 0. Then

$$C_{bc} = \frac{f_1(\eta_{bc})}{4\pi} \tag{53}$$

where $\eta_{bc} = y_{bc}/(b_c/2)$ is the span station of the wing with elliptic loading at which wing bending moments are taken. Two conditions on η_{bc} can be made. These two moment conditions are pictured as follows:

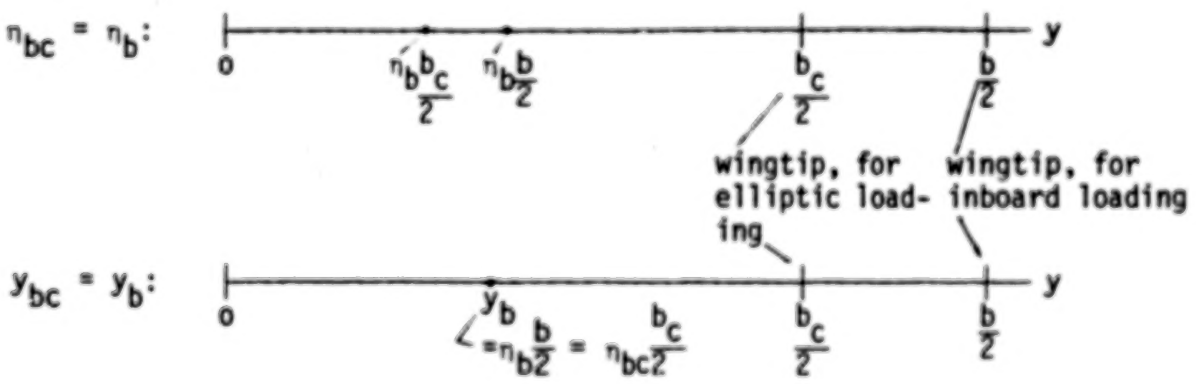

Then for the same y_b

$$\eta_{bc} = \frac{b}{b_c} \eta_b \tag{54}$$

For these two cases of moment definition, equation (53) becomes

$$\text{Same } \eta_b: \quad C_{bc} = \frac{f_1(\eta_b)}{4\pi} \tag{55}$$

$$\text{Same } y_b: \quad C_{bc} = \frac{f_1(\frac{b}{b_c} \eta_b)}{4\pi} \tag{56}$$

with equations (55), (56), and (35), equation (51) becomes

$$\text{Same } \eta_b: \quad \frac{b}{b_c} = \frac{1}{1 - \frac{k}{f_1} t} \tag{57}$$

$$\text{Same } y_b: \quad \frac{b}{b_c} = \frac{f_1(\frac{b}{b_c} \eta_b)}{f_1 - kt} \tag{58}$$

Solving for t leads to

$$\text{Same } \eta_b: \quad t = \frac{1}{k/f_1} \left(1 - \frac{1}{b/b_c}\right) \tag{59}$$

$$\text{Same } y_b: \quad t = \frac{1}{k/f_1} - \frac{f_1(\frac{b}{b_c} \eta_b)}{k\ b/b_c} \tag{60}$$

where k and f_1 are given in equations (36) and (37), and in table 1, and $f_1(b\eta_b/b_c)$ is

$$f_1(\frac{b}{b_c} \eta_b) = \frac{2}{3} [2 + (\frac{b}{b_c} \eta_b)^2] [1 - (\frac{b}{b_c} \eta_b)^2]^{\frac{1}{2}} - 2 \frac{b}{b_c} \eta_b \cos^{-1}(\frac{b}{b_c} \eta_b) \tag{61}$$

When b/b_c is specified then t can be determined from either of equations (59) or (60) for a given value of η_b. With this value of t, induced drag efficiency, e, is computed from equation (38), induced drag ratio from equation (52), η_{cp} from equation (32), C_b from equation (35), and induced velocity is the wake from

$$\frac{\pi A}{2C_L}\alpha_w = \left(\frac{b}{b_c}\right)^2 \frac{\alpha_w}{\alpha_{wc}} = 1 + t\left\{f_1 - \begin{bmatrix} 0, & |\eta| \le \eta_b \\ (|\eta| - \eta_b), & |\eta| \ge \eta_b \end{bmatrix}\right\} \tag{62}$$

When t is specified, such as for the condition of wingtip zero-slope loading of equation (29), then b/b_c can be determined from either of equations (57) or (58). An iteration for b/b_c is required in equation (58) when t is specified.

The data presented in tables 4 through 8 applies also to the case of same η_b when comparing this data with that due to elliptic loading. This can be seen by noting that equations (46) and (59) are identical when $C_{bc}/C_b = b/b_c$. From the relations of equations (51), (52), and (62), the data of tables 4 through 8 can be written as

$$\frac{C_{bc}}{C_b} = \frac{b}{b_c} \; ; \; \frac{\pi A}{2C_L}\alpha_w = \left(\frac{b}{b_c}\right)^2 \frac{\alpha_w}{\alpha_{wc}} \; ; \; \frac{C_b{}^2/e}{(C_b{}^2/e)_c} = \frac{1}{e}\left(\frac{b}{b_c}\right)^{-2} = \frac{D_i}{D_{ic}} \tag{63}$$

which relations apply when comparing with elliptic loading which has the same value of η_b, $\eta_{bc} = \eta_b$.

Data for the case of same η_b is tabulated as a function of b/b_c in table 9. A similar table for the case of same y_b is presented in table 10 with corresponding spanwise loading values given in table 11.

MINIMIZED INDUCED DRAG OF NONPLANAR WINGS WITH EITHER THE CONSTRAINT OF LIFT OR OF LIFT PLUS BENDING MOMENT

In the yz-plane or cross section plane the trailing vorticity system is assumed to analytically follow the downstream projection of the aft view geometry of the aircraft. Thus a staggered wing biplane will appear as two planar vorticity sheets separated by a vertical distance. The term nonplanar means that the vertical position of the vorticity sheet or wake is a function of the lateral coordinate. Nonplanar can also mean multiple independent vorticity systems which, however, can influence or interfere with each other. A flat straight vorticity sheet is the simple planar wing.

The general approach to a minimization solution is first to analytically determine the induced angles normal to the wake. These angles factored by the vorticity in the sheet form the induced drag integral. The vorticity in the wake is represented as a Fourier series in loading. Then the drag integral develops into an infinite series in terms of unknown Fourier loading coefficients and induced drag influence coefficients. Constraint conditions are specified on the Fourier loading coefficients. Then the induced drag series is minimized with respect to the Fourier loading coefficients, that is, partial derivatives are taken with respect to a given a_m. Solutions for the Fourier loading coefficients, a_n, are obtained from these minimization equations. Constraint conditions can be as simple as that for a given lift, then a_1 is constant in the derivative process, or for a given rolling moment, then a_2 is constant, or for wing bending moment with a given lift, then the induced drag series times the bending moment series in a_n is minimized. Thus, exact analytical solutions in terms of induced drag influence coefficients can be attained which provide the spanwise loading for minimized induced drag, subject to specified constraint conditions, for any nonplanar wing shape or number of wings.

Biplane and Wing in Ground-Effect Solutions

The biplane configuration provides an example for a nonplanar minimization solution. The wing in ground-effect is the same but with opposite sign of the vorticity from the lower wing. Shown on the right are the trailing vorticity

sheets from wings a and b. The normal induced downwash at sheet a, due to both trailing vorticity sheets is

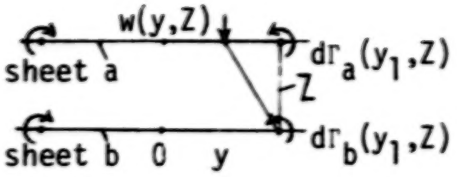

$$w(y,z) = \frac{1}{2\pi}\int_{-b_{a/2}}^{b_{a/2}} \frac{\frac{d\Gamma_a}{dy_1}\,dy_1}{y-y_1} + \frac{1}{2\pi}\int_{-b_{b/2}}^{b_{b/2}} \frac{(y-y_1)\,\frac{d\Gamma_b}{dy_1}\,dy_1}{(y-y_1)^2 + Z^2} \tag{64}$$

For the same wing span and vorticity strength, in trignometric coordinates, equation (64) becomes

$$\alpha_w(\phi) = \frac{1}{\pi}\int_0^{\pi} \frac{G'(\phi_1)d\phi_1}{\cos\phi_1-\cos\phi} + \frac{1}{\pi}\int_0^{\pi} \frac{(\cos\phi_1-\cos\phi)\,G'(\phi_1)d\phi_1}{(\cos\phi_1-\cos\phi)^2 + \zeta^2} \tag{65}$$

where G and $\cos\phi = \eta$ are defined in equations (1) and (2), and $\zeta = 2Z/b$. The Fourier series for G from equation (1) is

$$G(\phi_1) = \sum_{n=1}^{\infty} a_n \sin n\phi_1, \quad G'(\phi_1) = \sum_{n=1}^{\infty} n\,a_n \cos n\phi_1$$

The first integral is

$$\frac{1}{\pi}\int_0^{\pi} \frac{\cos n\phi_1\, d\phi_1}{\cos\phi_1-\cos\phi} = \frac{\sin n\phi}{\sin\phi} \tag{66}$$

and the second integral is defined by

$$I_n = \frac{1}{\pi}\int_0^{\pi} \frac{(\cos\phi_1-\eta)\cos n\phi_1\, d\phi_1}{(\cos\phi_1-\eta)^2 + \zeta^2} \tag{67}$$

where $\eta = \cos\phi$ and I_n is evaluated in equations (B5) through (B11) in appendix B. With equations (66) and (67) equation (65) can be reduced to

$$\alpha_w = \sum_{n=1}^{\infty} \left(\frac{\sin n\phi}{\sin\phi} + I_n\right) n\,a_n \tag{68}$$

The induced drag coefficient (eq. 13) becomes

$$C_{D_i} = \frac{A}{2}\int_0^{\pi} G\,\alpha_w \sin\phi\, d\phi = \frac{A}{2}\int_0^{\pi} \sum_{n=1}^{\infty} a_n \sin n\phi \sum_{n^*=1}^{\infty} \left(\frac{\sin n^*\phi}{\sin\phi} + I_{n^*}\right) n^* a_{n^*} \sin\phi\, d\phi \tag{69}$$

$$= \frac{A}{2}\left(\frac{\pi}{2}\sum_{n=1}^{\infty} n\, a_n^2 + \sum_{n=1}^{\infty} a_n \sum_{n^*=1}^{\infty} n^* a_{n^*} \int_0^{\pi} I_{n^*} \sin\phi \sin n\phi\, d\phi\right)$$

Define

$$I_{nn^*} = \frac{1}{\pi}\int_0^{\pi} I_{n^*} \sin\phi \sin n\phi\, d\phi \tag{70}$$

then with equation (4) for C_L, equation (69) becomes

$$\frac{\pi A\, C_{D_i}}{C_L^{\,2}} = \frac{1}{e} = \sum_{n=1}^{\infty} n\left(\frac{a_n}{a_1}\right)^2 + 2\sum_{n=1}^{\infty} \frac{a_n}{a_1} \sum_{n^*=1}^{\infty} n^* \frac{a_{n^*}}{a_1} I_{nn^*} \tag{71}$$

These lift and drag coefficients and aspect ratio are based on wing area and wing span of one wing only in this equal winged biplane. The I_{nn^*}'s represent induced drag influence coefficients due to a second wake vorticity sheet. The I_{nn^*} integral of equation (70) is evaluated in equations (B25), (B26), (B27), (B39), and (B40) of appendix B, also in table 12 for $\zeta = 1/2$.

For symmetric spanwise loading only odd numbered n and n* apply, then equation (71) can be written

$$\frac{1}{e} = 1 + 2\,I_{11} + \sum_{\substack{n=3\\ \text{odd}}}^{\infty} n\left(\frac{a_n}{a_1}\right)^2 + 2\sum_{\substack{n=3\\ \text{odd}}}^{\infty} (n\,I_{1n} + I_{n1})\frac{a_n}{a_1} + 2\sum_{\substack{n=3\\ \text{odd}}}^{\infty} \frac{a_n}{a_1} \sum_{\substack{n^*=3\\ \text{odd}}}^{\infty} n^*\, I_{nn^*} \frac{a_{n^*}}{a_1} \tag{72}$$

Equation (72) applies for a biplane with equal wings. Since I_{nn^*} denotes the influence of one wing on the other, then for a monoplane wing in ground effect the I's in equation (72) are all preceded by a negative sign. For elliptic

loading, $a_n = 0$ for $n>1$, then $e^{-1} = 1 + 2I_{11}$ for the wing in a biplane, and $e^{-1} = 1 - 2I_{11}$ for the wing at $h/b = \zeta/4$ above the ground. In ground effect the ground vortex images are in opposite sense to the vortices of the model.

<u>a_n/a_1 coefficients for minimized induced drag.</u> - Objective is to minimize equation (72) for a given lift but without any other constraint. Following the procedure leading to equation (17), taking partial derivatives of 1/e of equation (72) with respect to a_3/a_1, a_5/a_1, . . ., a_m/a_1, results in

$$\frac{\partial(1/e)}{\partial(a_m/a_1)} = 2\,m\,\frac{a_m}{a_1} + 2(m\,I_{1m} + I_{m1}) + 2\sum_{\substack{n=3\\ \text{odd}}}^{\infty} m\,I_{nm}\,\frac{a_n}{a_1} + 2\sum_{\substack{n^*=3\\ \text{odd}}}^{\infty} n^*\,I_{nn^*}$$

$$\frac{a_{n^*}}{a_1} = 2\left[m\,I_{1m} + I_{m1} + m\,\frac{a_m}{a_1} + \sum_{\substack{n=3\\ \text{odd}}}^{\infty}(m\,I_{nm} + n\,I_{mn})\,\frac{a_n}{a_1}\right] \qquad (73)$$

where m is an odd integer greater than one, and the I's are from equation (70) or appendix B with corresponding subscript integers. For minimal induced drag, equation (73) is zero, then

$$m\,I_{1m} + I_{m1} + m\,\frac{a_m}{a_1} + \sum_{\substack{n=3\\ \text{odd}}}^{N}(m\,I_{nm} + n\,I_{mn})\,\frac{a_n}{a_1} = 0;\ m=3,5,7,\ldots N \qquad (74)$$

where N is an odd integer made large enough to insure accuracy. There are (N-1)/2 m-equations with (N-1)/2 a_n/a_1 unknowns. A simultaneous solution of these equations leads to evaluation of the a_n/a_1 ratios. As an example, for N=5, equation (74) appears as

$$\left.\begin{aligned} 3I_{13} + I_{31} + 3(1 + 2I_{33})\,\frac{a_3}{a_1} + (3I_{53} + 5I_{35})\,\frac{a_5}{a_1} &= 0 \\ 5I_{15} + I_{51} + (3I_{53} + 5I_{35})\,\frac{a_3}{a_1} + 5(1 + 2I_{55})\,\frac{a_5}{a_1} &= 0 \end{aligned}\right\} \qquad (75)$$

For the wing in ground effect a negative sign must be inserted before the I values of equations (74) and (75). Examination of equation (74) shows that minimum induced drag is not attained with elliptic loading. For elliptic

loading, $a_n = 0$ for $n>1$, then equation (74) is not satisfied because $m I_{1m} + I_{m1}$ is not zero, except when $\zeta = \infty$ where $I = 0$. With the a_n/a_1 ratios known, then $1/e$ can be determined from equation (72), induced angle in the wake from equation (68), wing bending moment ratio from equation (11), η_{cp} from equation (12), and spanwise loading by equation (5).

<u>a_n/a_1 coefficients for minimized induced drag and wing bending moment.</u> - The ratio C_b/e is minimized as in the development leading to equation (17). Then

$$\frac{\partial(C_b/e)}{\partial(a_m/a_1)} = C_b \frac{\partial(1/e)}{\partial(a_m/a_1)} + \frac{1}{e} \frac{\partial C_b}{\partial(a_m/a_1)} = 0 \tag{76}$$

where $\partial(1/e)/\partial(a_m/a_1)$ is given in equation (73) and $\partial C_b/\partial(a_m/a_1)$ is given in equation (18). With these values, equation (76) becomes

$$m I_{1m} + I_{m1} + m \frac{a_m}{a_1} \sum_{\substack{n=3 \\ \text{odd}}}^{N} (m I_{nm} + n I_{mn}) \frac{a_n}{a_1} + m t f_m = 0;$$

$$m=1,3,5,\ldots N \tag{77}$$

where t is a constant similar to that in equation (20), and f_m is given in equation (10). Equation (77) is equal to equation (74) plus the added term $m t f_m$. The solution procedure for determining a_n/a_1 is the same as that of equation (74).

<u>Antisymmetric loading a_n/a_2 coefficients for minimized induced drag.</u> - The wing rolling moment coefficient is given by

$$C_\ell = \frac{L}{qSb} = \frac{A}{2} \int_{-1}^{1} G\eta d\eta = \frac{A}{4} \int_{0}^{\pi} G \sin 2\phi d\phi = \frac{\pi A}{8} a_2 \tag{78}$$

where L is the wing rolling moment, and G is defined in equation (1). With this C_ℓ and a_2 relation, equation (69) can be written as

$$\frac{C_{D_i}}{\frac{\pi A}{2} a_2^2} = \frac{\pi A C_{D_i}}{\partial 2 C_\ell^2} = \frac{1}{2} \sum_{n=1}^{\infty} n \left(\frac{a_n}{a_2}\right)^2 + \sum_{n=1}^{\infty} \frac{a_n}{a_2} \sum_{n^*=1}^{\infty} n^* \frac{a_{n^*}}{a_2} I_{nn^*} = \frac{1}{e_r} \tag{79}$$

For antisymmetric loading only even integer values of n and n* apply. Then

$$\frac{1}{e_r} = 1 + 2I_{22} + \frac{1}{2} \sum_{\substack{n=4 \\ \text{even}}}^{\infty} n\left(\frac{a_n}{a_2}\right)^2 + \sum_{\substack{n=4 \\ \text{even}}}^{\infty} (nI_{2n} + 2I_{n2}) \frac{a_n}{a_2} + \sum_{\substack{n=4 \\ \text{even}}}^{\infty} \frac{a_n}{a_2}$$

$$\sum_{\substack{n^*=4 \\ \text{even}}}^{\infty} n^* I_{nn^*} \frac{a_{n^*}}{a_2} \qquad (80)$$

where e_r is a drag efficiency factor for loading due to rolling. The partial derivative of equation (80) leads to the equations for minimized induced drag. Thus,

$$\frac{\partial(1/e_r)}{\partial(a_m/a_2)} = mI_{2m} + 2I_{m2} + m\frac{a_m}{a_2} + \sum_{\substack{n=4 \\ \text{even}}}^{N} (mI_{nm} + nI_{mn}) \frac{a_n}{a_2} = 0,$$

$$m = 4,6,8 \ldots N \qquad (81)$$

which applies to the biplane. For wing in-ground effect the signs of the I's, are changed.

Example numerical solution with $\zeta = 1/2$ of biplane and wing ground effect models. - For N = 9, equation (74) is written as

$$\left.\begin{aligned}
&3I_{13}+I_{31}+3(1+2I_{33})\frac{a_3}{a_1}+(3I_{53}+5I_{35})\frac{a_5}{a_1}+(3I_{73}+7I_{37})\frac{a_7}{a_1}+(3I_{93}+9I_{39})\frac{a_9}{a_1} = 0 \\
&5I_{15}+I_{51}+(3I_{53}+5I_{35})\frac{a_3}{a_1}+5(1+2I_{55})\frac{a_5}{a_1}+(5I_{75}+7I_{57})\frac{a_7}{a_1}+(5I_{95}+9I_{59})\frac{a_9}{a_1} = 0 \\
&7I_{17}+I_{71}+(3I_{73}+7I_{37})\frac{a_3}{a_1}+(5I_{75}+7I_{57})\frac{a_5}{a_1}+7(1+2I_{77})\frac{a_7}{a_1}+(7I_{97}+9I_{79})\frac{a_9}{a_1} = 0 \\
&9I_{19}+I_{91}+(3I_{93}+9I_{39})\frac{a_3}{a_1}+(5I_{95}+9I_{59})\frac{a_5}{a_1}+(7I_{97}+9I_{79})\frac{a_7}{a_1}+9(1+2I_{99})\frac{a_9}{a_1} = 0
\end{aligned}\right\} \qquad (82)$$

where I_{nn^*} is given in equation (70) and in appendix B. Using the I_{nn^*} for $\zeta = 1/2$ given in table 12, equation (82) becomes

$$
\left.
\begin{aligned}
-.139103 + 3.348175\,\frac{a_3}{a_1} - .155810\,\frac{a_5}{a_1} + .009726\,\frac{a_7}{a_1} - .004216\,\frac{a_9}{a_1} &= 0 \\
-.004910 - .155810\,\frac{a_3}{a_1} + 5.179748\,\frac{a_5}{a_1} - .078668\,\frac{a_7}{a_1} + .010699\,\frac{a_9}{a_1} &= 0 \\
.001489 + .009726\,\frac{a_3}{a_1} - .078668\,\frac{a_5}{a_1} + 7.077076\,\frac{a_7}{a_1} - .044194\,\frac{a_9}{a_1} &= 0 \\
-.003196 - .004216\,\frac{a_3}{a_1} + .010699\,\frac{a_5}{a_1} - .044194\,\frac{a_7}{a_1} + 9.008733\,\frac{a_9}{a_1} &= 0
\end{aligned}
\right\} \quad (83)
$$

The simultaneous solution of these four linear equations provides the Fourier loading coefficients. Convergence accuracy can be assessed by also doing the solution of the top three, top two, and top equations. These are

	$\frac{a_3}{a_1}$	$\frac{a_5}{a_1}$	$\frac{a_7}{a_1}$	$\frac{a_9}{a_1}$
4 eq. solution	.041649	.002196	-.000241	.000370
3 eq. solution	.041649	.002197	-.000243	
2 eq. solution	.041648	.002201		
1 eq. solution	.041546			

(84)

From equation (5), the spanwise loading distribution is

$$
\frac{c_\ell c}{C_L c_{av}} = \frac{4}{\pi}\left(\sin\phi + \sum_{\substack{n=3 \\ \text{odd}}}^{\infty} \frac{a_n}{a_1} \sin n\phi\right) \quad (85)
$$

where a_n/a_1 values are given in equation (84), and $\phi = \cos^{-1}\eta$. This loading is that for minimum induced drag of a biplane wing with the wings vertically separated by $\zeta = 1/2$. This optimized loading is outboard relative to elliptic loading.

With the $\zeta = 1/2$, I_{nn^*} values of table 12, the drag efficiency factor of equation (72) becomes

$$\frac{1}{e} = 1 \pm .422074 + \sum_{\substack{n=3 \\ \text{odd}}}^{9} n \left(\frac{a_n}{a_1}\right)^2 \pm \left[-.278206 \frac{a_3}{a_1} - .009820 \frac{a_5}{a_1} + .002979 \right.$$

$$\frac{a_7}{a_1} + \frac{a_3}{a_1} \left(.348175 \frac{a_3}{a_1} - .274717 \frac{a_5}{a_1} + .019452 \frac{a_7}{a_1} - .008431 \frac{a_9}{a_1}\right) + \frac{a_5}{a_1}$$

$$\left(.179748 \frac{a_5}{a_1} - .157336 \frac{a_7}{a_1} + .021397 \frac{a_9}{a_1}\right) + \frac{a_7}{a_1} \left(.077076 \frac{a_7}{a_1} - .088388\right.$$

$$\left.\left.\frac{a_9}{a_1}\right) + .008733 \left(\frac{a_9}{a_1}\right)^2 - .006391 \frac{a_9}{a_1}\right] \tag{86}$$

where in the ± signs, plus applies for the biplane a_n/a_1's and minus for the ground effect a_n/a_1's.

The spanwise center of pressure of equation (12) simplifies to

$$\eta_{cp} = \frac{4}{3\pi} \left(1 + \frac{3}{5} \frac{a_3}{a_1} - \frac{1}{7} \frac{a_5}{a_1} + \frac{1}{15} \frac{a_7}{a_1} - \frac{3}{77} \frac{a_9}{a_1}\right) \tag{87}$$

With the a_n/a_1 values of equation (84) used in equations (86) and (87), the 4 through 1 equation solutions compare as follows:

	4 eq. sol.	3 eq. sol.	2 eq. sol.	1 eq. sol.	elliptic loading
$\frac{1}{e}$	1.416271	1.416272	1.416273	1.416294	1.422074
η_{cp}	.434873	.434879	.434885	.434993	.424413

(88)

which shows 0.4080 percent less induced drag than that with elliptic loading.

The minimum induced drag and root bending moment solution for the biplane is obtained from the simultaneous solution of the equations of equation (77). That is, to add mtf_n to the left side of equations (82) and (83). For the wing root case, $\eta_b = 0$, and using equation (10a)

$$mtf_m \overset{m=3}{=} \frac{4}{5}t \overset{m=5}{=} -\frac{4}{21}t \overset{m=7}{=} \frac{4}{45}t \overset{m=9}{=} -\frac{4}{77}t \tag{89}$$

Choosing t = 1, these values are added to equation (83), and its solution for a_n/a_1 results in

$$\frac{a_n}{a_1}\overset{n=3}{=} -.195876 \overset{n=5}{=} .031633 \overset{n=7}{=} -.012113 \overset{n=9}{=} .005932 \tag{90}$$

and for odd n > 9 $$\frac{a_n}{a_1}\overset{n>9}{=} \frac{4(-1)^{\frac{n-1}{2}}}{n(n^2-4)} \tag{91}$$

where for n > 9, a_n/a_1 is obtained from equation (20). With equation (91) the following summation is:

$$\sum_{\substack{n=11\\ \text{odd}}}^{\infty} n\left(\frac{a_n}{a_1}\right)^2 = 2.04061 \times 10^{-4} \tag{92}$$

Also

$$\frac{1}{e} = \left(\frac{1}{e}\right)_{\text{eq. (82)}} + t^2 \sum_{\substack{n=1\\ \text{odd}}}^{\infty} n\left(\frac{a_n}{a_1}\right)^2, \quad \eta_{cp} = \left(\eta_{cp}\right)_{\text{eq. (83)}} + \frac{4}{3\pi}\left[\frac{3}{4}t^2 \sum_{\substack{n=11\\ \text{odd}}}^{\infty} n\left(\frac{a_n}{a_1}\right)^2\right] \tag{93}$$

Then with the a_n/a_1 values of equation (90) and t = 1

$$\left.\begin{aligned} \frac{1}{e} &= 1.613214, \quad & \eta_{cp} &= .372175 \\ \frac{1}{e_c} &= 1.422074, \quad & \eta_{cpc} &= .424413 \end{aligned}\right\} \tag{94}$$

$$\frac{e_c}{e} = 1.134410, \quad \frac{C_b}{C_{bc}}\overset{\eta_b=0}{=} \frac{\eta_{cp}}{\eta_{cpc}} = .876764 \tag{95}$$

With equations (49) and (50), for same lift and same wing root bending moment

$$\frac{b}{b_c} = 1.140558, \quad \frac{D_i}{D_{ic}} = .872038 \tag{96}$$

The spanwise loading distribution for these minimized conditions is equation (5) in which the a_n/a_1's are those given in equations (90) and (91). These results show the minimum induced drag for a given root bending moment due to t = 1 inboard loading of a wing in a biplane with $\zeta = 1/2$. Compared with the biplane wing with elliptic loading and same lift and wing root bending moment, it has 12.8 percent less induced drag, 14 percent greater wing span, and spanwise center of pressure is 12.3 percent less, that is loading is inboard.

For ground effect solutions the I_{nn^*}'s in equation (82) change sign. This sign change can be taken into account in equation (83) by replacing the numbers 3.348175, 5.179748, 7.077076, and 9.008733 by -2.651825, -4.820252, -6.922924, and -8.991268, respectively. With these numbers substituted into equation (83), the 4 through 1 equation, simultaneous solutions result in

	$\frac{a_3}{a_1}$	$\frac{a_5}{a_1}$	$\frac{a_7}{a_1}$	$\frac{a_9}{a_1}$
4 eq. solution	-.052494	.000675	.000136	-.000331
3 eq. solution	-.052495	.000676	.000134	
2 eq. solution	-.052495	.000678		
1 eq. solution	-.052455			

(97)

where as before in equation (84), excellent convergence is demonstrated. The a_n/a_1's of equation (97) inserted into equation (85) gives the optimized spanwise loading distribution for minimum induced drag of a wing in ground effect at $h/b = \zeta/4 = 1/8$ above ground. This optimized loading is inboard relative to elliptic loading. For elliptic loading, $a_n/a_1 = 0$ for $n > 1$.

With the a_n/a_1 values of equation (97) used in equations (86) and (87), the 4 through 1 equation solutions compare as follows:

	4 eq. sol.	3 eq. sol.	2 eq. sol.	1 eq. sol.	elliptic loading
$\frac{1}{e}$	.570628	.570629	.570629	.570630	.577927
η_{cp}	.411014	.411008	.411004	.411056	.424413

(98)

which shows 1.2627 percent less induced drag than that with elliptic loading.

The minimum induced drag and root bending moment solution for the wing in ground effect is obtained by the simultaneous solution of the equations of equation (83) which is changed by substituting the four numbers listed above equation (97), and by adding equation (89), t = 1, values with changed signs. The solution results in

$$\frac{a_n}{a_1} \overset{n=3}{=} -.357148 \overset{n=5}{=} .050279 \overset{n=7}{=} -.013734 \overset{n=9}{=} .005717 \tag{99}$$

and for odd n > 9 $$\frac{a_n}{a_1} \overset{n>9}{=} \frac{4(-1)^{\frac{n-1}{2}}}{n(n^2-4)} \tag{100}$$

These a_n/a_1 values are inserted into equation (93) for t = 1, then

$$\left.\begin{aligned} \frac{1}{e} &= .826212, & \eta_{cp} &= .330000 \\ \frac{1}{e_c} &= .577927, & \eta_{cpc} &= .424413 \end{aligned}\right\} \tag{101}$$

$$\frac{e_c}{e} = 1.429613, \qquad \frac{C_b}{C_{bc}} \overset{\eta_b=0}{=} \frac{\eta_{cp}}{\eta_{cpc}} = .777544 \tag{102}$$

With equations (49) and (50), for same lift and same wing root bending moment

$$\frac{b}{b_c} = 1.286101, \qquad \frac{D_i}{D_{ic}} = .864307 \tag{103}$$

The spanwise loading distribution for these minimized conditions is equation (5) in which the a_n/a_1's are those given in equations (99) and (100). These results show the minimum induced drag for a given root bending moment due to t = 1 inboard loading of a wing in ground effect at h/b = ζ/4 = 1/8 height. Compared with the wing in ground effect with elliptic loading and same lift and wing root bending moment, it has 13.6% less induced drag, 28.6% greater wing span, and spanwise center of pressure is 22.2% 'ess.

The antisymmetric loading solution for minimum induced drag for the biplane with $\zeta = 1/2$ is obtained with equation (81) in which the I's are the even n and n* integer values of I_{nn*} listed in table 12. Then for an N = 6 solution

$$\left.\begin{aligned} -.158416 + 4.256811\,\frac{a_4}{a_2} - .107350\,\frac{a_6}{a_2} &= 0 \\ .004993 - .107350\,\frac{a_4}{a_2} + 6.121520\,\frac{a_6}{a_2} &= 0 \end{aligned}\right\} \tag{104}$$

Then 2-equation and 1-equation solutions are

$$\begin{aligned} &\text{2 eq. sol.} \qquad \frac{a_4}{a_2} = .037211, \qquad \frac{a_6}{a_2} = -.000163 \\ &\text{1 eq. sol.} \qquad \frac{a_4}{a_2} = .037215 \end{aligned} \tag{105}$$

The induced drag efficiency parameter of equation (80) with even integer values of n and n* for I_{nn*} of table 12, becomes

$$\frac{1}{e_r} = 1 \pm .215435 + 2\left(\frac{a_4}{a_2}\right)^2 + 3\left(\frac{a_6}{a_2}\right)^2 \pm \left[-.158416\,\frac{a_4}{a_2} + .004993\,\frac{a_6}{a_2} + .128406\left(\frac{a_4}{a_2}\right)^2 + .060760\left(\frac{a_6}{a_2}\right)^2 - .107350\,\frac{a_4}{a_2}\,\frac{a_6}{a_2}\right] \tag{106}$$

where in the ± term, the + sign is for biplane, and the - sign is for ground effect values. Then with equation (105) for

$$\text{2 eq. sol.,}\ \frac{1}{e_r} = 1.212487; \qquad \text{1 eq. sol.,}\ \frac{1}{e_r} = 1.212487 \tag{107}$$

that is, the same to the sixth decimal place. This is 0.253% less than the elliptic loading equivalent sin 2ϕ loading value which is $1/e_r = 1.215435$. The spanwise loading is given in equation (1) which for antisymmetric loading is

$$\frac{c_\ell c}{2ba_2} = \sum_{\substack{n=2 \\ \text{even}}}^{\infty} \frac{a_n}{a_2} \sin n\phi \tag{108}$$

where from equation (78), $a_2 = 8C_L/\pi A$. The spanwise loading resulting from inserting a_n/a_2 values of equation (105) into equation (108), is outboard of the sin 2ϕ loading. This minimized induced drag loading is for a biplane with only antisymmetric loading.

The antisymmetric loading for minimum induced drag for the wing in ground effect at $h/b = \zeta/4 = 1/8$ height from ground is obtained with equation (81) but with sign changes on the I's from table 12.

$$\left.\begin{aligned} .158416 + 3.743189\,\frac{a_4}{a_2} + .107350\,\frac{a_6}{a_2} &= 0 \\ -.004993 + .107350\,\frac{a_4}{a_2} + 5.878480\,\frac{a_6}{a_2} &= 0 \end{aligned}\right\} \qquad (109)$$

$$\begin{aligned} &\text{2 eq. sol.} && \frac{a_4}{a_2} = -.042368, \quad \frac{a_6}{a_2} = .001623 \\ &\text{1 eq. sol.} && \frac{a_4}{a_2} = -.042321 \end{aligned} \qquad (110)$$

Using equation (106)

$$\text{2 eq. sol.,}\ \frac{1}{e_r} = .781205; \quad \text{1 eq. sol.,}\ \frac{1}{e_r} = .781213 \qquad (111)$$

which is 0.428% less than sin 2ϕ loading value which is $1/e_r = .784565$. The spanwise loading is equation (108) with the a_n/a_2 values of equation (110). This loading is inboard of the sin 2ϕ loading.

Unsymmetric spanwise loading is a combination of symmetric and antisymmetric loading, that is, it includes both odd and even integer values of n and n* in the loading series. A solution for minimized induced drag starts with equation (69), written as

$$C_{D_i} = \frac{\pi A}{4}\left(\sum_{n=1}^{\infty} n\,a_n^2 + 2\sum_{n=1}^{\infty} a_n \sum_{n^*=1}^{\infty} n^*\,I_{nn^*}\,a_{n^*}\right) \qquad (112)$$

Then

$$\frac{\partial C_{D_i}}{\partial a_m} = \frac{\pi A}{2}\left[m\, a_m + \sum_{n=1}^{\infty} (mI_{mn} + nI_{mn})\, a_n\right],\ m = 3,4,5 \ldots \tag{113}$$

For a minimized induced drag solution, equation (113) is equal to zero, then the equations are solved simultaneously to obtain $a_3, a_4, \ldots a_n$. The coefficients a_1 and a_2 are specified for given values of C_L and C_ℓ of equation (4) and (78). For a single wing, the I's of equation (113) are zero, then $a_n = 0$ for $n > 2$, which means that minimal induced drag is with $a_1 \sin\phi$ and $a_2 \sin 2\phi$ loading combinations.

Flow-Field Solution of a Flat Vorticity Sheet

A spinoff of the biplane drag minimization solution provides mathematically exact equations for downwash and sidewash about a vorticity sheet having arbitrary loading distribution. The downwash at point (y,z) due to the vorticity sheet is the second integral of equation (64), then

$$w_s(y,z) = \frac{1}{2\pi}\int_{-b/2}^{b/2} \frac{(y-y_1)\,\frac{d\Gamma}{dy_1}\,dy_1}{(y-y_1)^2 + Z^2} \tag{114}$$

where subscript s symbolizes, from sheet. Similarly, the sidewash is the horizontal component of the induced velocity, that is, $z/(y-y_1)$ times the integrant of equation (114). Thus

$$v_s(y,z) = \frac{Z}{2\pi}\int_{-b/2}^{b/2} \frac{\frac{d\Gamma}{dy_1}\,dy_1}{(y-y_1)^2 + Z^2} \tag{115}$$

where the v_s is positive in the y-direction. In terms of the dimensionless coordinates of equations (1) and (2), equations (114) and (115) become

$$\frac{w_s}{V}(\eta,\zeta) = \sum_{n=1}^{\infty} n\, a_n \frac{1}{\pi}\int_0^{\pi} \frac{(\cos\phi_1 - \eta)\cos n\phi_1\, d\phi_1}{(\cos\phi_1 - \eta)^2 + \zeta^2} \tag{116}$$

$$\frac{v_s}{V}(\eta,\zeta) = -\zeta \sum_{n=1}^{\infty} n\, a_n \frac{1}{\pi} \int_0^{\pi} \frac{\cos n\phi_1 \, d\phi_1}{(\cos\phi_1 - \eta)^2 + \zeta^2} \tag{117}$$

where a_n are the Fourier coefficients of loading, given in equation (1). The integrals of equations (116) and (117) are defined in equations (67) and (B12) of appendix B, then

$$\frac{w_s}{V} = \sum_{n=1}^{\infty} n\, I_n\, a_n \tag{118}$$

$$\frac{v_s}{V} = -\zeta \sum_{n=1}^{\infty} n\, J_n\, a_n \tag{119}$$

where for arbitrary values of η and ζ, I_n is determined from equations (B5) through (B11), J_n from equations (B11), (B13), (B14), and (B18) through (B20). It should be noted that a sign change in η influences the sign on I_n and J_n as shown in equations (B6) and (B16).

For n = 1 the loading distribution is elliptic and equations (118) and (14) can be expressed as a ratio so that

$$\frac{w_s}{w_w} = I_1 \tag{120}$$

where w_w is the downwash at the wake and is constant spanwise for elliptic loading. The elliptic loading solution for w_s/w_w is given in the literature, for example, solutions by conformal transformation in references 10 and 11, however, it appears as a function in elliptical coordinates. The general solutions for w_s/V and v_s/V such as those of equations (118) and (119) were not found in the literature. Computed values of equation (120) for various η and ζ correlate with values in the table on page 150 of reference 11.

Cruciform Wing Solution

The cruciform wing or x-wing is a nonplanar type configuration. An aft view of this wing and coordinate system is shown on the next page. The induced

velocity normal to the upper right wing panel due to the crossing wing with $d\Gamma$ vorticity is

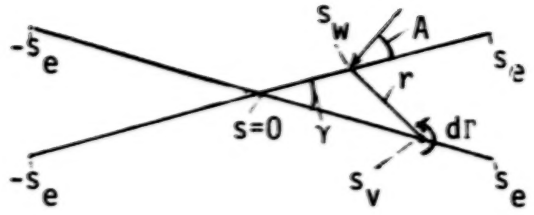

$$dw_{wv} = -\frac{d\Gamma}{2\pi r} \sin A \qquad (121)$$

where $r^2 = s_v^2 + s_w^2 - 2 s_v s_w \cos\gamma$, $\sin A = -\frac{1}{r}(s_w - s_v \cos\gamma)$ which relations come from the cosine and sine formulas, respectively. The total normal velocity along the upper right wing panel is the sum of that induced by the wing on itself and equation (121). Thus for the x-wing the induced angle in the wake is

$$\alpha_w(\phi) = \frac{1}{\pi}\int_0^\pi \frac{G'(\phi_1)\, d\phi_1}{\cos\phi_1 - \cos\phi} + \frac{1}{\pi}\int_0^\pi \frac{(\cos\gamma\cos\phi_1 - \eta)\, G'(\phi_1)\, d\phi_1}{(\cos\phi_1 - \eta\cos\gamma)^2 + \eta^2\sin^2\gamma} \qquad (122)$$

where the dimensionless terms are

$$\cos\phi = \eta = s/s_e, \quad G = \Gamma/2s_eV \qquad (123)$$

With the Fourier series for G in equation (1) and with equation (66), equation (122) simplifies to

$$\alpha_w = \sum_{n=1}^{\infty} \left(\frac{\sin n\phi}{\sin\phi} + P_n\right) n\, a_n \qquad (124)$$

where

$$P_n = \frac{1}{\pi}\int_0^\pi \frac{(\cos\gamma\, \cos\phi_1 - \eta)\, \cos n\phi_1\, d\phi_1}{(\cos\phi_1 - \eta\cos\gamma)^2 + \eta^2\, \sin^2\gamma} \qquad (125)$$

This integral is evaluated in equations (C2) through (C8) in appendix C. The P_n integral is similar to the I_n integral of equation (69). Equation (124) can be derived directly from equation (68) by a transformation of the variables. From the components of η_v shown at the right, the relations for η_v and ζ_v are

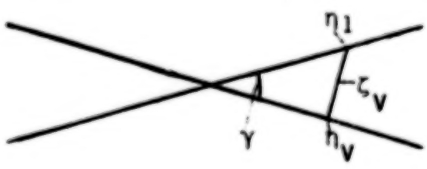

$$\eta_v = \eta_1 \cos\gamma = \cos\gamma \cos\phi_1, \quad \zeta_v = \eta_1 \sin\gamma = \sin\gamma \cos\phi_1 \tag{126}$$

These values of η_v and ζ_v are substituted into equation (67) for $\cos\phi_1$ and ζ, respectively, in the term which factors cos $n\phi_1$. Then I_n of equation (67) becomes P_n as given in equation (125). This transformation method can be applied to any two or more spatial arrangements of separate planar vorticity sheets.

The induced drag expression, derived in a similar manner to that of equation (69), is

$$C_{D_i} = \frac{\pi A}{4} \left(\sum_{n=1}^{\infty} n\, a_n^2 + 2 \sum_{n=1}^{\infty} a_n \sum_{n^*=1}^{\infty} n^*\, P_{nn^*}\, a_{n^*} \right) \tag{127}$$

where

$$P_{nn^*} = \frac{1}{\pi} \int_0^{\pi} P_{n^*} \sin\phi \sin n\phi \, d\phi \tag{128}$$

where P_{n^*} is given in equation (125), but with $n = n^*$, and $\eta = \cos\phi$. The drag influence coefficients, P_{nn^*}, are developed into a recurrence formula in appendix C, equations (C15) through (C19).

The lift coefficient given in equation (4) is with the lift normal to the wing from the aft view. For a cruciform wing or a tilted or rolled wing, the lift upwards is a component of the value given in equation (4), then

$$C_L = \frac{A}{2\pi} a_1 \cos\frac{\gamma}{2} \tag{129}$$

where C_L, A, and C_{D_i} are based on one wing of the crossed wings of the cruciform, i.e., the lift, induced drag, wing area, and width ($-s_e$ to s_e), of one of the two equal wings. Thus

$$S = 2s_e c_{av}, \quad A = \frac{(2s_e)^2}{S}, \quad C_L = \frac{L}{qS}, \quad C_{D_i} = \frac{D_i}{qS} \tag{130}$$

For symmetric spanwise loading only odd integers n and n* apply, then equation (127) with (129) becomes

$$\frac{\pi A C_{D_i}}{C_L{}^2} = \frac{1}{e} = \frac{1}{\cos^2\frac{\gamma}{2}} \left[1 + 2P_{11} + \sum_{\substack{n=3 \\ \text{odd}}}^{\infty} n\left(\frac{a_n}{a_1}\right)^2 + 2\sum_{\substack{n=3 \\ \text{odd}}}^{\infty} (nP_{1n} + P_{n1})\frac{a_n}{a_1}\right.$$

$$\left. + 2\sum_{\substack{n=3 \\ \text{odd}}}^{\infty} \frac{a_n}{a_1} \sum_{\substack{n^*=3 \\ \text{odd}}}^{\infty} n^* P_{nn^*} \frac{a_{n^*}}{a_1}\right] \qquad (131)$$

<u>a_n/a_1 coefficients for minimized induced drag.</u> - Derivatives of equation (131) are obtained in the same procedure as that leading to equations (73) and (74). Then

$$mP_{1m} + P_{m1} + m\frac{a_m}{a_1} + \sum_{\substack{n=3 \\ \text{odd}}}^{N} (mP_{nm} + nP_{mn})\frac{a_n}{a_1} = 0;\ m = 3,5,7, \ldots N \qquad (132)$$

where N is an odd integer. A simultaneous solution of these (N - 1)/2 equations results in the evaluation of the a_n/a_1 ratios. These a_n values, through equation (1), define the spanwise loading distribution for minimum induced drag for a cruciform wing where the wings are angled γ to each other in the yz plane. With the a_n/a_1 ratios known, then 1/e can be determined from equation (131), induced angle in the wake from equation (124), wing bending moment ratio from equation (11), η_{cp} from equation (12), and spanwise loading from equations (1) or (5).

<u>a_n/a_1 coefficients for minimized induced drag and wing bending moment, and antisymmetric loading.</u> - The added constraint of minimized wing bending moment is taken into account identically as done in the derivation of equation (77). For the cruciform wing solution the I_{nm}'s of equation (77) are replaced by P_{nm}'s. Or the equations are simply, mtf_m added to the left side of equation (132).

An antisymmetric loading solution can be obtained similarly as that leading to the equation (81), except the I_{nm}'s are replaced by P_{nm}'s. With a_n/a_2 determined from equation (81), the drag efficiency factor is found from equation (80) in which I_{nm} is substituted by P_{nm}.

Cruciform wing with $\gamma = 90°$. - In a cruciform wing when $\gamma = 90°$ there is no induced normal velocity at one vorticity sheet due to the other. The solution thus simplifies to the case of a single planar wing banked at an angle $\gamma/2$. For the constraint condition of lift, the loading is elliptical along the span, $\eta = s/s_e$. The C_L is given in equation (129), then from equation (131), $e^{-1} = 2$. For constraint conditions of lift and bending moment the loading characteristics are the same as those of equations (30) through (33), except that since by equation (129), $C_L(\gamma) = C_L \cos(\gamma/2)$, then C_L is replaced by $2^{\frac{1}{2}} C_L$ in equations (35) and (38), then

$$C_b = \frac{2^{\frac{1}{2}}}{4\pi}(f_1 - kt), \quad e^{-1} = 2(1 + kt^2) \tag{133}$$

When $\gamma = 90°$, the influence coefficients P_n and P_{nm} should be zero if there is no normal velocity induced from one vorticity sheet onto the other. Examination of equations (C2) and (C15) shows that when $\gamma = 90°$, the P_n and P_{nm} are zero for odd integer values of n and m, that is, for symmetric spanwise loading. For antisymmetrical loading, P_n and P_{nm} have values and thus the two wings are not aerodynamically independent of each other.

Flow Field at a γ Banked Plane, Induced by a Flat Vorticity Sheet

The cruciform wing solution is also the solution for determining the flowed field about a banked plane, as shown at the right. At the polar coordinate point (η,γ) the normal velocity to the γ plane is given by the second term in equation (124). Thus

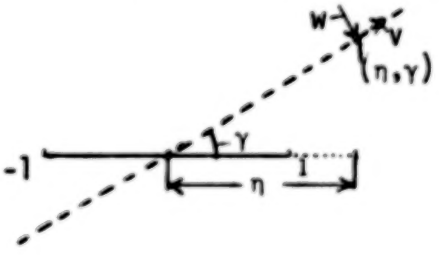

$$\frac{w(\eta,\gamma)}{V} = \sum_{n=1}^{\infty} n P_n a_n \tag{134}$$

The lateral velocity along the γ plane is analytically similar to equation (121), except that it is the cosine component, thus

$$dv = -\frac{d\Gamma}{2\pi r}\cos A$$

where by the sine formula, $\cos A = (s_v \sin\gamma)/r$. In dimensionless parameters, with equation (1), and integrating

$$\frac{v}{V} = -\sin\gamma \sum_{n=1}^{\infty} n\, a_n \frac{1}{\pi} \int_0^{\pi} \frac{\cos\phi_1 \cos n\phi_1\, d\phi_1}{(\cos\phi_1 - \eta\cos\gamma)^2 + \eta^2 \sin^2\gamma} \tag{135}$$

Since $2\cos\phi_1 \cos n\phi_1 = \cos(n+1)\phi_1 + \cos(n-1)\phi_1$, then equation (135) reduces to

$$\frac{v(\eta,\gamma)}{V} = -\frac{\sin\gamma}{2} \sum_{n=1}^{\infty} n\,(J_{n+1} + J_{n-1})\, a_n \tag{136}$$

where the J_n values are given in equations (C11) through (C13). The P_n values of equation (134) are given in equations (C2) through (C8). Equations (134) and (136) are exact solution equations for predicting the normal and tangential induced velocities on a γ-banked plane, induced by a flat vorticity sheet of arbitrary loading distribution, i.e., arbitrary a_n (see eq. 1).

V-Wing

The V-wing induced angle equation is similar to that of the cruciform wing, except the spanwise integration for velocity normal to the surface is made only over the upper wing panels. Then equation (122) becomes

$$\alpha_w(\phi) = \frac{1}{\pi} \int_0^{\pi/2} \frac{G'(\phi_1)\, d\phi_1}{\cos\phi_1 - \cos\phi} + \frac{1}{\pi} \int_{\pi/2}^{\pi} \frac{(\cos\gamma\cos\phi_1 - \eta)\, G'(\phi_1)\, d\phi_1}{(\cos\phi_1 - \eta\cos\gamma)^2 + \eta^2 \sin^2\gamma} \tag{137}$$

By adding and subtracting the first integral with limits $\pi/2$ to π and noting that the pertinent geometric parameter for the V-wing is the dihedral angle related to γ by

$$\Gamma = \frac{1}{2}\gamma \tag{138}$$

then equation (137) becomes

$$\alpha_w(\phi) = \frac{1}{\pi} \int_0^{\pi} \frac{G'(\phi_1)\, d\phi_1}{\cos\phi_1 - \cos\phi} - \frac{1}{\pi}(1 - \cos 2\Gamma) \int_{\pi/2}^{\pi} \frac{(\cos\phi_1 + \eta)\cos\phi_1\, G'(\phi_1)\, d\phi_1}{(\cos\phi_1 - \eta)[(\cos\phi_1 - \eta\cos 2\Gamma)^2 + \eta^2 \sin^2 2\Gamma]} \tag{139}$$

With the G series of equation (1)

$$\alpha_w(\phi) = \sum_{n=1}^{\infty} \left(\frac{\sin n\phi}{\sin\phi} + Q_n\right) n\, a_n \tag{140}$$

where

$$Q_n = -\frac{2}{\pi} \sin^2\Gamma \int_{\pi/2}^{\pi} \frac{(\cos\phi_1+\eta)\cos\phi_1 \cos n\phi_1\, d\phi_1}{(\cos\phi_1-\eta)[(\cos\phi_1-\eta\cos 2\Gamma)^2 + \eta^2\sin^2 2\Gamma]} \tag{141}$$

Using equation (140), the induced drag equation, derived similarly to that of equation (69), is

$$C_{D_i} = \frac{\pi A}{4}\left(\sum_{n=1}^{\infty} n\, a_n^2 + 2 \sum_{n=1}^{\infty} a_n \sum_{n^*=1}^{\infty} n^*\, Q_{nn^*}\, a_{n^*}\right) \tag{142}$$

where

$$Q_{nn^*} = \frac{1}{\pi}\int_0^{\pi} Q_{n^*} \sin\phi \sin n\phi\, d\phi \tag{143}$$

where Q_{n^*} is given in equation (141) in which n is replaced by n*, and $\eta = \cos\phi$. The lift coefficient is

$$C_L = \frac{\pi A}{4} a_1 \cos\Gamma \tag{144}$$

where C_L, A, and C_{D_i} are based on $S = 2s_e c_{av}$, $A = (2s_e)^2/S$, $C_L = L/qS$, $C_{D_i} = D_i/qS$. For symmetric spanwise loading only odd integer n and n* apply, then equation (142) with (144) becomes

$$\frac{\pi A C_{D_i}}{C_L^2} = \frac{1}{e} = \frac{1}{\cos^2\Gamma}\left[1 + 2\,Q_{11} + \sum_{\substack{n=3 \\ \text{odd}}}^{\infty} n\left(\frac{a_n}{a_1}\right)^2 + 2 \sum_{\substack{n=3 \\ \text{odd}}}^{\infty} (n\,Q_{1n} + Q_{n1})\frac{a_n}{a_1} + 2 \sum_{\substack{n=3 \\ \text{odd}}}^{\infty} \frac{a_n}{a_1} \sum_{\substack{n^*=3 \\ \text{odd}}}^{\infty} n^*\, Q_{nn^*} \frac{a_{n^*}}{a_1}\right] \tag{145}$$

Recurrence formula for Q_n and Q_{nn^*}. - To formulate a recurrence formula for the induced velocity influence coefficient it is simpler to work with Q_n

in the form

$$Q_n = q_n - r_n \tag{146}$$

where

$$q_n = \frac{1}{\pi}\int_{\pi/2}^{\pi} \frac{(\cos 2\Gamma \cos\phi_1 - \eta)\cos n\phi_1 \, d\phi_1}{(\cos\phi_1 - \eta\cos 2\Gamma)^2 + \eta^2 \sin^2 2\Gamma} \tag{147}$$

$$r_n = \frac{1}{\pi}\int_{\pi/2}^{\pi} \frac{\cos n\phi_1 \, d\phi_1}{\cos\phi_1 - \eta} \tag{148}$$

The recurrence formula for q_n and r_n are derived in the same manner as detailed in appendices B and C. Then

$$q_{n+2} = \left[\begin{array}{l} -\frac{4}{\pi}\cos 2\Gamma - 2\eta, \; n = 0 \\ \cos 2\Gamma + \frac{4}{\pi}\eta, \; n = 1 \\ \frac{4}{\pi}\left(\frac{\cos 2\Gamma}{n^2-1}\cos\frac{n\pi}{2} + \frac{\eta}{n}\sin\frac{n\pi}{2}\right), \; n > 1 \end{array}\right] + 4\eta\cos 2\Gamma \, q_{n+1} - 2(1+2\eta^2)q_n + 4\eta\cos 2\Gamma \, q_{n-1} - q_{n-2} \tag{149}$$

Noting that $q_{-n} = q_n$ and $r_{-n} = r_n$, then

$$\left.\begin{aligned} q_2 &= -\frac{2}{\pi}\cos 2\Gamma - \eta + 4\eta\cos 2\Gamma \, q_1 - (1+2\eta^2)\, q_0 \\ q_3 &= \cos 2\Gamma + \frac{4}{\pi}\eta + 4\eta\cos 2\Gamma \, q_2 - (3+4\eta^2)\, q_1 + 4\eta\cos 2\Gamma \, q_0 \end{aligned}\right\} \tag{150}$$

$$r_{n+1} = \left[\begin{array}{l} 1, \; n = 0 \\ \frac{-2}{\pi n}\sin\frac{n\pi}{2}, \; n > 0 \end{array}\right] + 2\eta \, r_n - r_{n-1} \tag{151}$$

$$\left.\begin{aligned} r_1 &= \frac{1}{2} + \eta \, r_0 \\ r_2 &= -\frac{2}{\pi} + 2\eta \, r_1 - r_0 \end{aligned}\right\} \tag{152}$$

The induced drag influence coefficient in terms of q and r, is equation (146) with $n = n^*$, inserted into (143), then

$$Q_{nn^*} = q_{nn^*} - r_{nn^*} \tag{153}$$

where

$$q_{nn^*} = \frac{1}{\pi}\int_0^{\pi} q_{n^*} \sin\phi \sin n\phi \, d\phi \tag{154}$$

$$r_{nn^*} = \frac{1}{\pi}\int_0^{\pi} r_{n^*} \sin\phi \sin n\phi \, d\phi \tag{155}$$

Then using the recurrence formulas of equations (149) and (151)

$$q_{n,n^*+2} = \begin{bmatrix} -\frac{2}{\pi}\cos 2\Gamma\,, & n = 1,\ n^* = 0 \\ -\frac{1}{2}\,, & n = 2,\ n^* = 0 \\ \frac{1}{2}\cos 2\Gamma\,, & n = 1,\ n^* = 1 \\ \frac{1}{\pi}\,, & n = 2,\ n^* = 1 \\ \frac{2}{\pi}\frac{\cos 2\Gamma}{n^{*2}-1}\cos\frac{n^*\pi}{2}, & n = 1,\ n^* > 1 \\ \frac{1}{\pi n^*}\sin\frac{n^*\pi}{2}, & n = 2,\ n^* > 1 \end{bmatrix} + 2\cos 2\Gamma\left(q_{n+1,n^*+1}+q_{n-1,n^*+1}\right) - 4q_{nn^*} - q_{n+2,n^*} - q_{n-2,n^*} + 2\cos 2\Gamma\left(q_{n+1,n^*-1}+q_{n-1,n^*-1}\right) - q_{n,n^*-2} \tag{156}$$

Noting that $q_{n,-n^*} = q_{nn^*}$ and $r_{n,-n^*} = r_{nn^*}$, then

$$q_{n2} = \begin{bmatrix} -\frac{1}{\pi}\cos 2\Gamma, & n = 1 \\ -\frac{1}{4}\,, & n = 2 \end{bmatrix} + 2\cos 2\Gamma\left(q_{n+1,1}+q_{n-1,1}\right) - 2q_{n0} - \frac{1}{2}q_{n+2,0} - \frac{1}{2}q_{n-2,0} \tag{157}$$

$$r_{n,n^*+1} = \begin{bmatrix} \frac{1}{2}\,, & n = 1,\ n^* = 0 \\ -\frac{1}{\pi n^*}\sin\frac{n^*\pi}{2}, & n = 1,\ n^* > 1 \end{bmatrix} + r_{n+1,n^*} + r_{n-1,n^*} - r_{n,n^*-1} \tag{158}$$

$$r_{n1} = \left[\frac{1}{4}\,, \quad n = 1\right] + \frac{1}{2}r_{n+1,0} + \frac{1}{2}r_{n-1,0} \tag{159}$$

a_n/a_1 coefficients for minimized induced drag. - In equation (145), since a_1 represents lift, this equation has the constraint condition of lift, that is, induced drag per unit lift. The partial derivative of equation (145)

with respect to a_m/a_1 is identically similar to that of equation (73) and (74). In equation (74) I_{mn} is replaced by Q_{mn}, then

$$mQ_{1m} + Q_{m1} + m\frac{a_m}{a_1} + \sum_{\substack{n=3 \\ \text{odd}}}^{N} (mQ_{nm} + nQ_{mn})\frac{a_n}{a_1} = 0;\ m = 3,5,7. \ . \ .N \qquad (160)$$

A simultaneous solution of these equations leads to evaluation of the a_n/a_1 ratios. With the a_n/a_1 values known, then the spanwise loading is determined from equation (5). This is the loading distribution for minimum induced drag per unit lift of the V-wing. Other aerodynamic characteristics are 1/e from equation (145), induced angle normal to the wake from equation (140), wing bending moment ratio, $C_b \cos\Gamma$, from equation (11), and η_{cp} from equation (12).

The solution for the constraint conditions of lift plus bending moment is obtained from equation (160) which is modified by adding the term mtf_m, similar to that shown in equation (77).

V-wing in ground effect. - When the apex of the V-wing touches ground the vorticity sheet system including ground images becomes that of the cruciform wing except the sense of the ground image vorticity is reversed. This can be taken into account by reversing the sign on the integrals in equation (122) when integrating along the lower panels of the sheet. Thus

$$\alpha_w(\phi) = \frac{1}{\pi}\int_0^{\pi/2} \frac{G'(\phi_1)\,d\phi_1}{\cos\phi_1 - \eta} - \frac{1}{\pi}\int_{\pi/2}^{\pi} \frac{G'(\phi_1)\,d\phi_1}{\cos\phi_1 - \eta} + \frac{1}{\pi}\int_{\pi/2}^{\pi}$$

$$\frac{(\cos 2\Gamma\cos\phi_1 - \eta)\,G'(\phi_1)\,d\phi_1}{(\cos\phi_1 - \eta\cos 2\Gamma)^2 + \eta^2\sin^2 2\Gamma} - \frac{1}{\pi}\int_0^{\pi/2} \frac{(\cos 2\Gamma\cos\phi_1 - \eta)\,G'(\phi_1)\,d\phi_1}{(\cos\phi_1 - \eta\cos 2\Gamma)^2 + \eta^2\sin^2 2\Gamma}$$

$$= \frac{1}{\pi}\int_0^{\pi} \frac{G'(\phi_1)\,d\phi_1}{\cos\phi_1 - \eta} - \frac{1}{\pi}\int_0^{\pi} \frac{(\cos 2\Gamma\cos\phi_1 - \eta)\,G'(\phi_1)\,d\phi_1}{(\cos\phi_1 - \eta\cos 2\Gamma)^2 + \eta^2\sin^2 2\Gamma} + \frac{2}{\pi}\int_{\pi/2}^{\pi}$$

$$\frac{(\cos 2\Gamma\cos\phi_1 - \eta)\,G'(\phi_1)\,d\phi_1}{(\cos\phi_1 - \eta\cos 2\Gamma)^2 + \eta^2\sin^2 2\Gamma} - \frac{2}{\pi}\int_{\pi/2}^{\pi} \frac{G'(\phi_1)\,d\phi_1}{\cos\phi_1 - \eta} \qquad (161)$$

With $G'(\phi_1) = \sum_{n=1}^{\infty} n\,a_n \cos n\phi_1$, comparing with equation (124), the first integral of equation (161), has the term $\sin n\phi/\sin\phi$, the second integral,

comparing with equation (125), has the term $-P_n$, and the third and fourth integrals, comparing with equations (146) through (148), has the term $2Q_n$. Then equation (161) becomes

$$\alpha_w(\phi) = \sum_{n=1}^{\infty} \left(\frac{\sin n\phi}{\sin\phi} + 2Q_n - P_n\right) n\, a_n \qquad (162)$$

The solution for the V-wing in ground effect follows the same procedure as that for the V-wing, but with the substitution of $2Q_n - P_n$ for Q_n, and $2Q_{nn^*} - P_{nn^*}$ for Q_{nn^*} in equations (141), (142), (145), and (160). The influence coefficients of P_n and P_{nn^*}, in which $\gamma = 2\Gamma$, are given in appendix C.

Planar-Wing Winglet Configuration

An aft view of this configuration consists of a flat wing span with winglets at the tips, as shown below.

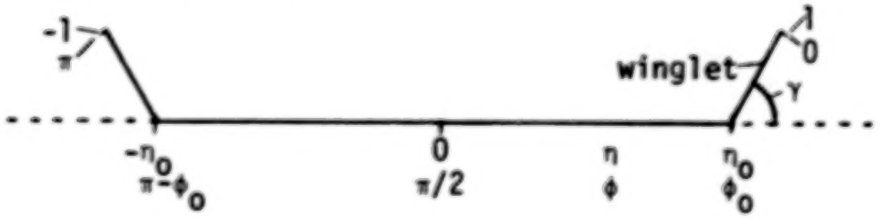

The dihedral cant angle, γ, of the winglet is the angle between the extended wing and the winglet. Theoretical aerodynamic characteristics of the planar-winglet have been developed in reference 9. The minimization method objective is to determine the loading distribution along the span extent of the wing and up the winglet such that induced drag for a given lift, and induced drag for a given root bending moment, are minimum.

Planar-wing winglet aerodynamic characteristics from reference 9. - From equation (69) of reference 9, the induced drag coefficient of a planar-wing winglet configuration with symmetric loading is

$$C_{D_i} = \frac{\pi A}{4}\left(\sum_{\substack{n=1\\ \text{odd}}}^{N} n\, a_n^2 + \sum_{\substack{n=1\\ \text{odd}}}^{N} a_n \sum_{\substack{n^*=1\\ \text{odd}}}^{N} n^* \frac{4}{\pi} D_{nn^*}\, a_{n^*}\right) \qquad (163)$$

where

$$D_{nn^*} = 2 \int_0^{\pi/2} L_{n^*_w} \sin\phi \sin n\phi \, d\phi \tag{164}$$

where for $\phi_0 \leq \phi \leq \frac{\pi}{2}$

$$L_{n^*_w} = \frac{1}{2\pi} \int_0^{\phi_0} L_- \cos n^*\phi_1 \, d\phi_1 + \frac{1}{2\pi} \int_{\pi-\phi_0}^{\pi} L_+ \cos n^*\phi_1 \, d\phi_1 \tag{165}$$

and for $0 \leq \phi \leq \phi_0$

$$L_{n^*_w} = \frac{1}{2\pi} \int_{\phi_0}^{\pi-\phi_0} L_- \cos n^*\phi_1 \, d\phi_1 + \frac{1}{2\pi} \int_{\pi-\phi_0}^{\pi} L_0 \cos n^*\phi_1 \, d\phi_1 \tag{166}$$

where (noting that $\eta_0 = \cos\phi_0$)

$$L_\pm = - \frac{(\cos\phi_1 \pm \eta_0)\,(\cos\phi_1 + \cos\phi \pm 2\eta_0)\,(1 - \cos\gamma)}{[(\cos\phi_1 - \cos\phi)^2 + 2(\cos\phi_1 \pm \eta_0)\,(\cos\phi \pm \eta_0)(1 - \cos\gamma)]\,(\cos\phi_1 - \cos\phi)} \tag{167}$$

$$L_0 = - \frac{(1 - 2\cos^2\gamma)\cos\phi_1 + \cos\phi + 2\eta_0\,(1 - \cos\gamma)\cos\gamma}{[(\cos\phi_1 - \cos\phi)\cos\gamma - 2\eta_0\,(1 - \cos\gamma)]^2 + (\cos\phi_1 + \cos\phi)^2 \sin^2\gamma} - \frac{1}{\cos\phi_1 - \cos\phi} \tag{168}$$

For the winglet span position of $\phi_0 = 5\pi/32$, or $\eta_0 = .881921$, values of D_{nn^*} had been computed for $\gamma = 90°$, and 75°, and presented in table II of reference 9. This table of D_{nn^*} has been reproduced as table 13 in the present report.

From equations (55) and (59) of reference (9), the lift coefficient and wing root bending moment coefficient are

$$C_L = \pi A a_1 \left[1 - \frac{2}{\pi}(1 - \cos\gamma)\left(\bar{T}_1 + \sum_{\substack{n=3 \\ \text{odd}}}^{N} \bar{T}_n \frac{a_n}{a_1}\right)\right] \tag{169}$$

$$C_{mbb} = \frac{Aa_1}{2}\left\{\frac{1}{3} - \frac{1}{2}(1 - \cos\gamma)n_0 T_1 + \sum_{\substack{n=3\\ \text{odd}}}^{N}\left[\frac{(-1)^{\frac{n+1}{2}}}{n-4} - \frac{1}{2}(1-\cos\gamma)n_0 T_n\right]\frac{a_n}{a_1}\right\} \tag{170}$$

where

$$\left.\begin{aligned} T_1 &= \phi_0 - n_0 \sin\phi_0 \\ T_n &= \frac{\sin(n-1)\phi_0}{n-1} - \frac{\sin(n+1)\phi_0}{n+1} \end{aligned}\right\} \tag{171}$$

Equations (163) and (169) are combined to form $e^{-1} = \pi A C_{D_i}/C_L^2$, then

$$\frac{1}{e} = \frac{1 + \frac{4}{\pi} D_{11} + \sum_{\substack{n=3\\ \text{odd}}}^{N} n\left(\frac{a_n}{a_1}\right)^2 + \sum_{\substack{n=3\\ \text{odd}}}^{N}\left(\frac{4}{\pi} D_{n1} + n\frac{4}{\pi} D_{1n}\right)\frac{a_n}{a_1} + \sum_{\substack{n=3\\ \text{odd}}}^{N}\frac{a_n}{a_1}\sum_{\substack{n^*=3\\ \text{odd}}}^{N}\frac{4}{\pi} D_{nn^*}\frac{a_{n^*}}{a_1}}{\left[1 - \frac{2}{\pi}(1-\cos\gamma)\left(T_1 + \sum_{\substack{n=3\\ \text{odd}}}^{N} T_n \frac{a_n}{a_1}\right)\right]^2} \tag{172}$$

The ratio of equation (170) to (169) leads to

$$C_b = \frac{\frac{1}{3} - \frac{1}{2}(1-\cos\gamma)n_0 T_1 + \sum_{\substack{n=3\\ \text{odd}}}^{N}\left[\frac{(-1)^{\frac{n+1}{2}}}{n^2-1} - \frac{1}{2}(1-\cos\gamma)n_0 T_n\right]\frac{a_n}{a_1}}{\pi\left[1 - \frac{2}{\pi}(1-\cos\gamma)\left(T_1 + \sum_{\substack{n=3\\ \text{odd}}}^{N} T_n \frac{a_n}{a_1}\right)\right]} \tag{173}$$

These induced drag, lift, and bending moment coefficients and aspect ratio are based on the extended span of the planar-wing span plus winglet spans, and on surface area of the planar-wing area plus the winglet areas.

<u>a_n/a_1 coefficients for minimized induced drag for a given lift.</u> - The partial derivative of equation (172) with respect to a_m/a_1 is

$$\frac{\partial(1/e)}{\partial a_m/a_1} = \frac{1}{[1 - \frac{2}{\pi}(1-\cos\gamma)\ (T_1 + \sum_{\substack{n=3 \\ \text{odd}}}^{N} T_n \frac{a_n}{a_1})]^2} \left\{ 2m \frac{a_m}{a_1} + \frac{4}{\pi} D_{m1} + m \frac{4}{\pi} D_{1m} + \sum_{\substack{n=3 \\ \text{odd}}}^{N} \right.$$

$$(m \frac{4}{\pi} D_{nm} + n \frac{4}{\pi} D_{mn}) \frac{a_n}{a_1} + \frac{4}{\pi e}(1 - \cos\gamma)\ T_m [1 - \frac{2}{\pi}(1 - \cos\gamma)$$

$$\left. (T_1 + \sum_{\substack{n=3 \\ \text{odd}}}^{N} T_n \frac{a_n}{a_1})] \right\} \qquad (174)$$

where m = 3, 5, 7, . . .N. The minimization solution is with equation (174) equal to zero. That is, the quantity within the braces in equation (174) must equal zero. Then

$$2m \frac{a_m}{a_1} + \frac{4}{\pi} D_{m1} + m \frac{4}{\pi} D_{1m} + \sum_{\substack{n=3 \\ \text{odd}}}^{N} (m \frac{4}{\pi} D_{nm} + n \frac{4}{\pi} D_{mn}) \frac{a_n}{a_1} + \frac{4}{\pi e}(1 - \cos\gamma)$$

$$T_m [1 - \frac{2}{\pi}(1 - \cos\gamma)\ (T_1 + \sum_{\substack{n=3 \\ \text{odd}}}^{N} T_n \frac{a_n}{a_1})] = 0,\ m=3,5,7,\ldots .N. \qquad (175)$$

Equation (175) involves the solution of (N-1)/2 nonlinear simultaneous equations. It is nonlinear because of e in the last term. A method of solution is to iterate e with estimates for e computed from equation (172), then equation (175) can be solved as linear simultaneous equations. With these new values of a_n/a_1, e is recomputed from equation (172), and the linear solution repeated. A first estimate for 1/e is that for elliptic loading, then $a_n/a_1 = 0$ for $n > 1$. Then from equation (172) for elliptic loading

$$\frac{1}{e} = \frac{1 + \frac{4}{\pi} D_{11}}{[1 - \frac{2}{\pi}(1-\cos\gamma)\ T_1]^2} \qquad (176)$$

a_n/a_1 coefficients for minimized induced drag and wing root bending moment. - For this minimization process, equation (76) must be satisfied, thus

$$\frac{\partial(1/e)}{\partial(a_m/a_1)} + \frac{1}{eC_b}\frac{\partial C_b}{\partial(a_m/a_1)} = 0 \tag{177}$$

where the first term is given in equation (174). The partial derivative of equation (173) with respect to a_m/a_1, inserted into equation (177) leads to

$$2m\frac{a_m}{a_1} + \frac{4}{\pi}D_{m1} + m\frac{4}{\pi}D_{1m} + \sum_{\substack{n=3\\ \text{odd}}}^{N}\left(m\frac{4}{\pi}D_{nm} + n\frac{4}{\pi}D_{mn}\right)\frac{a_n}{a_1} + \frac{4}{\pi e}(1-\cos\gamma)T_m$$

$$\left[1 - \frac{2}{\pi}(1-\cos\gamma)\left(T_1 + \sum_{\substack{n=3\\ \text{odd}}}^{N}T_n\frac{a_n}{a_1}\right)\right] + 8t\left(\left[\frac{(-1)^{\frac{m+1}{2}}}{m^2-4} - \frac{1}{2}(1-\cos\gamma)T_m\right.\right.$$

$$\cos\phi_0\left]\left[1 - \frac{2}{\pi}(1-\cos\gamma)\left(T_1 + \sum_{\substack{n=3\\ \text{odd}}}^{N}T_n\frac{a_n}{a_1}\right)\right] + \frac{2}{\pi}(1-\cos\gamma)T_m\left\{\frac{1}{3} - \frac{1}{2}\right.\right.$$

$$\left.\left.\left.(1-\cos\gamma)T_1\cos\phi_0 + \sum_{\substack{n=3\\ \text{odd}}}^{N}\left[\frac{(-1)^{\frac{n+1}{2}}}{n^2-4} - \frac{1}{2}(1-\cos\gamma)T_n\cos\phi_0\right]\frac{a_n}{a_1}\right\}\right) = 0$$

$$m = 3, 5, 7, \ldots N \tag{178}$$

where t is a constant similar to that developed in equation (20). The solution of equation (178) with respect to a_n/a_1 is the same as that of equation (175), but with the addition of the t term to the linear solution as e is iterated.

Example numerical solution with $\phi_0 = 5\pi/32$. - With the D_{nn*} for $\gamma = 90°$, and T_n, of tables 13 and 14, inserted into equation (175), this equation simplifies to the numerical form, for m = 3, 5, and 7

$$\left.\begin{aligned} .001665 + 2.821910\,\frac{a_3}{a_1} - .166305\,\frac{a_5}{a_1} - .016025\,\frac{a_7}{a_1} + .117625\,\frac{E}{e} &= 0 \\ -.002125 - .166305\,\frac{a_3}{a_1} + 4.908620\,\frac{a_5}{a_1} + .099925\,\frac{a_7}{a_1} + .126340\,\frac{E}{e} &= 0 \\ .011935 - .016025\,\frac{a_3}{a_1} + .099925\,\frac{a_5}{a_1} + 7.184340\,\frac{a_7}{a_1} + .076970\,\frac{E}{e} &= 0 \end{aligned}\right\} \quad (179)$$

where

$$E = .952165 - .117625\,\frac{a_3}{a_1} - .126340\,\frac{a_5}{a_1} - .076970\,\frac{a_7}{a_1} \quad (180)$$

Equation (172) becomes

$$\frac{1}{e} = \frac{1}{E^2}\left[1.03335 + .00333\,\frac{a_3}{a_1} - .00425\,\frac{a_5}{a_1} + .02387\,\frac{a_7}{a_1} + 2.82191\,\left(\frac{a_3}{a_1}\right)^2 + 4.90862\,\left(\frac{a_5}{a_1}\right)^2 + 7.18434\,\left(\frac{a_7}{a_1}\right)^2 - .33261\,\frac{a_3}{a_1}\frac{a_5}{a_1} - .03205\,\frac{a_3}{a_1}\frac{a_7}{a_1} + .19985\,\frac{a_5}{a_1}\frac{a_7}{a_1}\right] \quad (181)$$

and equation (173) becomes

$$C_b = \frac{1}{\pi E}\left(.30020 + .11853\,\frac{a_3}{a_1} - .13513\,\frac{a_5}{a_1} - .03109\,\frac{a_7}{a_1}\right) \quad (182)$$

For elliptic loading, equations (176) or (181), and (182) become

$$\frac{1}{e_c} = 1.139785,\ C_{bc} = .100357 \quad (183)$$

A one equation solution is obtained from the first equation of equation (179), starting with the e value of equation (183) and iterating until e converges. Similarly for a two equation solution, but starting with the 1 - eq. solution of e, etc. The converged three through one equation solutions are listed as follows:

	$\frac{1}{e}$	$\frac{a_3}{a_1}$	$\frac{a_5}{a_1}$	$\frac{a_7}{a_1}$	C_b
3 eq. solution	1.127466	-.047592	-.028843	-.012991	.098846
2 eq. solution	1.128776	-.047542	-.029110		.098826
1 eq. solution	1.133285	-.045823			.097987

(184)

The three equation result is an accurate solution for the wing with a winglet at $\phi_0 = 5\pi/32$, or $\eta_0 = .881921$, with $\gamma = 90$ degrees. The loading is given by inserting these a_n/a_1 values into equation (85). This loading is along the span extent of the wing and up the winglet to the winglet tip. The spanwise loading for minimum induced drag for a given lift is inboard from elliptic loading, particularly the loading is substantially less over the winglet as indicated by the negative values of a_n/a_1. Compared with elliptic loading values the minimized solution has a -1.081 percent smaller e^{-1}, and a -1.506 percent smaller C_b. The e^{-1} value of 1.127466 is with C_L, C_{D_i}, and A based on the combined areas and spans of the planar wing and winglet. When based only on the planar wing area and span, this e^{-1} value is multiplied by η_0^2, then $e^{-1} = .876926$. This means that the addition of two 13.39 percent wing semi-span winglets at $\gamma = 90$ degrees, to a planar wing, can reduce e^{-1} from one or larger to .877.

The equations for the minimized induced drag and bending moment solution are given in equation (178). These equations are the same as those of equation (175) but with an addition of a t term. For $\phi_0 = 5\pi/32$, $\gamma = 90$ degrees, the t terms to add to equation (179) are

$$\left.\begin{aligned} &t\left(.592669 - .123477\,\frac{a_5}{a_1} - .051120\,\frac{a_7}{a_1}\right) \\ &t\left(-.362955 + .123477\,\frac{a_3}{a_1} + .025891\,\frac{a_7}{a_1}\right) \\ &t\left(-.025992 + .051120\,\frac{a_3}{a_1} - .025891\,\frac{a_5}{a_1}\right) \end{aligned}\right\} \qquad (185)$$

For t = 1 in equation (185) and adding to equation (179), gives

$$\left.\begin{aligned} .594334 + 2.82191\,\frac{a_3}{a_1} - .289782\,\frac{a_5}{a_1} - .067145\,\frac{a_7}{a_1} + .117625\,\frac{E}{e} &= 0 \\ -.365080 - .042828\,\frac{a_3}{a_1} + 4.90862\,\frac{a_5}{a_1} + .125816\,\frac{a_7}{a_1} + .126340\,\frac{E}{e} &= 0 \\ -.014057 + .035095\,\frac{a_3}{a_1} + .074034\,\frac{a_5}{a_1} + 7.18434\,\frac{a_7}{a_1} + .076970\,\frac{E}{e} &= 0 \end{aligned}\right\} \qquad (186)$$

where E and 1/e are given in equations (180) and (181). In the iteration of e it is simpler to do a one equation solution of equation (186) for the first estimate of e. The three equation iterative solution of equation (186) gives

$$\left.\begin{aligned} &\frac{a_3}{a_1} = -.25932,\ \frac{a_5}{a_1} = .03994,\ \frac{a_7}{a_1} = -.01069 \\ &\frac{1}{e} = 1.2887,\ C_b = .086015 \end{aligned}\right\} \qquad (187)$$

where C_b is determined from equation (182). The spanwise loading is given in equation (85) which with these a_n/a_1 coefficients shows that this loading is strongly inboard of elliptic loading.

Combining equations (183) and (187), the e and C_b ratios are

$$\frac{e_c}{e} = 1.13065,\ \frac{C_b}{C_{bc}} = .85709 \qquad (188)$$

From equations (49) and (50), for the same lift and wing root bending moment

$$\frac{s_e}{s_{ec}} = \frac{C_{bc}}{C_b} = 1.16674 \qquad (189)$$

$$\frac{D_i}{D_{ic}} = \left(\frac{s_{ec}}{s_e}\right)^2 \frac{e_c}{e} = .83058 \qquad (190)$$

where subscript c denotes a configuration with elliptic loading, and s_e is the semispan of the planar wing plus the span length or height of the winglet. Equations (189) and (190) means that for $\phi_0 = 5\pi/32$, $\gamma = 90$ degrees, if the wing with the inboard loading of equation (187), has a span length 16.67 percent longer than the wing of elliptic loading, then the induced drag will be 17 percent less, for the same lift and the same wing root bending moment.

RESULTS AND DISCUSSION

In the present theory, minimization solutions are obtained by expressing the spanwise loading in a Fourier series, determining the induced angle normal to the wake, formulating the induced drag as a series of products of Fourier loading coefficients and induced drag influence coefficients, imposing constraint conditions, then minimizing the constraint conditioned induced drag with respect to the Fourier loading coefficients. This results in a set of unknown Fourier loading coefficients with an equal number of equations. The solution of these simultaneous equations leads to values of the Fourier loading coefficients and thus the loading for minimum induced drag.

Planar Wings

Constraint that either lift or rolling moment is specified. - Example solutions are shown at the beginning of the planar wing chapter. For the constraint that lift is specified the solution is

$$\frac{c_\ell c}{C_L c_{av}} = \frac{4}{\pi} \sin\phi, \; C_{D_i} = \frac{C_L^2}{\pi A}, \; e = 1, \; C_b = \frac{f_1}{4\pi}, \; \eta_{cp} = \frac{4}{3\pi} \tag{191}$$

where $\sin\phi = (1 - \eta^2)^{\frac{1}{2}}$, i.e., elliptic, and f_1 is given in equations (9), (10a), or (36).

For the constraint condition that rolling moment is specified, the solution for a planar wing is

$$\frac{c_\ell c}{C_\ell c_{av}} = \frac{16}{\pi} \sin 2\phi, \; C_{D_i} = \frac{32 C_\ell^2}{\pi A}, \; e_r = 1, \; \eta_{cp} = \frac{3\pi}{16} \tag{192}$$

where $\sin 2\phi = 2\eta(1 - \eta^2)^{\frac{1}{2}}$, and C_ℓ is wing rolling moment coefficient.

Constraints of lift and of wing bending moment about η_b. - The minimization solution in terms of infinite series is presented in equations (21) through (26). The solution is in terms of a constant, t, which governs the quantity of the bending moment constraint. When t is zero the solution simplifies to that of equation (191). An upper limit for t is given in equation (29) at

which point the loading becomes negative at the wing tips when $t > t_1$. Series summation methods are developed in appendix A so that equations (21) through (26) can also be represented in terms of closed functions. In terms of closed functions the planar wing solution of minimized induced drag for a given lift and a given wing bending moment about span station η_b, is presented in equations (30) through (39). For the constraint condition of wing root bending moment, $\eta_b = 0$, then equations (30) through (38) simplify to equations (40) through (44). For $\eta_b = 0$, equation (41) can be written as $t = 6 - 9\pi\eta_{cp}/2$, which substituted into equations (40) and (44), results in a loading function and induced drag function which correlate exactly with those presented in reference 2 which is a wing-root bending moment method. Equations (30) through (39) represent an independent solution as determined by the use of the present minimization theory, and developed originally without knowledge of the previous work of references 1 through 4. In terms of η_b, equations (30) through (39) are unique in the literature.

Numerical values of k, k_1, f_1, and k_0 for various values of η_b are presented in tables 1 and 2. With these constants the loading distribution, spanwise center of pressure, induced angle in the wake, wing bending moment parameter, and induced drag efficiency factor, are given in equations (30), (32), (34), (35) and (38), respectively, for arbitrary values of t. From equation (30) it can be seen that the loading distribution is elliptic loading times the factor, $1 - k_0 t$. With positive values of t, and since in table 2 k_0 is negative inboard and positive outboard on the span, then this optimum loading will be inboard of elliptic loading. The aerodynamic characteristics for specified values of t are given in tables 4 through 8. Greater detail is given in the section 'Numerical values of loading characteristics for various η_b and t'. A measure of the efficiency of wings with inboard loading is to compare induced drag with a wing with elliptic loading having the same lift and same wing bending moment. This is done in the section entitled 'Comparison with Elliptic Loading'. Aerodynamic characteristics ratioed to those of the wing with elliptic loading, for same η_b, are presented in table 9. Corresponding spanwise loadings are given in table 8. In addition the data of tables 4 through 7 contain some comparisons, that is, the C_b^2/e ratios are the same as

D_i/D_{ic}, and $C_{bc}/C_b = b/b_c$.

Tables 10 and 11 contain data for the condition that wing bending moments are equal about the same $y_b = y_{bc}$ span station. Since the elliptic loading span is smaller, then when $y_b = y_{bc}$, the dimensionless coordinates become, $\eta_b > \eta_{bc}$. The smaller η_b favors a higher bending moment which means there must be a larger inboard shift of loading which, in turn, increases induced drag. The induced drag ratios of table 10 are higher than those of table 9 where $\eta_b = \eta_{bc}$. Corresponding spanwise loading coefficients are presented in table 11. When $b/b_c = 1$, the loading is elliptic, that is $4(1-\eta^2)^{1/2}/\pi$. The loading for the asterisk marked lines in table 10 is wingtip zero-slope loading presented at the top of table 8.

Derivation of t for minimal induced drag and wing span. - Shown in the data of table 9 is a relative decrease of induced drag with increase in wing span, for wings with constant lift and constant wing bending moment. A design objective could be to get the smallest induced drag for the least increase in span. That is, to minimize the product of the span ratio and the induced drag ratio. The product of equations (52) and (57) gives, for same η_b

$$\frac{bD_i}{b_c D_{ic}} = \frac{1}{e\,\frac{b}{b_c}} = (1 + kt^2)\left(1 - \frac{k}{f_1}t\right) \tag{193}$$

where e is from equation (38). Equation (193) is minimized by taking the partial derivative with respect to t and equating to zero. This produces

$$t = \frac{f_1}{3k}\left[1 - \left(1 - \frac{3k}{f_1^2}\right)^{1/2}\right] \tag{194}$$

$$\frac{b}{b_c} = \frac{1}{1 - \frac{k}{f_1}t} = \frac{3}{2 + \left(1 - \frac{3k}{f_1^2}\right)^{1/2}} \tag{195}$$

$$\frac{1}{e} = 1 + kt^2 = \frac{2}{3} + \frac{2f_1^2}{9k}\left[1 - \left(1 - \frac{3k}{f_1^2}\right)^{1/2}\right] \tag{196}$$

$$\frac{D_i}{D_{ic}} = \frac{1}{e}\left(\frac{b}{b_c}\right)^{-2} = (1 + kt^2)\left(1 - \frac{k}{f_1}t\right)^2 \qquad (197)$$

Equations (194) through (197) are valid when the span-drag product of equation (193) is minimum, and when both wings have the same η_b.

For the constraint condition of wing-root bending moment, $\eta_b = 0$. Then from equations (36) and (37), or table 1, $k = 2/9$, and $f_1 = 4/3$. Using equations (193) through (197) gives

$$\left.\begin{aligned} &t = .418861 && e = \frac{C_L^2}{\pi A C_{D_i}} = .962475 \\ &\frac{b}{b_c} = 1.075049 && \frac{D_i}{D_{ic}} = .898987, \quad \frac{b\,D_i}{b_c\,D_{ic}} = .966456 \end{aligned}\right\} \qquad (198)$$

Using the above t, the spanwise loading distribution, and η_{cp}, α_w, and C_b, are determined from equations (40), (41), (42), and (43), respectively. The values of equation (198) show that for a wing with the loading of equation (40), with just a 7.5 percent increase in span, a 10.1 percent decrease in induced drag can be realized compared to a wing with elliptic loading, with both wings at same lift and same wing root bending moment.

For the constraint condition of wing bending moment about span station, $\eta_b = .2$, then $k = .176851$, $f_1 = .784747$, which are obtained from equations (36) and (37), or from table 1. Using equations (193) through (197) gives

$$\left.\begin{aligned} &t = .928705 && e = \frac{C_L^2}{\pi A C_{D_i}} = .867654 \\ &\frac{b}{b_c} = 1.264693 && \frac{D_i}{D_{ic}} = .720582, \quad \frac{b\,D_i}{b_c\,D_{ic}} = .911315 \end{aligned}\right\} \qquad (199)$$

Using the above t and η_b, the spanwise loading distribution, and η_{cp}, α_w, and C_b, are determined from equations (30), (32), (34), and (35), respectively. The values of equation (199) show that for a wing with the loading of equation (30), with a 26.47 percent increase in span, a 27.94 percent decrease in induced drag can be realized compared to a wing with elliptic loading, with both wings at

the same lift and wing bending moment about span station $\eta_b = .2 = \eta_{bc}$. Data from table 9 for $\eta_b = .2$ show that with just a 7.5 percent increase in span, a 11.8 percent decrease in induced drag can be realized.

Nonplanar Wings

Example applications of the minimization theory are made to the configurations described as, biplane, wing in ground effect, cruciform wing, V-wing, V-wing in ground effect, and planar-wing winglet. The biplane solution is obtained from equation (74). This equation is valid for a biplane with wings of equal span and same spanwise loading distribution; is independent of stagger; and is only dependent on height between wings or gap since I_{nn*} is a function of ζ. Equation (74) is also valid for the case of a planar wing in ground effect, provided that I_{nm} is substituted by $-I_{nm}$, and that $\zeta = 4h/b$, where h is height from ground. For $\zeta = 1/2$, the solution for minimum induced drag for a given lift, for the biplane, the loading characteristics are those given in equations (84) and (88), which show an outboard shift of loading compared with elliptic. Similarly, for $\zeta = 1/2$, or $h/b = 1/8$, for the wing in ground effect, the loading characteristics are those given in equations (97) and (98), which show an inboard shift of loading compared with elliptic. For $\zeta = 1/2$, the solution for minimum induced drag for a given lift and a given wing root bending moment, for the biplane, the loading characteristics are given in equations (90) through (96), while for the wing in ground effect, in equations (99) through (103). Compared to a wing with elliptic loading, the biplane with a 14.1 percent greater span, has 12.8 percent less induced drag, while the wing in ground effect with 28.6 percent greater span, has 13.6 percent less induced drag.

The minimization theory application to a cruciform wing is similar to that for the biplane. The primary difference is that the induced drag influence coefficient, P_{nn*}, replaces I_{nn*} of the biplane. Minimized induced drag solutions are obtained from either equation (132) or equation (132) plus mtf_m, which are analogous to equations (74) and (77), respectively. The P_{nn*} integrals are evaluated in appendix C.

The analyses for a V-wing is the same as that for the cruciform wing except that the spanwise integrations for the induced velocity influence coefficient

is for half the wing span. The induced drag influence coefficient is denoted by Q_{nn^*}. Minimized induced drag solutions are obtained from either equation (160) or equation (160) plus mtf_m, which equations are analogous to equations (74) and (77) with I_{nn^*}, or equation (132) with P_{nn^*}. When the pointed end of the V-wing touches ground, the vortex sheet plus ground image vorticity resembles in part the cruciform wing (see eq. 161). The solution for the V-wing in ground effect (V-wing apex touching ground) follows the same procedure as that for the V-wing, but with the substitution of $2Q_n - P_n$ for Q_n, and $2Q_{nn^*} - P_{nn^*}$ for Q_{nn^*} in equations (141), (142), (145), and (160). The P_n and P_{nn^*} coefficients, in which $\gamma = 2\Gamma$, are given in appendix C.

The planar-wing winglet configuration influence coefficients are derived in reference 9 and reproduced in the present report in equations (164) through (168) and in table 13. The minimization solution is obtained from equations (175) for a given lift, and (178) for a given lift and a given wing-root bending moment. The numerical solution for $\phi_0 = 5\pi/32$ (winglets starting at $\eta_0 = \pm.88192$) with winglets at right angle to the wing, is presented in equation (184) for the constraint of a given lift. This optimized loading is inboard relative to elliptic loading, particularly the loading is less than elliptical over the winglet. Comparing the same planar wing with and without added winglets, the induced drag is 12.3 percent less for the wing with winglets. The solution with constraints of lift and wing-root bending moment is presented in equation (187). The results show that if a wing-winglet with the optimized inboard loading has a span length 16.7 percent longer than that of the wing-winglet with elliptic loading, then the induced drag will be 17 percent less, for the same lift and wing-root bending moment.

Other Applications of the Analysis

An exact solution for the flow field about a flat vorticity sheet or planar wake is presented in equations (118) and (119). These equations are the vertical velocity or downwash, and lateral velocity or sidewash, induced by a flat vorticity sheet of arbitrary spanwise vorticity or loading distribution. The loading distribution is represented in equation (1) in which the a_n are Fourier loading coefficients which can have arbitrary values. Similarly,

equations (134) and (136) are presented for predicting the normal and tangential induced velocities on a γ-banked plane, induced by a flat vorticity sheet of arbitrary loading distribution.

With equations (118) and (119), the induced velocities can be predicted at any point in space. These equations can thus be used to set up the minimization solution for such configurations as multi-wings, wings in formation flying in arbitrary pattern, and banked wings. The minimization equation for the V-wing in ground effect is given in equation (162). The V-wing with apex at the boundary of an open wind tunnel has an identical solution to the cruciform wing presented in the section Cruciform Wing. The biplane solution is also the solution for wing flying near a wake, that is, over or under a wake which has the same loading distribution as that of the wing. The minimum induced drag solution for a wing under an arbitrarily loaded wake, is obtained by following the procedure in the biplane section. Let the wake loading be

$$G_w = \sum_{n=1}^{\infty} b_n \sin n\phi \tag{200}$$

then

$$\alpha_w = \sum_{n=1}^{\infty} \frac{\sin n\phi}{\sin \phi} n a_n + \sum_{n=1}^{\infty} I_n n b_n \tag{201}$$

With equation (201), 1/e of the wing becomes

$$\frac{1}{e} = \sum_{n=1}^{\infty} n \left(\frac{a_n}{a_1}\right)^2 + 2 \frac{C_{L_w}}{C_L} \sum_{n=1}^{\infty} \frac{a_n}{a_1} \sum_{n^*=1}^{\infty} n^* I_{nn^*} \frac{b_{n^*}}{b_1} \tag{202}$$

The a_n/a_1 coefficients for minimized induced drag are obtained by taking the derivative of 1/e with respect to a_m/a_1, and setting equal to zero. This solution gives

$$\frac{a_n}{a_1} = -\frac{C_{L_w}}{C_L} \frac{1}{n} \sum_{n^*=1}^{\infty} n^* \frac{b_{n^*}}{b_1} I_{nn^*} \tag{203}$$

where the lift coefficient ratio is that of the wake loading to that of the wing. The values of equation (203) in equation (1) give the loading distribution

of the wing with minimum induced drag, flying at a ζ distance above or below a wake which has the loading of equation (200). When the wake loading distribution is elliptic, then $b_n = 0$ for $n > 1$, and equation (203) reduces to

$$\frac{a_n}{a_1} = -\frac{C_{L_w}}{C_L}\,\frac{I_{n1}}{n} \tag{204}$$

which loading is outboard relative to elliptic loading.

The following two sections contain other applications in greater detail.

Flow Field Solution of a Thin Wing Chordwise Vortex Sheet

Two-dimensional thin wing theory and wake theory are in principle the same, differing only by coordinate definitions. In equations (114) and (115), substitute the longitudinal coordinate x for y, γ for $d\Gamma/dy_1$, c for b, and $-u_s(x,z)$ for $v_s(y,z)$. Then

$$w_s(x,z) = \frac{1}{2\pi}\int_0^c \frac{(x-x_1)\,\gamma\,dx_1}{(x-x_1)^2 + Z^2} \tag{205}$$

$$u_s(x,z) = \frac{Z}{2\pi}\int_0^c \frac{\gamma\,dx_1}{(x-x_1)^2 + Z^2} \tag{206}$$

where γ is circulation per unit length along the wing chord, related to total circulation and local lift coefficient by

$$\frac{\Gamma}{cV} = \int_0^1 \frac{\gamma}{V}\,d\,\frac{x}{c} = \frac{C_l}{2} \tag{207}$$

In terms of dimensionless coordinates, chordwise trigonometric coordinates, and chordwise loading represented by a cotangent term plus Fourier series, define

$$\frac{x}{c} = \zeta = \frac{1}{2}(1 - \cos\theta),\ \frac{z}{c} = \Omega \tag{208}$$

$$\frac{\gamma}{V} = -\frac{\Delta p}{2q} = -\frac{1}{2}\Delta C_p = 2A_0 \cot\frac{\theta}{2} + 2\sum_{n=1}^{\infty} A_n \sin n\theta \tag{209}$$

With equations (208) and (209), equation (205) becomes

$$\frac{w_s(\xi,\Omega)}{V} = \frac{1}{\pi}\int_0^{\pi} \frac{[\cos\theta_1-(1-2\xi)]\left\{A_0(1+\cos\theta_1)+\frac{1}{2}\sum_{n=1}^{\infty} A_n[\cos(n-1)\theta_1-\cos(n+1)\theta_1]\right\}d\theta_1}{[\cos\theta_1-(1-2\xi)]^2+4\Omega^2} \tag{210}$$

These integrals compare with the integrals of equations (67) or (B1), then

$$\frac{w_s(\xi,\Omega)}{V} = A_0\,(I_0 + I_1) + \frac{1}{2}\sum_{n=1}^{\infty} A_n\,(I_{n-1} - I_{n+1}) \tag{211}$$

where $I_n = I_n\,(1 - 2\xi,\ 2\Omega)$. By a similar derivation, noting correspondence with the J_n integral of equation (B12), equation (206) becomes

$$\frac{u_s(\xi,\Omega)}{V} = 2\,[A_0\,(J_0 + J_1) + \frac{1}{2}\sum_{n=1}^{\infty} A_n\,(J_{n-1} - J_{n+1})]\Omega \tag{212}$$

where $J_n = J_n\,(1 - 2\xi\ ,\ 2\Omega)$. These I_n and J_n induced velocity influence coefficients are evaluated by substituting

$$\eta = 1 - 2\xi, \qquad \text{and } \zeta = 2\Omega \tag{213}$$

into equations (B7) through (B11), and into equations (B13), (B14) and (B18) through (B20). With these η and ζ substitutions the p and r values of I_n and J_n becomes (from eq. B11)

$$p = 4(\xi^2 + \Omega^2), \quad r = 4[(1 - \xi)^2 + \Omega^2] \tag{214}$$

The dimensionless coordinate ξ is measured from the leading edge of the chordwise vortex sheet, and Ω is measured from the sheet.

Equations (211) and (212) represent an exact analytical solution for induced downwash and induced longitudinal velocity, due to arbitrary chordwise loading as represented in equation (209). The total longitudinal velocity is

$$\frac{U}{V} = 1 + \frac{u_s(\xi,\Omega)}{V} \tag{215}$$

where V is freestream velocity.

Formation Flying of Wings with Wingtips Linked

The objective is to link wings together and determine the spanwise loading such that induced drag is minimum with the constraint conditions that the bending moments at the wing connections be zero. This is because the term linked here means hinged and cannot support a bending moment. A three wing symmetrical combination shown here, has wings spanning the distances -1 to $-\eta_b$, $-\eta_b$ to η_b, and η_b to 1. The constraint condition when no lift transfers through the link is that the center of pressure of the outer wing loading, η_{cpb}, be at the midpoint of the η_b to 1 span.

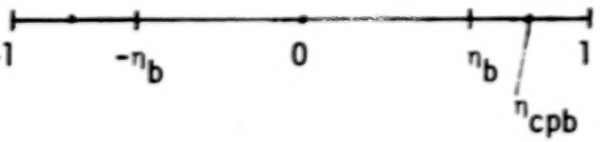

The minimization of induced drag for a given lift and wing bending moment has already been developed in the present planar wing chapter. These results are valid for an arbitrary value of t. For this linked wing problem, t must be determined such that the constraint condition on η_{cpb} is satisfied. The span position, η_{cpb}, is the sum of η_b and the ratio of bending moment about η_b, to wing lift from η_b to 1. Then

$$\eta_{cpb} = \eta_b + \frac{2C_b}{L_b/L} \tag{216}$$

where L_b/L is the fraction of lift of the outer wing compared to the total lift of all the wings. Using the relation $a_n/a_1 = -tf_n$ from equation (20), this ratio is

$$\frac{L_b}{L} = \frac{\int_{\eta_b}^{1} G d\eta}{\int_{-1}^{1} G d\eta} = \frac{1}{\pi}\left(h_1 - t \sum_{\substack{n=3 \\ \text{odd}}}^{\infty} h_n f_n\right) \tag{217}$$

where

$$h_1 = \phi_b - \sin\phi_b \cos\phi_b, \quad \phi_b = \cos^{-1}\eta_b \tag{218}$$

$$h_n = \frac{\sin(n-1)\phi_b}{n-1} - \frac{\sin(n+1)\phi_b}{n+1} \tag{219}$$

The constraint condition is that $\eta_{cpb} = (1 + \eta_b)/2$. Then equation (216), with equation (24) for C_b, and equation (217), leads to

$$t = \frac{f_1 - (1 - \eta_b)\, h_1}{k - (1 - \eta_b) \sum_{\substack{n = 3 \\ \text{odd}}}^{\infty} h_n f_n} \tag{220}$$

where f_1, f_n, and k are in equations (9), (10), and (37), respectively, or in tables 1 and 3.

Equation (220) represents the minimized induced drag solution for three symmetrically linked wings with arbitrary outer wing span. With t determined for a given η_b, the three-wing aerodynamic characteristics are evaluated from equations (30) through (38), and the lift ratio from equation (217). In the three-wing problem when lift is able or allowed to transfer through the links, then η_{cpb} can be reduced until the net three-wing optimum loading is elliptical and net e is unity.

For the case of $\eta_b = 0$, the solution reduces to a linked two-wing configuration. When $\eta_b = 0$, then $k = 2/9$, $k_1 = 1/6$, $f_1 = 4/3$, $h_1 = \pi/2$, $h_n = 0$ for $n > 1$, and equation (220) becomes

$$t = -\frac{3}{4}(3\pi - 8) = -1.068583 \tag{221}$$

then the two-wing aerodynamic characteristics from equations (40) through (44), and (217) become

$$\left.\begin{aligned} &\frac{c_\ell c}{C_L c_{av}} = \frac{3}{\pi}\left[(4 - \pi)(1 - \eta^2)^{\frac{1}{2}} + (3\pi - 8)\eta^2 \cosh^{-1}\frac{1}{|\eta|}\right] \\ &\eta_{cp} = \frac{1}{2} \qquad\qquad C_b = \frac{1}{8} \\ &\frac{\pi A}{2C_L}\alpha_w = -(3\pi - 9) + \frac{3\pi}{4}(3\pi - 8)|\eta| \qquad e = \left[1 + \frac{1}{8}(3\pi - 8)^2\right]^{-1} = .79761 \\ &\qquad = -.42478 + 3.35705|\eta| \qquad\qquad \frac{L_b}{L} = \frac{1}{2} \end{aligned}\right\} \tag{222}$$

Thus, two equal wings flying linked together with the optimal net spanwise loading in equation (222), with no rolling moments will have 0.6269 as much

induced drag as when the wings are flying separately with elliptic loading.

CONCLUSIONS

An analytical minimization theory has been developed which is applicable to complex aircraft nonplanar configurations, with simple or complex constraint conditions. The application of the theory to many configurations and flow conditions have proven to be not excessively complicated and show that the analyses remain mathematically manageable and viable. This is because the solution method is based on a Fourier series representation which, in effect, breaks up ultra complex expressions into a sequence of analytically workable terms. The solution remains analytically exact since a Fourier series can be carried out to convergence, or final terms can be summed. In the planar wing minimization solution, the spanwise loading distribution is determined for which the induced drag is minimum for a given lift and wing bending moment about a given span station. The planar wing solution aerodynamic characteristics are given in equations (30) through (38). These equations are unique. They also provide the solution for three wingtip-linked wings. Minimization solutions are made for nonplanar type configurations. These show the optimum spanwise loading for different constraint conditions. In many cases the reduction of induced drag can be substantial, particularly with either the constraint of wing bending moment, ground effect, or formation flying. Some of the solutions show marginal reductions in induced drag, relative to that due to elliptic loading, but do provide the analytical loading for the minimum.

For two of the simplified cases or conditions, previous theoretical solutions had been obtained by different analyses, which compare exactly with the present results. These include the planar wing with constraints of lift and wing-root bending moment ($\eta_b = 0$), and the flow field of a planar vorticity sheet with elliptic loading distribution. This minimization theory has proved to be a useful analytical tool for obtaining the exemplary minimization solutions in the present report. The method can be applied to many other problems of interest, such as, complex aircraft configurations, wings with arbitrary number of structural or performance constraint conditions, and optimized pattern for wings in flying formation.

Vought Corporation Hampton Technical Center
Hampton, Virginia 23666
January 22, 1979

APPENDIX A

MATHEMATICS OF TRIGONOMETRIC SUMMATIONS

Algebraic Series

Need to evaluate series summations of series with terms of the type

$$\frac{Z^n}{n\,(n+a)\,(n+b)\,\ldots\,(n+m)} \tag{A1}$$

where n are odd numbered integers and m are arbitrary numbers. This family of infinite series begins with the series of $\tanh^{-1}Z$, thus

$$\tanh^{-1}Z = \tfrac{1}{2}\ln\frac{1+Z}{1-Z} = Z + \frac{Z^3}{3} + \frac{Z^5}{5} + \ldots = Z + \sum_{\substack{n=3\\ \text{odd}}}^{\infty}\frac{Z^n}{n}$$

then

$$\sum_{\substack{n=3\\ \text{odd}}}^{\infty}\frac{Z^{n+a}}{n} = -Z^{a+1} + Z^a\tanh^{-1}Z \tag{A2}$$

Similarly

$$\tan^{-1}Z = Z - \frac{Z^3}{3} + \frac{Z^5}{5} - \ldots = Z + \sum_{\substack{n=3\\ \text{odd}}}^{\infty}\frac{(-1)^{\frac{n-1}{2}}Z^n}{n}$$

then

$$\sum_{\substack{n=3\\ \text{odd}}}^{\infty}\frac{(-1)^{\frac{n-1}{2}}Z^{n+a}}{n} = -Z^{a+1} + Z^a\tan^{-1}Z \tag{A3}$$

The $1/n(n+a)$ terms summation is obtained by dividing equations (A2) and (A3) by Z, then integrating from 0 to Z, thus

$$\sum_{\substack{n=3 \\ \text{odd}}}^{\infty} \frac{Z^{n+a+b}}{n(n+a)} = \left[- \frac{Z^{a+b+1}}{a+1} + \frac{Z^{a+b}}{a} \tanh^{-1} Z - \frac{Z^b}{a} \int \frac{Z^a}{1 - Z^2} \, dZ \right]_0^Z ,$$

$a \neq 0 \neq -$ (odd integers) (A4)

$$\sum_{\substack{n=3 \\ \text{odd}}}^{\infty} \frac{Z^{n+b}}{n^2} = \left[-Z^{b+1} + Z^b \int \frac{\tanh^{-1} Z}{Z} \, dZ \right]_0^Z , \; a = 0 \qquad \text{(A5)}$$

$$\sum_{\substack{n=3 \\ \text{odd}}}^{\infty} \frac{Z^{n+b}}{n(n-1)} = Z^{b+1} - \frac{Z^b}{2} (1 + Z) \ln (1 + Z) + \frac{Z^b}{2} (1 - Z) \ln (1 - Z),$$

$a = -1$ (A6)

$$\sum_{\substack{n=3 \\ \text{odd}}}^{\infty} \frac{(-1)^{\frac{n-1}{2}} Z^{n+a+b}}{n(n+a)} = \left[- \frac{Z^{a+b+1}}{a+1} + \frac{Z^{a+b}}{a} \tan^{-1} Z - \frac{Z^b}{a} \int \frac{Z^a \, dZ}{1 + Z^2} \right]_0^Z ,$$

$a \neq 0 \neq -$ (odd integers) (A7)

$$\sum_{\substack{n=3 \\ \text{odd}}}^{\infty} \frac{(-1)^{\frac{n-1}{2}} Z^{n+b}}{n^2} = \left[-Z^{b+1} + Z^b \int \frac{\tan^{-1} Z}{Z} \, dZ \right]_0^Z , \; a = 0 \qquad \text{(A8)}$$

$$\sum_{\substack{n=3 \\ \text{odd}}}^{\infty} \frac{(-1)^{\frac{n-1}{2}} Z^{n+b}}{n(n-1)} = Z^{b+1} - Z^b \tan^{-1} Z - \frac{Z^{b+1}}{2} \ln (1 + Z^2),$$

$a = -1$ (A9)

Apply equations (A4) and (A7) for various values of a, leads to

$$\sum_{\substack{n=3 \\ \text{odd}}}^{\infty} \frac{Z^{n+b}}{n(n+1)} = -\frac{Z^{b+1}}{2} + \frac{Z^{b-1}}{2}(1+Z)\ln(1+Z) + \frac{Z^{b-1}}{2}$$

$$(1-Z)\ln(1-Z) \tag{A10}$$

$$\sum_{\substack{n=3 \\ \text{odd}}}^{\infty} \frac{Z^{n+b}}{n(n+2)} = \frac{Z^{b-1}}{2} - \frac{Z^{b+1}}{3} - \frac{Z^{b-2}}{2}(1-Z^2)\tanh^{-1}Z \tag{A11}$$

$$\sum_{\substack{n=3 \\ \text{odd}}}^{\infty} \frac{Z^{n+b}}{n(n-2)} = \frac{Z^{b+1}}{2} - \frac{Z^{b}}{2}(1-Z^2)\tanh^{-1}Z \tag{A12}$$

$$\sum_{\substack{n=3 \\ \text{odd}}}^{\infty} \frac{(-1)^{\frac{n-1}{2}} Z^{n+b}}{n(n+1)} = -\frac{Z^{b+1}}{2} + Z^{b}\tan^{-1}Z - \frac{Z^{b-1}}{2}\ln(1+Z^2) \tag{A13}$$

$$\sum_{\substack{n=3 \\ \text{odd}}}^{\infty} \frac{(-1)^{\frac{n-1}{2}} Z^{n+b}}{n(n+2)} = -\frac{Z^{b-1}}{2} - \frac{Z^{b+1}}{3} + \frac{Z^{b-2}}{2}(1+Z^2)\tan^{-1}Z \tag{A14}$$

$$\sum_{\substack{n=3 \\ \text{odd}}}^{\infty} \frac{(-1)^{\frac{n-1}{2}} Z^{n+b}}{n(n-2)} = \frac{Z^{b+1}}{2} - \frac{Z^{b}}{2}(1+Z^2)\tan^{-1}Z \tag{A15}$$

In equations (A6), (A9), (A10), and (A13), let b = 0 then taking derivatives with respect to Z leads to

$$\sum_{\substack{n=3 \\ \text{odd}}}^{\infty} \frac{Z^{n+b}}{n-1} = -\frac{Z^{b+1}}{2}\ln(1-Z^2) \tag{A16}$$

$$\sum_{\substack{n=3 \\ \text{odd}}}^{\infty} \frac{Z^{n+b}}{n+1} = -\frac{Z^{b+1}}{2} - \frac{Z^{b-1}}{2}\ln(1-Z^2) \tag{A17}$$

$$\sum_{\substack{n=3 \\ \text{odd}}}^{\infty} \frac{(-1)^{\frac{n-1}{2}} Z^{n+b}}{n-1} = -\frac{Z^{b+1}}{2} \ln (1 + Z^2) \tag{A18}$$

$$\sum_{\substack{n=3 \\ \text{odd}}}^{\infty} \frac{(-1)^{\frac{n-1}{2}} Z^{n+b}}{n+1} = -\frac{Z^{b+1}}{2} + \frac{Z^{b-1}}{2} \ln (1 + Z^2) \tag{A19}$$

Extension of equation (A2) leads to the two summations

$$\sum_{\substack{n=3 \\ \text{odd}}}^{\infty} \frac{Z^{n+b}}{n+2} = -\frac{Z^{b+1}}{3} - Z^{b-1} + Z^{b-2} \tanh^{-1} Z \tag{A20}$$

$$\sum_{\substack{n=3 \\ \text{odd}}}^{\infty} \frac{Z^{n+b}}{n-2} = Z^{b+2} \tanh^{-1} Z \tag{A21}$$

The integrations of equations (A4), (A6), (A7), and (A9) result in the following summations where a and b have values such that no denominator vanishes:

$$\sum_{\substack{n=3 \\ \text{odd}}}^{\infty} \frac{Z^{n+a+b+c}}{n(n+a)(n+a+b)} = \left[-\frac{Z^{a+b+c+1}}{(a+1)(a+b+1)} + \frac{Z^{a+b+c}}{a(a+b)} \tanh^{-1} Z - \right.$$

$$\left. \frac{Z^c}{a(a+b)} \int \frac{Z^{a+b}\, dZ}{1-Z^2} - \frac{Z^c}{a} \int Z^{b-1} \left(\int \frac{Z^a}{1-Z^2}\, dZ \right) dZ \right]_0^Z \tag{A22}$$

$$\sum_{\substack{n=3 \\ \text{odd}}}^{\infty} \frac{Z^{n+b+c}}{n(n-1)(n+b)} = \left[\frac{b+2}{(b+1)^2} Z^{b+c+1} - \frac{Z^{b+c}}{b} \tanh^{-1} Z - \frac{Z^{b+c+1}}{2(b+1)} \right.$$

$$\left. \ln (1 - Z^2) + \frac{Z^c}{b(b+1)} \int \frac{Z^b}{1-Z^2}\, dZ \right]_0^Z \tag{A23}$$

$$\sum_{\substack{n=3 \\ \text{odd}}}^{\infty} \frac{Z^{n+c}}{n(n-1)^2} = \left[\frac{Z^c}{2} (1 + Z) \ln (1 + Z) - \frac{Z^c}{2} (1 - Z) \ln (1 - Z) - \frac{Z^{c+1}}{2} \int \frac{\ln (1-Z^2)}{Z} dZ \right]_0^Z \tag{A24}$$

$$\sum_{\substack{n=3 \\ \text{odd}}}^{\infty} \frac{(-1)^{\frac{n-1}{2}} Z^{n+a+b+c}}{n(n+a)(n+a+b)} = \left[- \frac{Z^{a+b+c+1}}{(a+1)(a+b+1)} + \frac{Z^{a+b+c}}{a(a+b)} \tan^{-1} Z - \frac{Z^c}{a(a+b)} \int \frac{Z^{a+b}}{1+Z^2} dZ - \frac{Z^c}{a} \int Z^{b-1} \left(\int \frac{Z^a \, dZ}{1+Z^2} \right) dZ \right]_0^Z \tag{A25}$$

$$\sum_{\substack{n=3 \\ \text{odd}}}^{\infty} \frac{(-1)^{\frac{n-1}{2}} Z^{n+b+c}}{n(n-1)(n+b)} = \left[\frac{b+2}{(b+1)^2} Z^{b+c+1} - \frac{Z^{b+c}}{b} \tan^{-1} Z - \frac{Z^{b+c+1}}{2(b+1)} \ln (1 + Z^2) + \frac{Z^c}{b(b+1)} \int \frac{Z^b}{1+Z^2} dZ \right]_0^Z \tag{A26}$$

$$\sum_{\substack{n=3 \\ \text{odd}}}^{\infty} \frac{(-1)^{\frac{n-1}{2}} Z^{n+b}}{n(n-1)^2} = \left[Z^{b+1} \ln Z - Z^{b+1} \int \frac{\tan^{-1} Z}{Z} dZ - \frac{Z^{b+1}}{2} \int \frac{\ln (1+Z^2)}{Z} dZ \right]_0^Z \tag{A27}$$

Series of the type given in equations (A22) through (A27) can be determined by using these equations or by solution with partial fractions. Thus to evaluate the example

$$\sum_{\substack{n=3 \\ \text{odd}}}^{\infty} \frac{Z^{n+1}}{n(n-2)(n+1)}$$

then in equation (A22), a = -2, b = 3, c = 0, hence the summation is

$$\left[\frac{Z^2}{2} - \frac{Z}{2} \tanh^{-1} Z + \tfrac{1}{2} \int \frac{Z\, dZ}{1-Z^2} + \tfrac{1}{2} \int Z^2 \left(\int \frac{dZ}{Z^2(1-Z^2)} \right) dZ \right]_0^Z$$

thus

$$\sum_{\substack{n=3 \\ \text{odd}}}^{\infty} \frac{Z^{n+1}}{n(n-2)(n+1)} = \frac{Z^2}{3} - \frac{1-Z}{6} \left(1 - \frac{Z}{2} - \frac{Z^2}{2}\right) \ln (1 - Z) -$$

$$\frac{1+Z}{6} \left(1 + \frac{Z}{2} - \frac{Z^2}{2}\right) \ln (1 + Z) \qquad \text{(A28)}$$

By partial fractions,

$$\frac{1}{n(n-2)(n+1)} = \frac{1}{3n(n-2)} - \frac{1}{3n(n+1)}$$

then the summation is 1/3 of the difference between equations (A12) and (A10), and equals that given in equation (A28).

Trigonometric Series

The trigonometric series can be obtained from the algebraic series by letting Z be a complex function. That is

$$\left.\begin{aligned} Z &= e^{i\phi} = \cos\phi + i \sin\phi \\ Z^n &= e^{in\phi} = \cos n\phi + i \sin n\phi \end{aligned}\right\} \qquad \text{(A29)}$$

thus the cosine series is the real part and the sine series the imaginary part of the algebraic series. The real and the imaginary part of the functions in the algebraic series are listed as follows where absolute values are taken in the log terms:

$$\left.\begin{aligned}
&\ln (1 + Z) = \ln 2 \cos \tfrac{\phi}{2} + i \tfrac{\phi}{2} \\
&\ln (1 - Z) = \ln 2 \sin \tfrac{\phi}{2} + i \left(-\tfrac{\pi\phi}{2|\phi|} + \tfrac{\phi}{2}\right) \\
&\ln (1 + Z^2) = \ln 2 \cos\phi + i \phi \\
&\ln (1 - Z^2) = \ln 2 \sin\phi + i \left(-\tfrac{\pi\phi}{2|\phi|} + \phi\right) \\
&\tanh^{-1} Z = \tfrac{1}{2} \tanh^{-1} \cos\phi + i \tfrac{\pi\phi}{4|\phi|} \\
&\tan^{-1} Z = \tfrac{\pi\phi}{4|\phi|} + i \tfrac{1}{2} \tanh^{-1} \sin\phi
\end{aligned}\right\} \qquad \text{(A30)}$$

In addition since $dZ/Z = id\phi$, then with equation (A30)

$$\int \frac{\tanh^{-1} Z}{Z}\, dZ = -\frac{\pi}{4}\phi + i\left[\frac{\phi}{2}(\ln 2 + 1 - \ln\phi) - \tfrac{1}{2} \sum_{m=1}^{\infty} \frac{(2^{2m-1} - 1) B_m}{m(2m+1)!}\right.$$

$$\left.\phi^{2m+1}\right] \qquad \text{(A31)}$$

where B_m are Bernoulli's numbers, 1/6, 1/30, 1/42, 1/30, 5/66, 691/2730, 7/6, . .

$$\int \frac{\tan^{-1} Z}{Z}\, dZ = \tfrac{1}{2}\left(\tfrac{\pi}{2} - \phi\right)\left[\ln 2 + 1 - \ln\left(\tfrac{\pi}{2} - \phi\right)\right] - \tfrac{1}{2} \sum_{m=1}^{\infty} \frac{(2^{2m-1} - 1) B_m}{m(2m+1)!} \qquad \text{(A32)}$$

$$\left(\tfrac{\pi}{2} - \phi\right)^{2m+1} + i\tfrac{\pi}{4}\phi$$

$$\int \frac{\ln (1+Z^2)}{Z} dZ = -\frac{\phi^2}{2} + i[\phi \ln 2 - \sum_{m=1}^{\infty} \frac{2^{2m-1} (2^{2m} - 1) B_m}{m(2m+1)!} \phi^{2m+1}] \quad (A33)$$

$$\int \frac{\ln (1-Z^2)}{Z} dZ = \tfrac{1}{2} (\pi - \phi) \phi + i [\phi (\ln 2 - 1 + \ln \phi) -$$

$$\sum_{m=1}^{\infty} \frac{2^{2m-1} B_m}{m(2m+1)!} \phi^{2m+1}] \quad (A34)$$

Bernoulli's number is related to the Zeta function by the relation

$$B_n = \frac{\pi(2m)!}{2^{2m-1} \pi^{2m+1}} \zeta(2m) \quad (A35)$$

where $\zeta(2m)$ is the Zeta function given by

$$\zeta(2m) = \sum_{k=1}^{\infty} \frac{1}{k^{2m}} \quad (A36)$$

For m = 1, 2, 3, $\zeta(2m) = \pi 2/6, \pi 4/90, \pi 6/945$, respectively. With equations (A35) and (A36)

$$\sum_{m=1}^{\infty} \frac{2^{2m-1} B_m}{m(2m+1)!} \phi^{2m+1} = \sum_{m=1}^{\infty} \frac{\zeta(2m)}{m(2m+1)} (\frac{\phi}{\pi})^{2m+1} = \sum_{k=1}^{\infty} \sum_{m=1}^{\infty} \frac{1}{m(2m+1)}$$

$$(\frac{\phi}{\pi k})^{2m+1} \quad (A37)$$

By partial fractions, $1/m(2m+1) = 1/m - 2/(2m+1)$, then the m-summation of equation (A37) is

$$\frac{2\phi}{\pi k} - 2 \tanh^{-1} \frac{\phi}{\pi k} - \frac{\phi}{\pi k} \ln [1 - (\frac{\phi}{\pi k})^2]$$

, also

$$\sum_{k=1}^{\infty} \ln\left[1 - \left(\frac{\phi}{\pi k}\right)^2\right] = \ln \sin \phi - \ln \phi$$

thus the summation term of equation (A34) simplifies to

$$\sum_{m=1}^{\infty} \frac{2^{2m-1} B_m}{m(2m+1)!} \phi^{2m+1} = -\int \ln \sin \phi \, d\phi + \phi - \phi \ln \phi$$

$$= \phi \ln \phi - \phi \ln \sin \phi + \sum_{k=1}^{\infty} 2\pi \left(\frac{\phi}{\pi} - k \tanh^{-1} \frac{\phi}{\pi k}\right) \quad \text{(A38)}$$

Similarly, the summation terms of equations (A31), (A32), and (A33) are

$$\sum_{m=1}^{\infty} \frac{(2^{2m-1} - 1) B_m}{m(2m+1)!} \phi^{2m+1} = \phi \ln \frac{4}{\phi} - \phi \ln \frac{2}{\tan \frac{\phi}{2}} - \sum_{k=1}^{\infty} 2\pi \left(\frac{\phi}{\pi} + k \right.$$

$$\left. \tanh^{-1} \frac{\phi}{\pi k} - 4k \tanh^{-1} \frac{\phi}{2\pi k}\right) \quad \text{(A39)}$$

, the summation term of equation (A32) is the same as that of equation (A39) but with $\frac{\pi}{2} - \phi$ replacing ϕ, also

$$\sum_{m=1}^{\infty} \frac{2^{2m-1} (2^{2m} - 1) B_m}{m(2m+1)!} \phi^{2m+1} = \frac{\pi}{2} \sum_{\substack{k=1 \\ \text{odd}}}^{\infty} \left[\frac{4\phi}{\pi} - k\left(1 + \frac{2\phi}{\pi k}\right) \ln \left(1 + \frac{2\phi}{\pi k}\right) + \right.$$

$$\left. k\left(1 - \frac{2\phi}{\pi k}\right) \ln \left(1 - \frac{2\phi}{\pi k}\right)\right] \quad \text{(A40)}$$

Example summations of trigonometric series. - With equations (A21), (A29), and (A30)

$$\sum_{\substack{n=3 \\ \text{odd}}}^{\infty} \frac{Z^{n+b}}{n-2} = Z^{b+2} \tanh^{-1} Z = [\cos (b+2)\,\phi + i \sin (b+2)\,\phi]$$

$$\left(\frac{1}{2} \tanh^{-1} \cos \phi + i \frac{\pi}{4} \frac{\phi}{|\phi|}\right)$$

then since the cosine series is the real part and the sine series the imaginery part

$$\sum_{\substack{n=3 \\ \text{odd}}}^{\infty} \frac{\cos(n+b)\phi}{n-2} = \frac{1}{2} \cos (b+2)\,\phi \tanh^{-1} \cos \phi - \frac{\pi\phi}{4|\phi|} \sin (b+2)\,\phi \qquad \text{(A41)}$$

$$\sum_{\substack{n=3 \\ \text{odd}}}^{\infty} \frac{\sin(n+b)\phi}{n-2} = \frac{1}{2} \sin (b+2)\,\phi \tanh^{-1} \cos \phi + \frac{\pi\phi}{4|\phi|} \cos (b+2)\,\phi \qquad \text{(A42)}$$

where an alternative function for $\tanh^{-1} \cos \phi$ is $-\ln \tan (\phi/2)$.

With equations (A12), (A29), and (A30)

$$\sum_{\substack{n=3 \\ \text{odd}}}^{\infty} \frac{Z^{n+b}}{n(n-2)} = \frac{1}{2} \cos (b+1)\,\phi + \frac{i}{2} \sin (b+1)\,\phi - \frac{1}{2} (\cos b\,\phi + i \sin b\,\phi)$$

$$(1 - \cos 2\,\phi - i \sin 2\,\phi)\left(\frac{1}{2} \tanh^{-1} \cos \phi + i \frac{\pi\phi}{4|\phi|}\right)$$

$$\sum_{\substack{n=3 \\ \text{odd}}}^{\infty} \frac{\cos(n+b)\phi}{n(n-2)} = \frac{\cos(b+1)\phi}{2} - \frac{\sin\phi}{2} [\sin (b+1)\,\phi \tanh^{-1} \cos \phi + \frac{\pi\phi}{2|\phi|}$$

$$\cos (b+1)\,\phi] \qquad \text{(A43)}$$

$$\sum_{\substack{n=3 \\ \text{odd}}}^{\infty} \frac{\sin(n+b)\phi}{n(n-2)} = \frac{\sin(b+1)\phi}{2} + \frac{\sin\phi}{2}\left[\cos\,(b+1)\,\phi\,\tanh^{-1}\cos\,\phi - \frac{\pi\phi}{2|\phi|}\right.$$

$$\left.\sin\,(b+1)\,\phi\right] \qquad \text{(A44)}$$

With equation (A28) divided by $Z^{\frac{1}{2}}$, and equations (A29) and (A30)

$$\sum_{\substack{n=3 \\ \text{odd}}}^{\infty} \frac{Z^{n-\frac{1}{2}}}{n(n-2)(n+1)} = \frac{Z^{\frac{1}{2}}}{3} - \frac{Z^{-\frac{1}{2}} - Z^{\frac{1}{2}}}{6}\left(Z^{-1} - \frac{1}{2} - \frac{Z}{2}\right)\ln\,(1-Z) - \frac{Z^{-\frac{1}{2}} + Z^{\frac{1}{2}}}{6}$$

$$\left(Z^{-1} + \frac{1}{2} - \frac{Z}{2}\right)\ln\,(1+Z)$$

$$= \frac{1}{3}\cos\frac{\phi}{2} - \frac{i}{3}\sin\frac{\phi}{2}\left(\sin^2\frac{\phi}{2} + i\,\frac{3}{2}\sin\phi\right)\left[\ln 2\sin\frac{\phi}{2} + i\right.$$

$$\left.\left(\frac{\phi}{2} - \frac{\pi\phi}{2|\phi|}\right)\right] - \frac{1}{3}\cos\frac{\phi}{2}\left(\cos^2\frac{\phi}{2} - i\,\frac{3}{2}\sin\phi\right)\left[\ln 2\cos\frac{\phi}{2} +\right.$$

$$\left.i\,\frac{\phi}{2}\right] + \frac{i}{3}\sin\frac{\phi}{2}$$

then letting $\phi = \phi/2$, the trigonometric summations become

$$\sum_{\substack{n=3 \\ \text{odd}}}^{\infty} \frac{\cos(2n-1)\phi}{n(n-2)(n+1)} = \frac{\cos\phi}{3} - \frac{\pi\phi}{6|\phi|}\sin^3\phi - \frac{\phi}{3}\sin 3\phi + \sin^2\phi\cos\phi\ln 2$$

$$\sin\phi - \frac{\cos^3\phi}{3}\ln 2\cos\phi \qquad \text{(A45)}$$

$$\sum_{\substack{n=3 \\ \text{odd}}}^{\infty} \frac{\sin(2n-1)\phi}{n(n-2)(n+1)} = \frac{\sin\phi}{3} - \frac{\pi\phi}{2|\phi|}\sin^2\phi\cos\phi - \frac{\phi}{3}\cos 3\phi + \sin\phi\cos^2\phi$$

$$\ln 2\cos\phi - \frac{\sin^3\phi}{3}\ln 2\sin\phi \qquad \text{(A46)}$$

Spanwise Loading Distribution

This loading function is given in equation (21) and contains the summation

$$\sum_{\substack{n=3 \\ \text{odd}}}^{\infty} f_n \sin n\phi \tag{A47}$$

Substituting equation (10) into equation (A47) results in

$$\sum_{\substack{n=3 \\ \text{odd}}}^{\infty} f_n \sin n\phi = \sum_{\substack{n=3 \\ \text{odd}}}^{\infty} \left[\frac{\sin(n-2)\phi_b \sin n\phi}{n(n-2)} - \frac{\sin(n+2)\phi_b \sin n\phi}{n(n+2)} - \right.$$

$$\left. \frac{2\cos\phi_b \sin(n-1)\phi_b \sin n\phi}{n(n-1)} + \frac{2\cos\phi_b \sin(n+1)\phi_b \sin n\phi}{n(n+1)} \right] \tag{A48}$$

The first term within the brackets, by trigonometric identities can be written as

$$\sin(n-2)\phi_b \sin n\phi = \frac{1}{2}\cos[n\phi - (n-2)\phi_b] - \frac{1}{2}\cos[n\phi + (n-2)\phi_b]$$

$$= \frac{1}{2}\cos\psi_+ \cos(n-1)\psi_- + \frac{1}{2}\sin\psi_+ \sin(n-1)\psi_- - \frac{1}{2}\cos\psi_- \cos(n-1)\psi_+$$

$$- \frac{1}{2}\sin\psi_- \sin(n-1)\psi_+ \tag{A49}$$

where ψ_+ and ψ_- are defined as

$$\psi_+ = \psi_b + \phi, \quad \psi_- = \phi_b - \phi \tag{A50}$$

Apply equation (A49) to equations (A43) and (A44) with b = -1, results in

$$\sum_{\substack{n=3 \\ \text{odd}}}^{\infty} \frac{\sin(n-2)\phi_b \sin n\phi}{n(n-2)} = \frac{1}{4}\left[\cos\psi_+ - \cos\psi_- + \frac{\pi}{2}\sin(\psi_+ - |\psi_-|) + \right.$$

$$\left. \sin\psi_+ \sin\psi_- (\tanh^{-1}\cos\psi_- - \tanh^{-1}\cos\psi_+)\right] \qquad \text{(A51)}$$

The second term in equation (A48) is of the form obtained from equation (A11). In trigonometric summation it becomes

$$\sum_{\substack{n=3 \\ \text{odd}}}^{\infty} \frac{\cos(n+b)\phi}{n(n+2)} = \frac{\cos(b-1)\phi}{2} - \frac{\cos(b+1)\phi}{3} - \frac{\sin\phi}{2}\left[\frac{\pi\phi}{2|\phi|}\cos(b-1)\phi + \right.$$

$$\left. \sin(b-1)\phi \tanh^{-1}\cos\phi\right] \qquad \text{(A52)}$$

$$\sum_{\substack{n=3 \\ \text{odd}}}^{\infty} \frac{\sin(n+b)\phi}{n(n+2)} = \frac{\sin(b-1)\phi}{2} - \frac{\sin(b+1)\phi}{3} - \frac{\sin\phi}{2}\left[\frac{\pi\phi}{2|\phi|}\sin(b-1)\phi - \right.$$

$$\left. \cos(b-1)\phi \tanh^{-1}\cos\phi\right] \qquad \text{(A53)}$$

The sine product is expanded as before, but with b = 1, then the second term summation of equation (A48) becomes

$$-\sum_{\substack{n=3 \\ \text{odd}}}^{\infty} \frac{\sin(n+2)\phi_b \sin n\phi}{n(n+2)} = \frac{1}{4}\left[-\cos\psi_+ + \cos\psi_- + \frac{4}{3}\sin\frac{3}{2}(\psi_+ + \psi_-)\right.$$

$$\left. \sin\frac{1}{2}(\psi_+ - \psi_-) - \frac{\pi}{2}\sin(\psi_+ - |\psi_-|) + \sin\psi_+ \sin\psi_- (\tanh^{-1}\cos\psi_- + \right.$$

$$\left. \tanh^{-1}\cos\psi_+)\right] \qquad \text{(A54)}$$

The third term in equation (A48) is of the form of equation (A6), then

$$\sum_{\substack{n=3 \\ \text{odd}}}^{\infty} \frac{\cos(n+b)\phi}{n(n-1)} = \cos\,(b+1)\,\phi - \frac{\pi\phi}{4|\phi|} \sin\frac{\phi}{2} \cos\,(b+\tfrac{1}{2})\,\phi + \frac{\phi}{2} \sin\,(b+1)\,\phi$$

$$-\cos\,(b+\tfrac{1}{2})\,\phi \cos\frac{\phi}{2} \ln 2\cos\frac{\phi}{2} + \sin\,(b+\tfrac{1}{2})\,\phi \sin\frac{\phi}{2} \ln 2\sin\frac{\phi}{2} \qquad \text{(A55)}$$

$$\sum_{\substack{n=3 \\ \text{odd}}}^{\infty} \frac{\sin(b+1)\phi}{n(n-1)} = \sin\,(b+1)\,\phi - \frac{\pi\phi}{2|\phi|} \sin\frac{\phi}{2} \sin\,(b+\tfrac{1}{2})\,\phi - \frac{\phi}{2} \cos\,(b+1)\,\phi$$

$$-\sin\,(b+\tfrac{1}{2})\,\phi \cos\frac{\phi}{2} \ln 2\cos\frac{\phi}{2} - \cos\,(b+\tfrac{1}{2})\,\phi \sin\frac{\phi}{2} \ln 2\sin\frac{\phi}{2} \qquad \text{(A56)}$$

The sine product is expanded in terms of $n - \frac{1}{2}$, then with $b = -\frac{1}{2}$ in equations (A55) and (A56) the third term of equation (A48) becomes

$$-2\cos\phi_b \sum_{\substack{n=3 \\ \text{odd}}}^{\infty} \frac{\sin(n-1)\phi_b \sin n\phi}{n(n-1)} = \frac{\cos\phi_b}{2}\left[\left(\frac{\pi\psi_-}{|\psi_-|} - \psi_- - \psi_+\right) \sin\frac{\psi_-}{2}\right.$$

$$\cos\frac{\psi_+}{2} - (\pi - \psi_- - \psi_+) \sin\frac{\psi_+}{2} \cos\frac{\psi_-}{2} + 2\cos\frac{\psi_+}{2} \cos\frac{\psi_-}{2} \ln\frac{\cos\frac{\psi_-}{2}}{\cos\frac{\psi_+}{2}} -$$

$$\left. 2\sin\frac{\psi_+}{2} \sin\frac{\psi_-}{2} \ln\frac{\sin\frac{\psi_+}{2}}{\sin\frac{\psi_-}{2}}\right] \qquad \text{(A57)}$$

Similarly the fourth term in equation (A48) is developed as

$$2\cos\phi_b \sum_{\substack{n=3 \\ \text{odd}}}^{\infty} \frac{\sin(n+1)\phi_b \sin n\phi}{n(n+1)} = \frac{\cos\phi_b}{2}\left[-2\sin\,(\psi_+ + \psi_-) \sin\tfrac{1}{2}\,(\psi_+ - \psi_-) -\right.$$

$$\left(\frac{\pi\psi_-}{|\psi_-|} - \psi_- - \psi_+\right) \sin\frac{\psi_-}{2} \cos\frac{\psi_+}{2} + (\pi - \psi_- - \psi_+) \sin\frac{\psi_+}{2} \cos\frac{\psi_-}{2} + 2$$

$$\left. \cos\frac{\psi_+}{2} \cos\frac{\psi_-}{2} \ln\frac{\cos\frac{\psi_-}{2}}{\cos\frac{\psi_+}{2}} - 2\sin\frac{\psi_+}{2} \sin\frac{\psi_-}{2} \ln\frac{\sin\frac{\psi_+}{2}}{\sin\frac{\psi_-}{2}}\right] \qquad \text{(A58)}$$

where ϕ_+ and ϕ_- are defined in equation (A50).

The desired summation of equation (A48) is obtained by adding together equations (A51), (A54), (A57), and (A58). Thus

$$\sum_{\substack{n=3 \\ \text{odd}}}^{\infty} f_n \sin n\phi = -\frac{\sin \phi_b}{3}(1 + 2\cos^2 \phi_b) \sin\phi + \frac{1}{2}(\cos \phi_b + \cos \phi)^2$$

$$\tanh^{-1} \frac{\sin \phi_b \sin \phi}{1 + \cos \phi_b \cos \phi} + \frac{1}{2}(\cos \phi_b - \cos \phi)^2 \quad \tanh^{-1}$$

$$\frac{\sin \phi_b \sin \phi}{1 - \cos \phi_b \cos \phi} \tag{A59}$$

where from equations (2) and (6), $\eta = \cos \phi$, $\eta_b = \cos \phi_b$. Using hyperbolic function identities, equation (A59) in terms of η and η_b becomes

$$\sum_{\substack{n=3 \\ \text{odd}}}^{\infty} f_n \sin n\phi = -\frac{1}{3}(1 + 2\eta_b^2)(1 - \eta_b^2)^{\frac{1}{2}}(1 - \eta^2)^{\frac{1}{2}} + \frac{1}{2}(\eta_b + \eta)^2 \cosh^{-1}$$

$$\frac{1+\eta_b \eta}{|\eta_b+\eta|} + \frac{1}{2}(\eta_b - \eta)^2 \cosh^{-1} \frac{1-\eta_b \eta}{|\eta_b-\eta|} \tag{A60}$$

The condition of wing bending moment taken about the midspan is $\eta_b = 0$, then equation (A60) reduces to

$$\sum_{\substack{n=3 \\ \text{odd}}}^{\infty} f_n \sin n\phi = -\frac{1}{3}(1 - \eta^2)^{\frac{1}{2}} + \eta^2 \cosh^{-1} \frac{1}{|\eta|} \tag{A61}$$

When either equation (A59) or (A60) is substituted into equation (21) the loading distribution becomes a closed function for any value of span station η_b about which bending moment is taken.

The k-Factor Summation

Combining equations (26) and (10) results in

$$k = \sum_{\substack{n=3 \\ \text{odd}}}^{\infty} nf_n^2 = \sum_{\substack{n=3 \\ \text{odd}}}^{\infty} \left\{ \frac{\sin^2(n-2)\phi_b}{n(n-2)^2} + \frac{\sin^2(n+2)\phi_b}{n(n+2)^2} - \frac{2\sin(n-2)\phi_b \sin(n+2)\phi_b}{n(n-2)(n+2)} \right.$$

$$4\cos\phi_b \left[- \frac{\sin(n-2)\phi_b \sin(n-1)\phi_b}{n(n-2)(n-1)} - \frac{\sin(n+1)\phi_b \sin(n+2)\phi_b}{n(n+2)(n+1)} + \frac{\sin(n-2)\phi_b \sin(n+1)\phi_b}{n(n-2)(n+1)} \right.$$

$$\left. + \frac{\sin(n-1)\phi_b \sin(n+2)\phi_b}{n(n-1)(n+2)} \right] + 4\cos^2\phi_b \left[- \frac{2\sin(n-1)\phi_b \sin(n+1)\phi_b}{n(n-1)(n+1)} + \frac{\sin^2(n-1)\phi_b}{n(n-1)^2} + \right.$$

$$\left. \left. \frac{\sin^2(n+1)\phi_b}{n(n+1)^2} \right] \right\} \qquad \text{(A62)}$$

The summations are obtained by using equations (A22) through (A24) with the trigonometric relations given in equations (A29) through (A34). An example the sixth term in equation (A62) has the form of the summation example of equation (A45). By trigonometric identity

$$\sin (n - 2)\, \phi_b \sin (n + 1)\, \phi_b = \frac{1}{2} \cos 3\phi_b - \frac{1}{2} \cos (2n - 1)\, \phi_b \qquad \text{(A63)}$$

then the desired summation is $\frac{1}{2} \cos 3\phi_b$ times equation (A45) in which $\phi = 0$, minus $\frac{1}{2}$ times equation (A45) in which $\phi = \phi_b$. Thus

$$\sum_{\substack{n=3 \\ \text{odd}}}^{\infty} \frac{\sin(n-2)\phi_b \sin(n+1)\phi_b}{n(n-2)(n+1)} = \frac{\phi_b}{6} \sin 3\phi_b + \frac{\pi}{12} \sin^3\phi_b - \frac{2}{3} \sin^2\phi_b \cos\phi_b - \frac{1}{2}$$

$$\sin^2\phi_b \cos\phi_b \ln \sin\phi_b + \frac{1}{6} \cos^3\phi_b \ln \cos\phi_b \qquad \text{(A64)}$$

This mathematical procedure is used to develop the other summations of equation (A62). The results are listed as follows:

$$\sum_{\substack{n=3 \\ \text{odd}}}^{\infty} \frac{\sin^2(n-2)\phi_b}{n(n-2)^2} = \frac{\pi}{8}\left(\phi_b - \frac{1}{4}\sin 4\phi_b\right) - \frac{1}{4}\sin^2\phi_b - \frac{1}{2}\sin^2\phi_b\cos^2\phi_b \ln$$

$$\tan\phi_b \tag{A65}$$

$$\sum_{\substack{n=3 \\ \text{odd}}}^{\infty} \frac{\sin^2(n+2)\phi_b}{n(n+2)^2} = -\frac{\pi}{8}\left(\phi_b - \frac{1}{4}\sin 4\phi_b\right) + \frac{1}{4}\sin^2\phi_b - \frac{1}{2}\sin^2\phi_b\cos^2\phi_b \ln$$

$$\tan\phi_b + \frac{7}{36} + \frac{\cos 6\phi_b}{18} - \frac{\cos 2\phi_b}{4} \tag{A66}$$

$$-2\sum_{\substack{n=3 \\ \text{odd}}}^{\infty} \frac{\sin(n-2)\phi_b\sin(n+2)\phi_b}{n(n-2)(n+2)} = -\frac{1}{6}\left(1 - 4\cos^2\phi_b\right)\sin^2\phi_b + \sin^2\phi_b\cos^2\phi_b \ln$$

$$\tan\phi_b \tag{A67}$$

$$-\sum_{\substack{n=3 \\ \text{odd}}}^{\infty} \frac{\sin(n-2)\phi_b\sin(n-1)\phi_b}{n(n-2)(n-1)} + \frac{\sin(n+1)\phi_b\sin(n+2)\phi_b}{n(n+1)(n+2)} = \frac{1}{6}\sin 2\phi_b \sin 3\phi_b +$$

$$\sin^2\phi_b\cos\phi_b \ln\sin\phi_b + \cos^3\phi_b \ln\cos\phi_b \tag{A68}$$

$$\sum_{\substack{n=3 \\ \text{odd}}}^{\infty} \frac{\sin(n-1)\phi_b\sin(n+2)\phi_b}{n(n-1)(n+2)} = -\frac{\phi_b}{6}\sin 3\phi_b - \frac{\pi}{12}\sin^3\phi_b + \frac{1}{2}\sin^2\phi_b\cos\phi_b\left(\frac{2}{3} -$$

$$\ln\sin\phi_b\right) + \frac{1}{6}\cos^3\phi_b \ln\cos\phi_b \tag{A69}$$

$$-2\sum_{\substack{n=3 \\ \text{odd}}}^{\infty} \frac{\sin(n-1)\phi_b\sin(n+1)\phi_b}{n(n-1)(n+1)} = \sin^2\phi_b \ln\sin\phi_b - \cos^2\phi_b \ln\cos\phi_b \tag{A70}$$

$$\sum_{\substack{n=3 \\ \text{odd}}}^{\infty} \frac{\sin^2(n-1)\phi_b}{n(n-1)^2} = -\frac{\phi_b^2}{2} + \frac{\pi}{4}\phi_b - \frac{\pi}{8}\sin 2\phi_b - \frac{1}{2}\sin^2\phi_b \ln \sin\phi_b - \frac{1}{2}$$

$$\cos^2\phi_b \ln \cos\phi_b \qquad \text{(A71)}$$

$$\sum_{\substack{n=3 \\ \text{odd}}}^{\infty} \frac{\sin^2(n+1)\phi_b}{n(n+1)^2} = \frac{\phi_b^2}{2} - \frac{\pi}{4}\phi_b + \frac{\pi}{8}\sin 2\phi_b - \frac{1}{4}\sin^2\phi_b - \frac{1}{2}\sin^2\phi_b \ln \sin\phi_b - \frac{1}{2}$$

$$\cos^2\phi_b \ln \cos\phi_b \qquad \text{(A72)}$$

Then by equation (A62) the k factor is the sum of equations (A65) through (A67), plus 4 $\cos\phi_b$ times the sum of equations (A68), (A64), and (A69), plus 4 $\cos^2\phi_b$ times the sum of equations (A70) through (A72). Thus with an extensive reduction the k factor simplifies to

$$k = \frac{2}{9}(\sin^6\phi_b - 3\sin^2\phi_b \cos^2\phi_b - 6\cos^4\phi_b \ln \cos^2\phi_b) \qquad \text{(A73)}$$

Since $\eta_b = \cos\phi_b$, k can be written as

$$k = \frac{2}{9}(1 - 6\eta_b^2 + 3\eta_b^4 + 2\eta_b^6 - 6\eta_b^4 \ln \eta_b^2) \qquad \text{(A74)}$$

The functional behavior of k as $\eta_b \to 1$ can be assessed by expanding the k factor in terms of $1 - \eta_b$. Then

$$k = \frac{16}{9}(1-\eta_b)^4 \left[1 - \frac{6}{5}(1-\eta_b) + \frac{3}{10}(1-\eta_b)^2 + 36 \sum_{\substack{n=3 \\ \text{odd}}}^{\infty} \frac{(n-1)!(1-\eta_b)^n}{(n+4)!}\right] \qquad \text{(A75)}$$

It can be seen that k decreases rapdily as η_t approaches unity and remains positive. The summation terms are quite small. When an analytical summation of this series is made, equation (A75) converts back to equation (A74).

Spanwise Center of Pressure, η_{cp}

The η_{cp} of the spanwise loading distribution of equation (21) is given in equation (22) which contains the summation

$$-3 \sum_{\substack{n=3 \\ \text{odd}}}^{\infty} \frac{(-1)^{\frac{n-1}{2}}}{n^2-4} f_n = \sum_{\substack{n=3 \\ \text{odd}}}^{\infty} \frac{-3(-1)^{\frac{n-1}{2}}}{n^2-4} \left[\frac{\sin(n-2)\phi_b}{n(n-2)} - \frac{\sin(n+2)\phi_b}{n(n+2)} - \right.$$

$$\left. \frac{2\cos\phi_b \sin(n-1)\phi_b}{n(n-1)} + \frac{2\cos\phi_b \sin(n+1)\phi_b}{n(n+1)} \right] \qquad \text{(A76)}$$

These summations are obtained by expanding the $n^2 - 4$ term in partial fractions, as

$$\frac{-3}{n^2-4} = \frac{3}{4}\left(\frac{-1}{n-2} + \frac{1}{n+2}\right) \qquad \text{(A77)}$$

With equation (A77) the individual summations of equation (A76) appear as those of equations (A25) through (A27), which can be converted to trigonometric series by application of equations (A29) through (A34). The first summation by using equation (A25) with a = -2, b = c = 0, is

$$-\sum_{\substack{n=3 \\ \text{odd}}}^{\infty} \frac{(-1)^{\frac{n-1}{2}} \sin(n-2)\phi_b}{n(n-2)^2} = -\,\text{Imag.}\left(-\frac{1}{4z} + \frac{1}{4}\tan^{-1}z + \frac{1}{4z^2}\tan^{-1}z - \frac{1}{2}\right.$$

$$\left. \int \frac{\tan^{-1}z}{z}\,dz\right) = \frac{\pi}{16}(2\phi_b + \sin 2\phi_b) - \frac{1}{4}\sin\phi_b - \frac{1}{4}\cos^2\phi_b \tanh^{-1}\sin\phi_b \qquad \text{(A78)}$$

The other summations are as follows:

$$\sum_{\substack{n=3 \\ \text{odd}}}^{\infty} \frac{(-1)^{\frac{n-1}{2}} \sin(n-2)\phi_b}{n(n-2)(n+2)} = -\frac{1}{12}\sin\phi_b - \frac{1}{2}\sin\phi_b \cos^2\phi_b + \frac{\pi}{4}\sin\phi_b \cos^3\phi_b -$$

$$\frac{1}{4}\cos^2\phi_b \cos 2\phi_b \tanh^{-1}\sin\phi_b \qquad \text{(A79)}$$

$$\sum_{\substack{n=3 \\ \text{odd}}}^{\infty} \frac{(-1)^{\frac{n-1}{2}} \sin(n+2)\phi_b}{n(n-2)(n+2)} = -\frac{1}{12}\sin\phi_b + \frac{5}{6}\sin\phi_b \cos^2\phi_b - \frac{\pi}{4}\sin\phi_b \cos^3\phi_b -$$

$$\frac{1}{4}\cos^2\phi_b \cos 2\phi_b \tanh^{-1}\sin\phi_b \qquad \text{(A80)}$$

$$-\sum_{\substack{n=3 \\ \text{odd}}}^{\infty} \frac{(-1)^{\frac{n-1}{2}} \sin(n+2)\phi_b}{n(n+2)^2} = -\frac{\pi}{8}\phi_b + \frac{23}{36}\sin\phi_b + \frac{4}{9}\sin\phi_b \cos^2\phi_b - \frac{\pi}{8}\sin\phi_b$$

$$\cos\phi_b - \frac{1}{4}\cos^2\phi_b \tanh^{-1}\sin\phi_b \qquad \text{(A81)}$$

$$\sum_{\substack{n=3 \\ \text{odd}}}^{\infty} \frac{(-1)^{\frac{n-1}{2}} \sin(n-1)\phi_b}{n(n-2)(n-1)} = \frac{\phi_b}{2} - \frac{\pi}{4}\sin\phi_b \qquad \text{(A82)}$$

$$-\sum_{\substack{n=3 \\ \text{odd}}}^{\infty} \frac{(-1)^{\frac{n-1}{2}} \sin(n-1)\phi_b}{n(n-1)(n+2)} = \frac{\phi_b}{6} - \frac{\pi}{12}\sin\phi_b - \frac{\pi}{6}\sin\phi_b \cos^2\phi_b + \frac{1}{3}\sin\phi_b \cos\phi_b +$$

$$\frac{1}{3}\cos^3\phi_b \tanh^{-1}\sin\phi_b \qquad \text{(A83)}$$

$$-\sum_{\substack{n=3 \\ \text{odd}}}^{\infty} \frac{(-1)^{\frac{n-1}{2}} \sin(n+1)\phi_b}{n(n-2)(n+1)} = -\frac{\phi_b}{6} + \frac{\pi}{12}\sin\phi_b + \frac{\pi}{6}\sin\phi_b \cos^2\phi_b - \frac{2}{3}\sin\phi_b$$

$$\cos\phi_b + \frac{1}{3}\cos^2\phi_b \tanh^{-1}\sin\phi_b \qquad \text{(A84)}$$

$$\sum_{\substack{n=3 \\ \text{odd}}}^{\infty} \frac{(-1)^{\frac{n-1}{2}} \sin(n+1)\phi_b}{n(n+1)(n+2)} = -\frac{\phi_b}{2} + \frac{\pi}{4}\sin\phi_b - \frac{1}{3}\sin\phi_b \cos\phi_b \qquad \text{(A85)}$$

The f_n summation term of equation (A76) is 3/4 times the sum of equations (A78) through (A81), plus 1.5 $\cos\phi_b$ times the sum of equations (A82) through (A85). Then, defining k_1 as follows:

$$k_1 = -3 \sum_{\substack{n=3 \\ \text{odd}}}^{\infty} \frac{(-1)^{\frac{n-1}{2}}}{n^2-4} f_n = -\frac{1}{4}\sin\phi_b + \frac{5}{12}\sin^3\phi_b + \frac{1}{4}\cos^4\phi_b \tanh^{-1}\sin\phi_b \qquad \text{(A86)}$$

In terms of $\eta_b = \cos\phi_b$, k_1 is

$$k_1 = \frac{1}{6}\left(1 - \frac{5}{2}\eta_b^2\right)\left(1-\eta_b^2\right)^{\frac{1}{2}} + \frac{1}{4}\eta_b^4 \cosh^{-1}\frac{1}{|\eta_b|} \qquad \text{(A87)}$$

Induced Downwash Angle in the Wake

The equation for induced angle is given in equation (23) which contains the summation

$$- \frac{1}{\sin\phi} \sum_{\substack{n=3 \\ \text{odd}}}^{\infty} nf_n \sin n\phi = \frac{1}{\sin\phi} \sum_{\substack{n=3 \\ \text{odd}}}^{\infty} \left[- \frac{\sin(n-2)\phi_b \sin n\phi}{n-2} + \frac{\sin(n+2)\phi_b \sin n\phi}{n+2} + \right.$$

$$\left. \frac{2\cos\phi_b \sin(n-1)\phi_b \sin n\phi}{n-1} - \frac{2\cos\phi_b \sin(n+1)\phi_b \sin n\phi}{n+1} \right] \qquad \text{(A88)}$$

where f_n is defined in equation (10). By trigonometric identities the general sine product is formulated as

$$\sin (n + c)\phi_b \sin n\phi = \frac{1}{2} \cos c\phi_b \cos n\psi_- - \frac{1}{2} \sin c\phi_b \sin n\psi_- - \frac{1}{2} \cos c\phi_b$$

$$\cos n\psi_+ + \frac{1}{2} \sin c\phi_b \sin n\psi_+ \qquad \text{(A89)}$$

where ψ_- and ψ_+ are defined in equation (A50). With c = -2 in equation (A89), the first summation of equation (A88) can be evaluated by using equations (A41) and (A42) in which b = 0, and ϕ equals ψ_- or ψ_+. Then

$$-\sum_{\substack{n=3 \\ \text{odd}}}^{\infty} \frac{\sin(n-2)\phi_b \sin n\phi}{n-2} = - \frac{\pi}{8} \left(1 + \frac{\psi_-}{|\psi_-|}\right) \sin 2\phi - \frac{1}{4} (\tanh^{-1}\cos\psi_- - \tanh^{-1}$$

$$\cos\psi_+) \cos 2\phi \qquad \text{(A90)}$$

Equation (A20) can be made into trigonmetric series by using the relations of equations (A29) and (A30). Thus

$$\sum_{\substack{n=3 \\ \text{odd}}}^{\infty} \frac{z^{n+b}}{n+2} = - \frac{1}{3} \cos (b + 1)\phi - \cos (b - 1)\phi - \frac{\pi\phi}{4|\phi|} \sin (b - 2)\phi + \frac{1}{2}$$

$$\cos (b - 2)\phi \tanh^{-1} \cos\phi + i \left[- \frac{1}{3} \sin (b + 1)\phi - \sin (b - 1)\phi + \frac{\pi\phi}{4|\phi|} \right.$$

$$\left. \cos (b - 2)\phi + \frac{1}{2} \sin (b - 2)\phi \tanh^{-1} \cos\phi \right] \qquad \text{(A91)}$$

where the summations of cos (n + b)ϕ and sin (n + b)ϕ are given by the real part and the imaginary part, respectively, of equation (A91). With c = 2 in equation (A89) and using equation (A91), the second summation of equation (A88) becomes

$$\sum_{\substack{n=3 \\ \text{odd}}}^{\infty} \frac{\sin(n+2)\phi_b \sin n\phi}{n+2} = \frac{4}{3}\sin^3\phi_b \sin\phi - \frac{\pi}{8}\left(1 + \frac{\phi_-}{|\phi_-|}\right)\sin 2\phi + \frac{1}{4}$$

$$(\tanh^{-1}\cos\phi_- - \tanh^{-1}\cos\phi_+)\cos 2\phi \qquad \text{(A92)}$$

In similar procedures, working with equations (16A), (17A), and (89A), the third and fourth summations of equation (88A) are evaluated as

$$\sum_{\substack{n=3 \\ \text{odd}}}^{\infty} \frac{\sin(n-1)\phi_b \sin n\phi}{n-1} = -\frac{1}{2}\phi_b \sin\phi + \frac{\pi}{8}\left(1 + \frac{\phi_-}{|\phi_-|}\right)\sin\phi + \frac{1}{4}\cos\phi \ln \frac{\sin\phi_+}{\sin\phi_-} \qquad \text{(A93)}$$

$$-\sum_{\substack{n=3 \\ \text{odd}}}^{\infty} \frac{\sin(n+1)\phi_b \sin n\phi}{n+1} = \sin\phi_b \cos\phi_b \sin\phi - \frac{1}{2}\phi_b \sin\phi + \frac{\pi}{8}\left(1 + \frac{\phi_-}{|\phi_-|}\right)$$

$$\sin\phi - \frac{1}{4}\cos\phi \ln \frac{\sin\phi_+}{\sin\phi_-} \qquad \text{(A94)}$$

The required summation is the sum of equations (A90) and (A92), plus $2\cos\phi_b$ times the sum of equations (A93) and (A94), then all divided by $\sin\phi$, thus

$$-\frac{1}{\sin\phi}\sum_{\substack{n=3\\ \text{odd}}}^{\infty} nf_n \sin n\phi = \frac{2}{3}(2+\cos^2\phi_b)\sin\phi_b - 2\phi_b\cos\phi_b - \frac{\pi}{2}\left(1+\frac{\phi_b-\phi}{|\phi_b-\phi|}\right)$$

$$(\cos\phi - \cos\phi_b) = f_1 - \frac{\pi}{2}\left(1+\frac{\eta-\eta_b}{|\eta-\eta_b|}\right)(\eta - \eta_b) \qquad \text{(A95)}$$

where f_1 is defined in equation (9). Shown in equation (A95) is a linear variation with spanwise coordinate η for $\eta \geq \eta_b$, and is a constant with η for $\eta \leq \eta_b$. That is, the induced downwash in the wake is constant inboard of η_b, then varies linearly with η at span stations outboard of η_b.

TABLE OF CONTENTS

APPENDIX B

EVALUATION OF I_n AND I_{nn*} INTEGRALS

Integral of Equation (67)

The I_n integral is

$$I_n = \frac{1}{\pi}\int_0^{\pi} \frac{(\cos\phi_1-\eta)\cos n\phi_1\, d\phi_1}{(\cos\phi_1-\eta)^2+\zeta^2} \tag{B1}$$

This integral was originally evaluated, for arbitrary integer n, in reference 14 in terms of a recurrence formula of a related integral. Here a simpler I_n recurrence formula will be developed. From trigonometric identities

$$\cos(n+2)\phi_1 = 2\cos 2\phi_1 \cos n\phi_1 - \cos(n-2)\phi_1 \tag{B2}$$

then integrating as in equation (B1)

$$I_{n+2} = \frac{2}{\pi}\int_0^{\pi} \frac{\cos 2\phi_1\,(\cos\phi_1-\eta)\cos n\phi_1\, d\phi_1}{(\cos\phi_1-\eta)^2+\zeta^2} - I_{n-2} \tag{B3}$$

In the integrant, $\cos 2\phi_1$ can be divided by the denominator, and noting that $2\cos\phi_1\cos n\phi_1 = \cos(n+1)\phi_1 + \cos(n-1)\phi_1$, then

$$I_{n+2} = \frac{2}{\pi}\int_0^{\pi} \left\{2(\cos\phi_1-\eta)\cos n\phi_1 + \frac{2\eta(\cos\phi_1-\eta)[\cos(n+1)\phi_1+\cos(n-1)\phi_1]}{(\cos\phi_1-\eta)^2+\zeta^2} - \frac{(1+2\eta^2+2\zeta^2)(\cos\phi_1-\eta)\cos n\phi_1}{(\cos\phi_1-\eta)^2+\zeta^2}\right\} d\phi_1 - I_{n-2} \tag{B4}$$

Then the recurrence formula for I_n is

$$I_{n+2} = \begin{bmatrix}2, & n=1\\ 0, & n\neq 1\end{bmatrix} - \begin{bmatrix}4\eta, & n=0\\ 0, & n\neq 0\end{bmatrix} + 4\eta\, I_{n+1} - 2(1+2\eta^2+2\zeta^2)\, I_n + 4\eta\, I_{n-1} - I_{n-2} \tag{B5}$$

Examination of equation (B1) shows

$$I_{-n} = I_n,\quad I_n(-\eta) = I_n(\eta) \text{ for odd } n,\quad I_n(-\eta) = -I_n(\eta) \text{ for even } n \tag{B6}$$

that is, I_n is symmetric with η for odd n and antisymmetric for even n. Then from equation (B5)

$$I_2 = -2\eta + 4\eta\, I_1 - (1 + 2\eta^2 + 2\zeta^2)\, I_0 \tag{B7}$$

$$I_3 = 2 + 4\eta\, I_2 - (3 + 4\eta^2 + 4\zeta^2)\, I_1 + 4\eta\, I_0 \tag{B8}$$

where based on the work in reference 14, I_0 and I_1 are

$$I_0 = \frac{(1-\eta)\, p^{-\frac{1}{2}} - (1+\eta) r^{-\frac{1}{2}}}{[(p^{\frac{1}{2}}+r^{\frac{1}{2}})^2 - 4]^{\frac{1}{2}}} \tag{B9}$$

$$I_1 = 1 - \frac{(-\eta+\eta^2+\zeta^2)\, p^{-\frac{1}{2}} - (\eta+\eta^2+\zeta^2)\, r^{-\frac{1}{2}}}{[(p^{\frac{1}{2}}+r^{\frac{1}{2}})^2 - 4]^{\frac{1}{2}}} = 1 + I_0 - \frac{\zeta^2(p^{-\frac{1}{2}}+r^{-\frac{1}{2}})}{[(p^{\frac{1}{2}}+r^{\frac{1}{2}})^2 - 4]^{\frac{1}{2}}} \tag{B10}$$

where

$$\left.\begin{aligned} p &= (1-\eta)^2 + \zeta^2 \\ r &= (1+\eta)^2 + \zeta^2 = p + 4\eta \end{aligned}\right\} \tag{B11}$$

Equations (B5) through (B11) gives the evaluation of the I_n integral of equation (B1) for all values of η, ζ, and n. Another method is, to define

$$J_n = \frac{1}{\pi}\int_0^{\pi} \frac{\cos n\phi_1\, d\phi_1}{(\cos\phi_1 - \eta)^2 + \zeta^2} \tag{B12}$$

From reference 14

$$J_0 = \frac{p^{-\frac{1}{2}} + r^{-\frac{1}{2}}}{[(p^{\frac{1}{2}}+r^{\frac{1}{2}})^2 - 4]^{\frac{1}{2}}} \tag{B13}$$

$$J_1 = \frac{p^{-\frac{1}{2}} - r^{-\frac{1}{2}}}{[(p^{\frac{1}{2}}+r^{\frac{1}{2}})^2 - 4]^{\frac{1}{2}}} \tag{B14}$$

Using a trigonometric identity, equation (B1) can be written

$$I_n = \frac{1}{2\pi} \int_0^{\pi} \frac{[\cos(n+1)\phi_1+\cos(n-1)\phi_1-2\eta\cos n\phi_1]\, d\phi_1}{(\cos\phi_1-\eta)^2 + \zeta^2}$$

then

$$I_n = \frac{1}{2} (J_{n+1} - 2\eta J_n + J_{n-1}) \tag{B15}$$

Since

$$J_{-n} = J_n;\ \ J_n(-\eta) = -J_n(\eta) \text{ for odd } n;\ J_n(-\eta) = J_n(\eta) \text{ for even } n \tag{B16}$$

that is, J_n is antisymmetric with η for odd n and symmetric for even n. Then

$$I_0 = J_1 - \eta J_0 \tag{B17}$$

Equation (B2) can be used to establish a recurrence formula for J_n in a manner similar to that for I_n. Then

$$J_{n+2} = \begin{bmatrix} 4, & n = 0 \\ 0, & n \neq 0 \end{bmatrix} + 4\eta J_{n+1} - 2(1+2\eta^2+2\zeta^2)J_n + 4\eta J_{n-1} - J_{n-2} \tag{B18}$$

then

$$J_2 = 2 + 4\eta J_1 - (1 + 2\eta^2 + 2\zeta^2) J_0 \tag{B19}$$

$$J_3 = 4\eta J_2 - (3 + 4\eta^2 + 4\zeta^2) J_1 + 4\eta J_0 \tag{B20}$$

Combining equation (B15) for n = 1, and equation (B19) gives

$$I_1 = 1 + \eta J_1 - (\eta^2 + \zeta^2) J_0 = 1 + \eta I_0 - \zeta^2 J_0 \tag{B21}$$

Inserting equations (B13) and (B14) into equations (B17) and (B21) leads to the I_0 and I_1 values of equations (B9) and (B10). The J_n recurrence formula of equation (B18), together with equations (B11), (B13), and (B14) provide an evaluation of the J_n type of integral (eq. B12) for arbitrary η, ζ, and n.

With J_n known, a second method, by applying (B15), is available for evaluating I_n.

Integral of Equation (70)

The I_{nn^*} integral is

$$I_{nn^*} = \frac{1}{\pi}\int_0^{\pi} I_{n^*} \sin\phi \sin n\phi \, d\phi \tag{B22}$$

where I_{n^*} is that in equation (B1) with $n = n^*$. Examination of equation (B22), taking into account the symmetric and antisymmetric characteristics of I_{n^*} in equation (B6), shows

$$\left.\begin{aligned} &I_{0n^*} = 0; \quad I_{-n,n^*} = -I_{nn^*}; \quad I_{n,-n^*} = I_{nn^*}; \\ &I_{n \text{ odd}, n^* \text{ even}} = 0; \; I_{n \text{ even}, n^* \text{ odd}} = 0 \end{aligned}\right\} \tag{B23}$$

which means that I_{nn^*} has a value only when n and n^* are both odd, or n and n^* are both even integers.

A recurrence formula for I_{nn^*} can be made by making the integration of equation (B22) on equation (B5). Then

$$I_{n,n^*+2} = \frac{1}{\pi}\int_0^{\pi}\left\{\begin{bmatrix}2, & n^* = 1\\ 0, & n^* \neq 1\end{bmatrix} - \begin{bmatrix}4\cos\phi, & n^* = 0\\ 0 \qquad , & n^* \neq 0\end{bmatrix} + 4I_{n^*+1}\cos\phi - \right.$$

$$\left. 2(1 + 2\zeta^2 + 2\cos^2\phi)\, I_{n^*} + 4\, I_{n^*-1}\cos\phi - I_{n^*-2}\right\} \sin\phi \sin n\phi \, d\phi \tag{B24}$$

Inserting the trigonometric identities

$$2 \sin n\phi \cos\phi = \sin (n + 1)\phi + \sin (n - 1)\phi$$

$$4 \sin n\phi \cos^2\phi = 2 \sin n\phi + \sin (n + 2)\phi + \sin (n - 2)\phi$$

into equation (B24), then the integrations can be made in terms of I-values with lower n^* integers, which is a recurrence formula. The recurrence formula for I_{nn^*} is

$$I_{n,n^*+2} = \begin{bmatrix} 1, & n = 1, & n^* = 1 \\ 0, & n \neq 1, & n^* \neq 1 \end{bmatrix} - \begin{bmatrix} 1, & n = 2, & n^* = 0 \\ 0, & n \neq 2, & n^* \neq 0 \end{bmatrix} + 2I_{n+1,n^*+1} +$$

$$2I_{n-1,n^*+1} - 4(1+\zeta^2)\, I_{nn^*} - I_{n+2,n^*} - I_{n-2,n^*} + 2I_{n+1,n^*-1} + 2I_{n-1,n^*-1}$$

$$- I_{n,n^*-2} \qquad \text{(B25)}$$

The I_{nn^*} terms for low values of n and n* are obtained from equation (B25) by taking into account the I_{nn^*} identity relations given in equation (B23). Thus letting n* be zero in equation (B25) results in

$$\left.\begin{aligned} I_{n2} &= -\frac{1}{2}\begin{bmatrix} 1, & n = 2 \\ 0, & n \neq 2 \end{bmatrix} + 2I_{n+1,1} + 2I_{n-1,1} - 2(1+\zeta^2)I_{n0} - \frac{1}{2} I_{n+2,0} - \frac{1}{2} I_{n-2,0} \\ I_{02} &= I_{12} = I_{n\ \text{odd},2} = 0 \\ I_{22} &= -\frac{1}{2} + 2I_{31} + 2I_{11} - 2(1+\zeta^2)I_{20} - \frac{1}{2} I_{40} \\ I_{42} &= 2I_{51} + 2I_{31} - 2(1+\zeta^2)I_{40} - \frac{1}{2} I_{60} - \frac{1}{2} I_{20} \end{aligned}\right\} \text{(B26)}$$

Letting n* be one in equation (B25) results in

$$\left.\begin{aligned} I_{n3} &= \begin{bmatrix} 1, & n = 1 \\ 0, & n \neq 1 \end{bmatrix} + 2I_{n+1,2} + 2I_{n-1,2} - (5+4\zeta^2)I_{n1} - I_{n+2,1} - I_{n-2,1} + 2I_{n+1,0} + 2I_{n-1,0} \\ I_{03} &= I_{00} = I_{23} = I_{n\ \text{even},3} = 0 \\ I_{13} &= 1 + 2I_{22} - 4(1+\zeta^2)I_{11} - I_{31} + 2I_{20} \\ I_{33} &= 2I_{42} + 2I_{22} - (5+4\zeta^2)I_{31} - I_{51} - I_{11} + 2I_{40} + 2I_{20} \end{aligned}\right\} \text{(B27)}$$

For higher values of n*, equation (B25) is used directly, without the bracketed terms since n* is greater than one.

With the recurrence formula of equation (B25) the I_{nn^*} terms can be evaluated to very large values of n*. However, as can be seen in equations (B26) and (B27), the recurrence formula starts with a low value of n*, namely n* = 0 and 1. Needed are evaluations of I_{n0} and I_{n1}.

For $\eta \ll 1$, by binomial theory, the radicals of equations (B13) and (B14) can be expanded into a power series of η, then

$$J_0 = \frac{1}{|\zeta|(1+\zeta^2)^{\frac{1}{2}}}\left[1 + \left(\frac{1}{2} - \zeta^2\right)\left(\frac{\eta}{1+\zeta^2}\right)^2 + \left(\frac{3}{8} - 3\zeta^2 + \zeta^4\right)\left(\frac{\eta}{1+\zeta^2}\right)^4 + \left(\frac{5}{16} - \frac{45}{8}\zeta^2 + \frac{15}{2}\zeta^2 - \zeta^6\right)\left(\frac{\eta}{1+\zeta^2}\right)^6\right] \tag{B28}$$

$$J_1 = \frac{1}{|\zeta|(1+\zeta^2)^{\frac{1}{2}}}\left[\frac{\eta}{1+\zeta^2} + \left(\frac{1}{2} - 2\zeta^2\right)\left(\frac{\eta}{1+\zeta^2}\right)^3 + \left(\frac{3}{8} - \frac{9}{2}\zeta^2 + 3\zeta^4\right)\left(\frac{\eta}{1+\zeta^2}\right)^5 + \left(\frac{5}{16} - \frac{15}{2}\zeta^2 + 15\zeta^4 - 4\zeta^6\right)\left(\frac{\eta}{1+\zeta^2}\right)^7\right] \tag{B29}$$

The influence coefficients I_0 and I_1 are obtained by combining equations (B28) and (B29) with equations (B17) and (B21). Thus

$$I_0 = \sum_{\substack{r=1 \\ \text{odd}}}^{13} \zeta_r \eta^r \tag{B30}$$

where

$$\left.\begin{aligned} \zeta_1 &= \frac{-|\zeta|}{(1+\zeta^2)^{3/2}}, \qquad \zeta_5 = \frac{-|\zeta|}{(1+\zeta^2)^{11/2}}\left(\frac{15}{8} - 5\zeta^2 + \zeta^4\right) \\ \zeta_3 &= \frac{-|\zeta|}{(1+\zeta^2)^{7/2}}\left(\frac{3}{2} - \zeta^2\right), \qquad \zeta_7 = \frac{-|\zeta|}{(1+\zeta^2)^{15/2}}\left(\frac{35}{16} - \frac{105}{8}\zeta^2 + \frac{21}{2}\zeta^4 - \zeta^6\right) \end{aligned}\right\} \tag{B31}$$

and ζ_9, ζ_{11}, and ζ_{13} are determined from the simultaneous solution of three equations, at η = .8, .9, and .95 of

$$\eta^9\zeta_9 + \eta^{11}\zeta_{11} + \eta^{13}\zeta_{13} = I_0(\eta) - \sum_{\substack{r=1 \\ \text{odd}}}^{7} \zeta_r \eta^r \tag{B32}$$

where $I_0(\eta)$ is given in equation (B9). The inverse of equation (B32) for $\eta = .8, .9,$ and $.95$, is

$$\left.\begin{aligned}
\zeta_9 &= \frac{29241}{1785}\frac{\Delta I_0(.8)}{.8^9} - \frac{23104}{629}\frac{\Delta I_0(.9)}{.9^9} + \frac{82944}{3885}\frac{\Delta I_0(.95)}{.95^9} \\
\zeta_{11} &= -\frac{13700}{357}\frac{\Delta I_0(.8)}{.8^9} + \frac{61700}{629}\frac{\Delta I_0(.9)}{.9^9} - \frac{46400}{777}\frac{\Delta I_0(.95)}{.95^9} \\
\zeta_{13} &= \frac{8000}{357}\frac{\Delta I_0(.8)}{.8^9} - \frac{40000}{629}\frac{\Delta I_0(.9)}{.9^9} + \frac{32000}{777}\frac{\Delta I_0(.95)}{.95^9}
\end{aligned}\right\} \tag{B33}$$

where

$$\Delta I_0(\eta) = I_0(\eta) - \sum_{\substack{r=1 \\ \text{odd}}}^{7} \zeta_r \eta^r \tag{B34}$$

And for I_1

$$I_1 = \sum_{\substack{r=0 \\ \text{even}}}^{12} \zeta_r \eta^r \tag{B35}$$

where

$$\left.\begin{aligned}
\zeta_0 &= 1 - \frac{|\zeta|}{(1+\zeta^2)^{1/2}}, \qquad \zeta_4 = \frac{-|\zeta|}{(1+\zeta^2)^{9/2}}\left(\frac{15}{8} - \frac{5}{2}\zeta^2\right) \\
\zeta_2 &= \frac{-3|\zeta|}{2(1+\zeta^2)^{5/2}}, \qquad \zeta_6 = \frac{-|\zeta|}{(1+\zeta^2)^{13/2}}\left(\frac{35}{16} - \frac{35}{4}\zeta^2 + \frac{7}{2}\zeta^4\right)
\end{aligned}\right\} \tag{B36}$$

$$\left.\begin{aligned}
\zeta_8 &= \frac{29241}{1785}\frac{\Delta I_1(.8)}{.8^8} - \frac{23104}{629}\frac{\Delta I_1(.9)}{.9^8} + \frac{82944}{3885}\frac{\Delta I_1(.95)}{.95^8} \\
\zeta_{10} &= -\frac{13700}{357}\frac{\Delta I_1(.8)}{.8^8} + \frac{61700}{629}\frac{\Delta I_1(.9)}{.9^8} - \frac{46400}{777}\frac{\Delta I_1(.95)}{.95^8} \\
\zeta_{12} &= \frac{8000}{357}\frac{\Delta I_1(.8)}{.8^8} - \frac{40000}{629}\frac{\Delta I_1(.9)}{.9^8} + \frac{32000}{777}\frac{\Delta I_1(.95)}{.95^8}
\end{aligned}\right\} \tag{B37}$$

where

$$\Delta I_1(\eta) = I_1(\eta) - \sum_{\substack{r=0 \\ \text{even}}}^{6} \zeta_r \eta^r \tag{B38}$$

For evaluating I_{n0} and I_{n1}, equations (B30) and (B35) are inserted into equation (B22). Since $\eta = \cos\phi$, and $\sin\phi \sin n\phi = 0.5\,[\cos(n-1)\phi - \cos(n+1)\phi]$, then

$$I_{n0} = \frac{1}{2\pi} \sum_{\substack{r=1 \\ \text{odd}}}^{13} \zeta_r \int_0^{\pi} \cos^r\phi\,[\cos(n-1)\phi - \cos(n+1)\phi]\,d\phi$$

which integrates to

$$I_{n0} = \frac{\zeta_1}{4}\left[1,\ n=2\right] + \frac{\zeta_3}{4}\left[\begin{matrix}\frac{1}{2}, & n=2\\ \frac{1}{4}, & 4\end{matrix}\right] + \frac{\zeta_5}{4}\left[\begin{matrix}\frac{5}{16}, & n=2\\ \frac{1}{4}, & 4\\ \frac{1}{16}, & 6\end{matrix}\right] + \frac{\zeta_7}{4}\left[\begin{matrix}\frac{7}{32}, & n=2\\ \frac{7}{32}, & 4\\ \frac{3}{32}, & 6\\ \frac{1}{64}, & 8\end{matrix}\right] +$$

$$\frac{\zeta_9}{4}\left[\begin{matrix}\frac{21}{128}, & n=2\\ \frac{3}{16}, & 4\\ \frac{27}{256}, & 6\\ \frac{1}{32}, & 8\\ \frac{1}{256}, & 10\end{matrix}\right] + \frac{\zeta_{11}}{4}\left[\begin{matrix}\frac{33}{256}, & n=2\\ \frac{165}{1024}, & 4\\ \frac{55}{512}, & 6\\ \frac{11}{256}, & 8\\ \frac{5}{512}, & 10\\ \frac{1}{1024}, & 12\end{matrix}\right] + \frac{\zeta_{13}}{4}\left[\begin{matrix}\frac{429}{4096}, & n=2\\ \frac{143}{1024}, & 4\\ \frac{429}{4096}, & 6\\ \frac{13}{256}, & 8\\ \frac{65}{4096}, & 10\\ \frac{3}{1024}, & 12\\ \frac{1}{4096}, & 14\end{matrix}\right] \tag{B39}$$

where the brackets indicate that a value exists at the cited n, but is zero for any other n integer. The ζ_r's for odd r are given in equations (B31) and (B33).

Similarly, with equations (B35) and (B22)

$$I_{n1} = \frac{\zeta_0}{4}\begin{bmatrix} 2, & n= \\ 1 & \end{bmatrix} + \frac{\zeta_2}{4}\begin{bmatrix} \frac{1}{2}, & n= \\ \frac{1}{2}, & 1 \\ \frac{1}{2}, & 3 \end{bmatrix} + \frac{\zeta_4}{4}\begin{bmatrix} \frac{1}{4}, & n= \\ \frac{3}{8}, & 1 \\ \frac{1}{8}, & 3 \\ & 5 \end{bmatrix} + \frac{\zeta_6}{4}\begin{bmatrix} \frac{5}{32}, & n= \\ \frac{9}{32}, & 1 \\ \frac{5}{32}, & 3 \\ \frac{1}{32}, & 5 \\ & 7 \end{bmatrix} +$$

$$\frac{\zeta_8}{4}\begin{bmatrix} \frac{7}{64}, & n= \\ \frac{7}{32}, & 1 \\ \frac{5}{32}, & 3 \\ \frac{7}{128}, & 5 \\ \frac{1}{128}, & 7 \\ & 9 \end{bmatrix} + \frac{\zeta_{10}}{4}\begin{bmatrix} \frac{21}{256}, & n= \\ \frac{45}{256}, & 1 \\ \frac{75}{512}, & 3 \\ \frac{35}{512}, & 5 \\ \frac{9}{512}, & 7 \\ \frac{1}{512}, & 9 \\ & 11 \end{bmatrix} + \frac{\zeta_{12}}{4}\begin{bmatrix} \frac{33}{512}, & n= \\ \frac{297}{2048}, & 1 \\ \frac{275}{2048}, & 3 \\ \frac{77}{1024}, & 5 \\ \frac{27}{1024}, & 7 \\ \frac{11}{2048}, & 9 \\ \frac{1}{2048}, & 11 \\ & 13 \end{bmatrix} \qquad (B40)$$

where ζ_r's for even r are given in equations (B36) and (B37).

Numerical example of I_{nn^*} for $\zeta = 1/2$. - An application of the equations for evaluating I_{nn^*} leads to the following values: From equations (B31) and (B36)

$$\left.\begin{aligned} \zeta_1 &= -.357771 & \zeta_0 &= .552786 \\ \zeta_3 &= -.286217 & \zeta_2 &= -.429325 \\ \zeta_5 &= -.100748 & \zeta_4 &= -.228973 \\ \zeta_7 &= .042497 & \zeta_6 &= -.025645 \end{aligned}\right\} \qquad (B41)$$

From equations (B9) and (B10)

$$\left.\begin{aligned} I_0(.8) &= -.442322 & I_1(.8) &= .199389 \\ I_0(.9) &= -.529048 & I_1(.9) &= .100090 \\ I_0(.95) &= -.569635 & I_1(.95) &= .051389 \end{aligned}\right\} \qquad (B42)$$

Using the ζ's of equation (B41)

η	$\sum_{r=1}^{7} \zeta_r \eta^r$ odd	η	$\sum_{r=0}^{6} \zeta_r \eta^r$ even
.8	-.456861	.8	.177508
.9	-.569810	.9	.041175
.95	-.633557	.95	-.040031

(B43)

By equations (B34) and (B38) the $\Delta I_0(\eta)$ and $\Delta I_1(\eta)$ terms are given by the differences between the values of equations (B42) and (B43). Then with equations (B33) and (B37)

$$\left.\begin{aligned} \zeta_9 &= .075149 & \zeta_8 &= .051299 \\ \zeta_{11} &= .107226 & \zeta_{10} &= .191347 \\ \zeta_{13} &= -.086553 & \zeta_{12} &= -.105817 \end{aligned}\right\} \quad \text{(B44)}$$

With the ζ_r values established in equations (B41) and (B44) the I_{n0} and I_{n1} coefficients are determined from equations (B39) and (B40). These coefficients are listed in the first two columns of table 12. In table 12 the I_{nn^*} for $n^* > 1$ are determined from the recurrence formula of equations (B25) through (B27).

APPENDIX C

EVALUATION OF P_n AND P_{nn*} INTEGRALS

Integral of Equation (125)

The recurrence formula of equation (125) is obtained in a similar manner as done for I_n in appendix B. With equation (B2), equation (125) becomes

$$P_{n+2} = \frac{2}{\pi} \int_0^{\pi} \frac{\cos 2\phi_1 \, (\cos\gamma\cos\phi_1 - \eta) \cos n\phi_1 \, d\phi_1}{(\cos\phi_1 - \eta \cos\gamma)^2 + \eta^2 \sin^2\gamma} - P_{n-2} \tag{C1}$$

In the integrant, $\cos 2\phi_1$ can be divided by the denominator, and noting that $2 \cos\phi_1 \cos n\phi_1 = \cos(n+1)\phi_1 + \cos(n-1)\phi_1$, equation (C1) becomes

$$P_{n+2} = \begin{bmatrix} -4\eta, & n = 0 \\ 2\cos\gamma, & n = 1 \\ 0, & n > 1 \end{bmatrix} + 4\eta \cos\gamma \, P_{n+1} - 2(1 + 2\eta^2) \, P_n + 4\eta \cos\gamma \, P_{n-1} - P_{n-2} \tag{C2}$$

which is the recurrence formula for P_n. Examination of equation (125) shows

$$P_{-n} = P_n, \quad P_n(-\eta) = P_n(\eta) \text{ for odd } n, \quad P_n(-\eta) = -P_n(\eta) \text{ for even } n \tag{C3}$$

Then from equation (C2)

$$P_2 = -2\eta + 4\eta \cos\gamma \, P_1 - (1 + 2\eta^2) \, P_0 \tag{C4}$$

$$P_3 = 2\cos\gamma + 4\eta \cos\gamma \, P_2 - (3 + 4\eta^2) \, P_1 + 4\eta \cos\gamma \, P_0 \tag{C5}$$

where

$$P_0 = \cos\gamma \, J_1 - \eta \, J_0 \tag{C6}$$

$$P_1 = \cos\gamma + \eta \cos 2\gamma \, J_1 - \eta^2 \cos\gamma \, J_0 \tag{C7}$$

where J_0 and J_1 are given in equations (B13) and (B14), respectively, but with the parameters $\eta\cos\gamma$ for η and $\eta\sin\gamma$ for ζ in p and r of equation (B11). Then

$$\left.\begin{aligned} p &= 1 - 2\,\eta\cos\gamma + \eta^2 \\ r &= 1 + 2\,\eta\cos\gamma + \eta^2 \end{aligned}\right\} \tag{C9}$$

Equations (C6) and (C7) are derived from a parameter similarity with the J_0 and J_1 integrals. Thus

$$P_0 = \frac{\cos\gamma}{\pi}\int_0^{\pi} \frac{\cos\phi_1\, d\phi_1}{(\cos\phi_1-\eta\cos\gamma)^2 + \eta^2\sin^2\gamma} - \frac{\eta}{\pi}\int_0^{\pi} \frac{d\phi_1}{(\cos\phi_1-\eta\cos\gamma)^2 + \eta^2\sin^2\gamma} \tag{C9}$$

which comparing with the J_n integral of equation (B12) results in

$$P_0 = \cos\gamma\, J_1\,(\eta\cos\gamma,\ \eta\sin\gamma) - \eta\, J_0\,(\eta\cos\gamma,\ \eta\sin\gamma)$$

that is, these J's are functions of $\eta\cos\gamma$ and $\eta\sin\gamma$ rather than the η and ζ of equation (B12). Equation (C7) is derived in a similar fashion.

In terms of the $\eta\cos\gamma$, $\eta\sin\gamma$ parameters the J_n integral is

$$J_n = \frac{1}{\pi}\int_0^{\pi} \frac{\cos n\phi_1\, d\phi_1}{(\cos\phi_1-\eta\cos\gamma)^2 + \eta^2\sin^2\gamma} \tag{C10}$$

Using the equation (B2) relation, a recurrence formula can be developed, thus

$$J_{n+2} = \begin{bmatrix} 4, & n = 0 \\ 0, & n \neq 0 \end{bmatrix} + 4\eta\cos\gamma\, J_{n+1} - 2(1+2\eta^2)\, J_n + 4\eta\cos\gamma\, J_{n-1} - J_{n-2} \tag{C11}$$

Since $J_{-n} = J_n$, then

$$J_2 = 2 + 4\eta\cos\gamma\, J_1 - (1+2\eta^2)\, J_0 \tag{C12}$$

$$J_3 = 4\eta\cos\gamma\, J_2 - (3+4\eta^2)\, J_1 + 4\eta\cos\gamma\, J_0 \tag{C13}$$

where J_0 and J_1 are given in equations (B13) and (B14) in which p and r are those in equation (C8).

When η and ζ are replaced by $\eta\cos\gamma$ and $\eta\sin\gamma$ in equations (B18) through (B20), then equations (C11) through (C13) are reproduced or checked. Equation (125) can be written as

$$P_n = \frac{1}{\pi}\int_0^{\pi} \frac{\left\{\frac{\cos\gamma}{2}\left[\cos(n+1)\phi_1 + \cos(n-1)\phi_1\right] - \eta\cos n\phi_1\right\} d\phi_1}{(\cos\phi_1-\eta\cos\gamma)^2 + \eta^2\sin^2\gamma}$$

$$P_n = \frac{1}{2}\left(J_{n+1}\cos\gamma - 2n\,J_n + J_{n-1}\cos\gamma\right) \qquad \text{(C14)}$$

Equation (C14) provides a second method (to eq. C2) for evaluating P_n.

Integral of Equation (128)

The recurrence formula for P_{nn^*} is made by making the integration of equation (128) on equation (C2) in which n is replaced by n*. Then in a derivation similar to that leading to equation (B25), the recurrence formula is

$$P_{n,\,n^*+2} = \begin{bmatrix}\cos\gamma, & n = 1,\ n^* = 1\\ -1, & n = 2,\ n^* = 0\end{bmatrix} + 2\cos\gamma\left(P_{n+1,\,n^*+1} + P_{n-1,\,n^*+1}\right) - 4P_{nn^*} - P_{n+2,\,n^*}$$

$$-P_{n-2,\,n^*} + 2\cos\gamma\left(P_{n+1,\,n^*-1} + P_{n-1,\,n^*-1}\right) - P_{n,\,n^*-2} \qquad \text{(C15)}$$

where the brackets indicate that this term is zero for values of n and n* other than those listed. The relations of equation (B23) apply also to P_{nn^*}. Then from equation (C15)

$$\left.\begin{aligned} P_{n2} &= \left[-\tfrac{1}{2},\ n=2\right] + 2\cos\gamma\left(P_{n+1,1}+P_{n-1,1}\right) - 2P_{n0} - \tfrac{1}{2}P_{n+2,0} - \tfrac{1}{2}P_{n-2,0}\\ P_{02} &= P_{12} = P_{n=\text{odd},2} = 0\\ P_{22} &= -\tfrac{1}{2} + 2\cos\gamma\left(P_{31} + P_{11}\right) - 2P_{20} - \tfrac{1}{2}P_{40}\end{aligned}\right\} \qquad \text{(C16)}$$

$$\left.\begin{aligned} P_{n3} &= \left[\cos\gamma, n=1\right] + 2\cos\gamma\left(P_{n+1,2}+P_{n-1,2}\right) - 5P_{n1} - P_{n+2,1} - P_{n-2,1} + 2\cos\gamma\left(P_{n+1,0}+P_{n-1,0}\right)\\ P_{03} &= P_{23} = P_{n=\text{even},3} = 0\\ P_{13} &= \cos\gamma + 2\cos\gamma\,P_{22} - 4P_{11} - P_{31} + 2\cos\gamma\,P_{20}\end{aligned}\right\} \qquad \text{(C17)}$$

Values of P_{n0} and P_{n1} are needed to start this recurrence formula. From equations (128), (C6), and (C7)

$$\left.\begin{aligned} P_{no} &= \frac{1}{\pi}\int_0^{\pi} (\cos\gamma\, J_1 - J_0\cos\phi)\sin\phi \sin n\phi\, d\phi \\ P_{00} &= P_{n=odd,0} = 0 \end{aligned}\right\} \qquad (C18)$$

where the zero values result because the term inside the parenthesis is antisymmetric about $\phi = \pi/2$, so when sin $n\phi$ is symmetric, the integral is zero.

$$\begin{aligned} P_{n1} &= [\tfrac{1}{2}\cos\gamma,\ n=1] + \frac{1}{2\pi}\int_0^{\pi} (\cos 2\gamma\, J_1 - \cos\gamma\, J_0\cos\phi)\sin 2\phi \sin n\phi\, d\phi \\ P_{01} &= P_{n=even,0} = 0 \end{aligned} \qquad (C19)$$

where as before the term inside the parenthesis is antisymmetric. These integrals can be evaluated by the expansion method used in appendix B, or by a quadrature formula given in reference 15, which has

$$\int_0^{\pi} f(\phi)d\phi = \frac{\pi}{M+1}\left[\tfrac{1}{2} f(\phi_0) + \tfrac{1}{2} f(\phi_{M+1}) + \sum_{\mu=1}^{M} f(\phi_\mu)\right] \qquad (C20)$$

where M is an odd integer and $\phi_\mu = \mu\pi/(M+1)$. The integrant of equation (C18) is symmetric about $\phi = \pi/2$ when n is even, also it is zero at $\phi = \pi/2$. Then with equation (C20), equation (C18) becomes

$$P_{n0} \overset{n=even}{=} \frac{2}{M+1}\sum_{\mu=1}^{\frac{M-1}{2}} (\cos\gamma\, J_1 - J_0\cos\phi_\mu)\sin\phi_\mu \sin n\phi_\mu \qquad (C21)$$

where J_0 and J_1 of equations (B13) and (B14) are evaluated with the p and r of equation (C8) at $\eta = \cos\phi_\mu$.

The integrant in equation (C19) is symmetric when n is odd, also it is zero at $\phi = \pi/2$. Then with equation (C20), equation (C19) becomes

$$P_{n1} \overset{n=odd}{=} [\tfrac{1}{2}\cos\gamma,\ n=1] + \frac{1}{M+1}\sum_{\mu=1}^{\frac{M-1}{2}} (\cos 2\gamma\, J_1 - \cos\gamma\, J_0\cos\phi_\mu)\sin 2\phi_\mu \sin n\phi_\mu \qquad (C22)$$

where as before, $\phi_\mu = \mu\pi/(M+1)$, and J_0 and J_1 are evaluated with $\eta = \cos\phi_\mu$ in equation (C8).

REFERENCES

1. Prandtl, Ludwig: Uber Tragflügel Kleinsten Induzierten Widerstandes. Zeitschrift Flugtechnik und Motorluftschiffahrt, Vol. 24, Nov. 1933, pp. 305-306.

2. Jones, Robert T.: The Spanwise Distribution of Lift for Minimum Induced Drag of Wings Having a Given Lift and a Given Bending Moment. NACA TN-2249, Dec. 1950.

3. Klein, Armin; and Viswanathan, Sathy P.: Minimum Induced Drag of Wings with Given Lift and Root-Bending Moment. Zeitschrift fuer Ange-wandte Mathematik und Physik, Vol. 24, Dec. 1973, pp. 886-892.

4. Klein, Armin; and Viswanathan, Sathy P.: Approximate Solution for Minimum Induced Drag of Wings with Given Structural Weight. Journal of Aircraft, Vol. 12, No. 2, Feb 1975, pp. 124-126.

5. Blackwell, Jr., James A.: Numerical Method to Calculate the Induced Drag or Optimum Loading for Arbitrary Non-Planar Aircraft. NASA SP-405, May 1976, pp. 49-70.

6. Feitel, Winfried M.: Optimization and Design of Three-Dimensional Aerodynamic Configurations of Arbitrary Shape by a Vortex Lattice Method. NASA SP-405, May 1976, pp. 71-88.

7. Heyson, Harry H.; Riebe, Gregory D.; and Fulton, Cynthia L.: Theoretical Parametric Study of the Relative Advantages of Winglets and Wing-Tip Extensions. NASA TM X-74003, Jan. 1977.

8. Cone, Clarence D., Jr.: The Theory of Induced Lift and Minimum Induced Drag of Nonplanar Lifting Systems. NASA TR R-139, 1962.

9. DeYoung, John: Nonplanar Wing Load-Line and Slender Wing Theory. NASA CR-2864, Aug. 1977.

10. Glauert, Hermann: The Elements of Aerofoil and Airscrew Theory, 2nd ed., Cambridge University Press, New York, 1947, pp. 138-142, pp. 164-165.

11. von Karman, Theodore; and Burgers, J. M.: General Aerodynamic Theory - Perfect Fluids, Vol. II of Aerodynamic Theory, div. E, W. F. Durand,

ed., First Dover edition, Dover Publications, New York, 1973, pp. 146-151, pp. 171-177.

12. DeYoung, J.: Wing Loading Theory Satisfying all Boundary Points. Ph.D. Dissertation, Dept. of Aerospace Engineering, The University of Texas at Arlington, Arlington, Texas, 1975, pp. 13-17.

13. DeYoung, John: Spanwise Loading for Wings and Control Surfaces of Low Aspect Ratio. NACA TN-2011, Jan. 1950.

14. DeYoung, John; and Barling, Jr., Walter H.: Prediction of Downwash Behind Swept-Wing Airplanes at Subsonic Speeds. NACA TN-3346, Jan. 1955, pp. 39-41.

15. DeYoung, John; and Harper, Charles W.: Theoretical Symmetric Span Loading at Subsonic Speeds for Wings Having Arbitrary Planform. NACA Report 921, 1948, p. 16.

TABLE 1. - CONSTANTS OF PLANAR WING MINIMIZATION SOLUTION

η_b	k	k_1	f_1	$\frac{k}{f_1}$
0	2/9	1/6	4/3	1/6
.05	.218893	.165424	1.181253	.185306
.10	.209570	.161760	1.039157	.201673
.15	.195126	.155839	.907010	.215131
.20	.176851	.147886	.784747	.225361
.25	.156042	.138175	.672280	.232109
.30	.133952	.127012	.569493	.235213
.40	.090328	.101679	.392358	.230218
.5	.053025	.074704	.251841	.210548
.6	.025900	.048928	.145912	.177501
.7	.009611	.026977	.071919	.133638
.8	.002196	.010978	.026398	.083197
.9	.000157	.002159	.004719	.033267
1.0	0	0	0	0

TABLE 2. - SPANWISE FUNCTION, k_o, OF PLANAR WING MINIMIZATION SOLUTION

η_b \ η	0	.2	.4	.6	.8	.9	.96	1
0	-1/3	-.239745	-.059810	.161042	.406024	.534748	.613552	2/3
.05	-.325360	-.238882	-.060532	.159478	.403914	.532429	.611122	.664168
.10	-.308364	-.236111	-.062646	.154815	.397606	.525492	.603852	.656692
.15	-.286239	-.230808	-.065990	.147144	.387168	.513998	.591800	.644294
.2	-.261029	-.221316	-.070279	.136621	.372713	.498050	.575063	.627069
.3	-.206572	-.183739	-.079716	.107996	.332454	.453424	.528138	.578723
.4	-.152579	-.139061	-.083345	.071782	.278779	.393352	.464721	.513248
.5	-.103773	-.096063	-.066443	.032844	.214672	.320444	.387268	.433013
.6	-.063166	-.059116	-.044010	.001076	.144553	.238432	.299239	.341333
.8	-.012386	-.011761	-.009496	-.003586	.020040	.071386	.113089	.144000
1.0	0	0	0	0	0	0	0	0

TABLE 3. - FOURIER SERIES COEFFICIENTS, $f_n \times 10$
OF THE SPANWISE LOADING OF EQUATION (21)

n \ η_b	0	.05	.10	.15	.20	.40	.60	.80*
3	2.6667	2.6500	2.6005	2.5192	2.4080	1.7245	.8738	.2074
5	-.3810	-.3710	-.3418	-.2951	-.2339	.0690	.2347	.1220
7	.1270	.1199	.0996	.0684	.0303	-.0966	-.0423	.0453
9	-.0577	-.0515	-.0366	-.0150	.0090	.0444	-.0269	.0003
11	.0311	.0266	.0147	-.0013	-.0166	-.0079	.0167	-.0105
13	-.0186	-.0149	-.0053	.0063	.0151	-.0080	.0040	-.0047
15	.0121	.0089	.0011	-.0072	-.0114	.0070	-.0077	.0021
17	-.0083	-.0055	.0009	.0066	.0077	-.0056	.0010	.0030
19	.0059	.0035	-.0018	-.0055	-.0045	.0005	.0034	-.0012
21	-.0044	-.0022	.0016	.0043	.0021	.0024	-.0019	-.0023
23	.0033	.0014	-.0022	-.0031	-.0003	-.0028	-.0011	-.0008
25	-.0026	-.0008	.0020	.0021	-.0007	.0015	.0016	.0005
27	.0020	.0005	-.0018	-.0012	.0013	.0001	0	.0007
29	-.0016	-.0002	.0016	.0006	-.0014	-.0011	-.0010	.0003
31	.0013	0	-.0013	-.0001	.0013	.0011	.0005	-.0005
33	-.0011	.0001	.0011	-.0003	-.0010	-.0005	.0005	-.0002
35	.0009	-.0002	-.0009	.0005	.0007	-.0002	-.0005	.0002
37	-.0008	.0002	.0007	-.0006	-.0003	.0006	-.0001	.0003
39	.0007	-.0002	-.0005	.0006	0	-.0005	.0004	0
41	-.0006	.0003	.0003	-.0006	.0002	.0002	-.0001	.0002
43	.0005	-.0003	-.0002	.0005	-.0003	.0002	-.0003	-.0001
45	-.0004	.0003	.0001	-.0004	.0004	-.0004	.0002	.0001
47	.0004	-.0003	0	.0003	-.0004	.0003	.0001	.0001
49	-.0003	.0003	-.0001	-.0002	.0003	-.0001	-.0002	0
51	.0003	-.0002	.0001	.0001	-.0002	-.0001	0	-.0001

* At $\eta_b = 1$, $f_n = 0$.

TABLE 4. - AERODYNAMIC CHARACTERISTICS OF WING WITH WINGTIP ZERO-SLOPE LOADING

η_b	$t=t_1$ eq. (29)	η_{cp}	$\frac{\pi A}{2C_L}\alpha_w$		$C_b \times 10$	e	$\frac{C_b^2}{e} \times 10^2$	$\frac{C_b^2/e}{(C_b^2/e)_c}$	$\frac{C_{bc}}{C_b}$
			$0 \le \eta \le \eta_b$	$\eta=1$					
0	3/2	.31831	3	-1.71239	.79577	2/3	.94989	.84375	4/3
.05	1.50564	.31871	2.77854	-1.71506	.67774	.66835	.68727	.77779	1.38697
.10	1.52278	.31987	2.58241	-1.72315	.57298	.67296	.48785	.71342	1.44322
.15	1.55209	.32176	2.40776	-1.73687	.48077	.68025	.33979	.65224	1.50128
.20	1.59472	.32432	2.25145	-1.75652	.40005	.68977	.23202	.59496	1.56101
.25	1.65247	.32751	2.11092	-1.78262	.32979	.70121	.15510	.54193	1.62220
.30	1.72794	.33127	1.98405	-1.81589	.26900	.71431	.10130	.49323	1.68473
.40	1.94837	.34033	1.76446	-1.90813	.17218	.74466	.03981	.40838	1.81340
.5	2.30940	.35119	1.58160	-2.04600	.10296	.77954	.01360	.33859	1.94643
.6	2.92969	.36358	1.42748	-2.25403	.05573	.81813	.00380	.28158	2.08343
.7	4.11847	.37726	1.29620	-2.58537	.02573	.85983	.00077	.23511	2.22412
.8	6.94444	.39206	1.18332	-3.18000	.00887	.90424	.00009	.19722	2.36830
.9	18.11177	.40782	1.08547	-4.60451	.00149	.95102	.00000	.16608	2.51588
1.0	∞	.42441	1	-∞	0	1	0	.14063	2.66667

BLANK PAGE

BLANK PAGE

TABLE 5. - AERODYNAMIC CHARACTERISTICS OF WING WITH $(C_{bc}/C_b) = 1.1$ LOADING

η_b	t eq. (46)	η_{cp}	$\frac{\pi A}{2C_L}\alpha_w$		$C_b \times 10$	e	$\frac{C_b^2}{e} \times 10^2$	$\frac{C_b^2/e}{(C_b^2/e)_c}$
			$0 \le \eta \le \eta_b$	$\eta = 1$				
0	6/11	.38583	1.72727	.01368	.96458	.93798	.99192	.88109
.1	.45077	.39347	1.46843	.19389	.75176	.95916	.58921	.86164
.2	.40339	.39909	1.31656	.30272	.56771	.97203	.33157	.85023
.3	.38650	.40358	1.22011	.37016	.41199	.98038	.17313	.84298
.4	.39488	.40737	1.15494	.41060	.28384	.98611	.08170	.83809
.6	.51216	.41378	1.07473	.43113	.10556	.99325	.01122	.83206
.8	1.09270	.41932	1.02885	.34228	.01910	.99738	.00037	.82861
1.0	∞	.42441	1	$-\infty$	0	0	0	.82645

TABLE 6. - AERODYNAMIC CHARACTERISTICS OF WING WITH $(C_{bc}/C_b) = 1.2$ LOADING

η_b	t eq. (46)	η_{cp}	$\frac{\pi A}{2C_L}\alpha_w$		$C_b \times 10$	e	$\frac{C_b^2}{e} \times 10^2$	$\frac{C_b^2/e}{(C_b^2/e)_c}$
			$0 \le \eta \le \eta_b$	$\eta = 1$				
0	1	.35368	2.33333	-.80826	.88419	.81818	.95553	.84877
.1	.82642	.36768	1.85878	-.47787	.68911	.87479	.54284	.79384
.2	.73955	.37800	1.58036	-.27834	.52040	.91180	.29701	.76162
.3	.70858	.38622	1.40353	-.15471	.37766	.93698	.15222	.74115
4	.72395	.39317	1.28405	-.08568	.26019	.95480	.07090	.72732
.6	.93896	.40491	1.13701	-.04293	.09676	.97768	.00958	.71030
.8	2.00328	.41508	1.05288	-.20581	.01751	.99126	.00031	.70057
1.0	∞	.42441	1	$-\infty$	0	1	0	.69444

///

TABLE 7. - AERODYNAMIC CHARACTERISTICS OF WING WITH $(C_{bc}/C_b) = 4/3$ LOADING

η_b	t eq. (46)	η_{cp}	$\frac{\pi A}{2C_L}\alpha_w$		$C_b \times 10$	e	$\frac{C_b^2}{e} \times 10^2$	$\frac{C_b^2/e}{(C_b^2/e)_c}$
			$0 \le \eta \le \eta_b$	$\eta = 1$				
0	3/2	.31831	3	-1.71239	.79577	2/3	.94989	.84375
.05	1.34912	.32969	2.59365	-1.43281	.70501	.71510	.69506	.78661
.10	1.23963	.33931	2.28817	-1.21680	.62020	.75641	.50852	.74365
.15	1.16208	.34755	2.05402	-1.04915	.54133	.79145	.37026	.71072
.20	1.10933	.35479	1.87054	- .91751	.46836	.82126	.26710	.68492
.25	1.07708	.36125	1.72410	- .81371	.40124	.84672	.19014	.66433
.30	1.06287	.36712	1.60530	- .73207	.33989	.86857	.13301	.64762
.40	1.08593	.37755	1.42607	- .62085	.23417	.90374	.06068	.62242
.5	1.18738	.38677	1.29903	- .56610	.15031	.93044	.02428	.60455
.6	1.40844	.39517	1.20551	- .56439	.08709	.95113	.00797	.59140
.7	1.87073	.40299	1.13454	- .62858	.04292	.96746	.00190	.58142
.8	3.00492	.41041	1.07932	- .80872	.01575	.98055	.00025	.57366
.9	7.51495	.41753	1.03546	-1.32543	.00282	.99121	.00001	.56749
1.0	∞	.42441	1	$-\infty$	0	1	0	.56250

TABLE 8. - SPANWISE LOADING DISTRIBUTION, $c_\ell c/C_L c_{av}$, OF WING WITH SPECIFIED CONDITION OF LOADING*

η_b	t \ η	0	.2	.4	.6	.8	.9	.96
Wingtip zero-slope loading								
0	3/2	1.90986	1.69614	1.27164	.77254	.29867	.10982	.02840
.1	1.52278	1.87112	1.69605	1.27827	.77846	.30140	.11088	.02869
.2	1.59472	1.80325	1.68781	1.29773	.79667	.30988	.11419	.02957
.4	1.94837	1.65175	1.58552	1.35644	.87613	.34900	.12965	.03371
.6	2.92969	1.50886	1.46357	1.31740	1.01538	.44042	.16731	.04397
.8	6.94444	1.38276	1.34940	1.24390	1.04396	.65763	.27986	.07653
elliptic loading, either t=0 or η_b=1		1.27324	1.24751	1.16694	1.01859	.76394	.55499	.35651
(C_{bc}/C_b) = 4/3 loading								
0	3/2	1.90986	1.69614	1.27164	.77254	.29867	.10982	.02840
.1	1.23963	1.75994	1.61265	1.25757	.82311	.38741	.19346	.08964
.2	1.10933	1.64193	1.55380	1.25792	.86422	.44808	.24836	.12908
.4	1.08593	1.48420	1.43590	1.27256	.93919	.53267	.31793	.17659
.6	1.40844	1.38651	1.35138	1.23928	1.01705	.60841	.36862	.20625
.8	3.00492	1.32063	1.29160	1.20024	1.02957	.71794	.43594	.23536
(C_{bc}/C_b) = 1.2 loading								
0	1	1.69765	1.54660	1.23674	.85456	.45376	.25821	.13777
.1	.82642	1.59771	1.49094	1.22736	.88827	.51292	.31397	.17860
.2	.73955	1.51903	1.45170	1.22760	.91568	.55337	.35057	.20489
.3	.70858	1.45961	1.40993	1.23286	.94065	.58398	.37668	.22309
.4	.72395	1.41388	1.37311	1.23735	.96566	.60976	.39695	.23657
.6	.93896	1.34876	1.31676	1.21516	1.01756	.66025	.43074	.25634
.8	2.00328	1.30483	1.27691	1.18914	1.02591	.73327	.47562	.27574
(C_{bc}/C_b) = 1.1 loading								
0	6/11	1.50474	1.41065	1.20501	.92912	.59475	.39311	.23720
.1	.45077	1.45022	1.38029	1.19990	.94751	.62702	.42353	.25947
.2	.40339	1.40731	1.35889	1.20003	.96246	.64908	.44349	.27381
.3	.38650	1.37489	1.33611	1.20290	.97608	.66578	.45773	.28373
.4	.39488	1.34995	1.31602	1.20535	.98972	.67985	.46879	.29108
.6	.51216	1.31443	1.28529	1.19325	1.01803	.70739	.48722	.30187
.8	1.09270	1.29047	1.26335	1.17905	1.02258	.74722	.51170	.31245

* Equation (63) and table 9 apply when comparing with elliptic loading with same η_b values.

TABLE 9. - COMPARISON OF AERODYNAMIC CHARACTERISTICS DUE TO OPTIMIZED SPANWISE LOADING WITH THAT DUE TO ELLIPTIC LOADING OF EQUAL LIFT AND BENDING MOMENT FOR BENDING MOMENTS AT THE SAME $\eta_b = \eta_{bc}$ NORMALIZED SPAN STATION

$\eta_b = \eta_{bc}$	$b/b_c = C_{bc}/C_b$	t eq. (59)	η_{cp}	α_w/α_{wc}		$C_b \times 10$	e	$\frac{D_i}{D_{ic}}$
				$0 \le \eta \le \eta_b$	$\eta = 1$			
0	.95	-.31579	.44675	.64149	1.74075	1.11688	.97832	1.13259
	1.00	0	.42441	1	1	1.06103	1	1
	1.05	.28571	.40420	1.25256	.43842	1.01051	.98218	.92348
	1.10	.54545	.38583	1.42750	.01131	.96458	.93798	.88109
	1.15	.78261	.36905	1.54516	-.31392	.92264	.88020	.85906
	1.20	1.00000	.35368	1.62037	-.56129	.88419	.81818	.84877
	1.25	1.20000	.33953	1.66400	-.74874	.84883	.75758	.84480
*	4/3	3/2	.31831	1.68750	-.96322	.79577	2/3	.84375
	1.60	2.25000	.26526	1.56250	-1.19867	.66315	.47059	.83008
	2.00	3	.21221	1.25000	-1.10619	.53052	.33333	.75000
.1	.95	-.26097	.43656	.80754	1.62515	.87046	.98593	1.12385
	1.00	0	.42441	1	1	.82693	1	1
	1.05	.23612	.40820	1.12958	.52404	.78756	.98845	.91763
	1.10	.45077	.39347	1.21358	.16024	.75176	.95916	.86164
	1.15	.64676	.38001	1.26434	-.11841	.71907	.91940	.82243
	1.20	.82642	.36768	1.29082	-.33185	.68911	.87479	.79384
*	1.44322	1.52278	.31987	1.23982	-.82729	.57298	.67296	.71342
	1.60	1.85945	.29676	1.14541	-.90828	.51683	.57985	.67367
	2.00	2.47926	.25420	.89409	-.85840	.41347	.43703	.57204
.2	.95	-.23354	.43907	.90496	1.55533	.65735	.99045	1.11872
	1.00	0	.42441	1	1	.62448	1	1
	1.05	.21130	.41115	1.05743	.57575	.59474	.99217	.91419
	1.10	.40339	.39909	1.08807	.25018	.56771	.97203	.85023
	1.15	.57878	.38809	1.09958	-.00033	.54303	.94407	.80094
	1.20	.73955	.37800	1.09747	-.19329	.52040	.91180	.76162
	1.35	1.15042	.35221	1.04405	-.54240	.46258	.81034	.67712
*	1.56101	1.59472	.32432	.92396	-.72084	.40005	.68977	.59496
	2.00	2.21866	.28516	.68527	-.70875	.31224	.53460	.46764
.4	.95	-.22862	.43428	1.00864	1.48613	.32866	.99530	1.11326
	1.00	0	.42441	1	1	.31223	1	1
	1.05	.20684	.41549	.98064	.62700	.29736	.99615	.91053
	1.10	.39488	.40737	.95450	.33934	.28384	.98611	.83809
	1.15	.56657	.39996	.92423	.11670	.27150	.97182	.77807
	1.20	.72395	.39317	.89170	-.05950	.26019	.95480	.72732
	1.40	1.24106	.37086	.75864	-.43490	.22302	.87787	.58119
*	1.81340	1.94837	.34033	.53657	-.58026	.17218	.74466	.40838
	2.00	2.17185	.33069	.46304	-.56043	.15611	.70123	.35652
.6	.95	-.29651	.43057	1.06009	1.47296	.12222	.99773	1.11056
	1.00	0	.42441	1	1	.11611	1	1
	1.05	.26827	.41884	.94253	.63675	.11058	.99814	.90872
	1.10	.51216	.41378	.88821	.35631	.10556	.99325	.83206
	1.15	.73484	.40915	.83722	.13898	.10097	.98621	.76672
	1.20	.93896	.40491	.78959	-.02981	.09676	.97768	.71030
	1.60	2.11266	.38054	.51104	-.52601	.07257	.89638	.43578

TABLE 9. - Continued.

$\eta_b = \eta_{bc}$	$b/b_c = C_{bc}/C_b$	t eq. (59)	η_{cp}	α_w/α_{wc}		$C_b \times 10$	e	$\frac{D_i}{D_{ic}}$
				$0 \le \eta \le \eta_b$	$\eta = 1$			
*	2.08343	2.92969	.36358	.32886	-.51929	.05573	.81813	.28158
.8	.95	-.63261	.42736	1.08953	1.52995	.02211	.99912	1.10706
	1.00	0	.42441	1	1	.02101	1	1
	1.05	.57236	.42175	.92073	.59454	.02001	.99928	.90768
	1.10	1.09270	.41932	.85029	.28288	.01910	.99738	.82861
	1.15	1.56778	.41711	.78744	.04259	.01827	.99463	.76023
	1.20	2.00328	.41508	.73117	-.14292	.01751	.99126	.70057
	1.60	4.50737	.40341	.48358	-.66917	.01313	.95729	.40806
*	2.36830	6.94444	.39206	.21097	-.56696	.00887	.90424	.19722

* Values for wingtip zero-slope loading, t of equation (29).

TABLE 10. - COMPARISON OF AERODYNAMIC CHARACTERISTICS DUE TO OPTIMIZED SPANWISE LOADING WITH THAT DUE TO ELLIPTIC LOADING OF EQUAL LIFT AND BENDING MOMENT FOR BENDING MOMENTS AT THE SAME $y_b = y_{bc}$ SPAN STATION

$\eta_b = b_c\eta_{bc}/b$	$b/b_c = C_{bc}/C_b$	t eq. (60)	η_{cp}	α_w/α_{wc}		$C_b \times 10$	e	$\frac{D_i}{D_{ic}}$
				$0 \le \eta \le \eta_b$	$\eta = 1$			
0	Same values as those in table 9 for $\eta_b = 0$.							
.1	.95	-.33009	.44708	.72796	1.76210	.88198	.97767	1.13334
	1.00	0	.42441	1	1	.82693	1	1
	1.05	.29820	.40394	1.18810	.42334	.77720	.98170	.92393
	1.10	.56887	.38536	1.31499	-.01429	.73206	.93649	.88250
	1.15	.81558	.36842	1.39699	-.34068	.69092	.87765	.86155
	1.20	1.04134	.35292	1.44592	-.59876	.65327	.81483	.85226
*	1.32306	1.52278	.31987	1.47525	-.98439	.57298	.67296	.84889
	1.6	2.32882	.26453	1.33594	-1.23617	.43856	.46804	.83460
	2.0	3.08624	.21253	1.05177	-1.12976	.31224	.33376	.74903
.2	.95	-.37441	.44791	.78247	1.82513	.67717	.97581	1.13550
	1.00	0	.42441	1	1	.62448	1	1
	1.05	.33663	.40328	1.14664	.37926	.57711	.98035	.92521
	1.10	.64065	.38420	1.24194	-.08874	.53432	.93233	.88643
	1.15	.91632	.36690	1.29987	-.44149	.49552	.87071	.86842
	1.20	1.16718	.35116	1.33051	-.70659	.46022	.80585	.86175
*	1.29721	1.59472	.32432	1.33796	-1.04383	.40005	.68977	.86154
	1.6	2.56054	.26370	1.17554	-1.33827	.26413	.46307	.84356
	2.0	3.32803	.21553	.90292	-1.18815	.15611	.33798	.73969
.4	.95	-.60668	.45059	.84428	2.11139	.35584	.96782	1.14487
	1.00	0	.42441	1	1	.31223	1	1
	1.05	.53345	.40139	1.09687	.18483	.27388	.97494	.93034
	1.10	1.00378	.38110	1.15193	-.41177	.24008	.91658	.90166
	1.15	1.41938	.36316	1.17725	-.84580	.21020	.84604	.89375
	1.20	1.78725	.34729	1.18142	-1.15809	.18376	.77608	.89481
*	1.22396	1.94837	.34033	1.17782	-1.27372	.17218	.74466	.89641
	1.6	3.56422	.27060	.93689	-1.68748	.05603	.46566	.83887
	2.0	4.19758	.24327	.66174	-1.31633	.01050	.38587	.64789
	2.5	4.34371	.23697	.43269	-.87735	0	.36978	.43269
.6	.95	-1.44623	.45445	.87421	2.88793	.14592	.94861	1.16806
	1.00	0	.42441	1	1	.11611	1	1
	1.05	1.20278	.39944	1.06621	-.30472	.09133	.96388	.94101
	1.10	2.19802	.37877	1.09150	-1.19123	.07081	.88879	.92986
*	1.14423	2.92969	.36358	1.09029	-1.72164	.05573	.81813	.93358
	1.15	3.01594	.36179	1.08889	-1.77684	.05396	.80933	.93428
	1.20	3.68188	.34796	1.06752	-2.14552	.04023	.74013	.93827
	1.40	5.21515	.31612	.89845	-2.44520	.00863	.58671	.86960
	5/3	5.63377	.30742	.65593	-1.09275	0	.54883	.65594
.8	.95	-7.85059	.46099	.87840	6.34397	.03472	.88079	1.25800
	1.00	0	.42441	1	1	.02101	1	1
	1.05	5.43663	.39908	1.03720	-2.05115	.01150	.93905	.96590
*	1.06860	6.94444	.39206	1.03627	-2.78482	.00827	.90424	.96847
	1.10	8.94496	.38274	1.02159	-3.62327	.00537	.85055	.97166
	1.15	10.94770	.37341	.97467	-4.22658	.00187	.79164	.95516
	1.25	12.01966	.36841	.84307	-3.99032	0	.75915	.84305

* Values for wingtip zero-slope loading, t of equation (29).

TABLE 11. - SPANWISE LOADING DISTRIBUTION*, $c_\ell c/C_L c_{av}$, FOR CONDITIONS OF TABLE 10

η_b	t \ η	0	.2	.4	.6	.8	.9	.96
(b/b_c) = 1.20 loading								
.1	1.04134	1.68209	1.55424	1.24307	.85438	.44764	.25129	.13233
.2	1.16718	1.66115	1.56977	1.26267	.85617	.43161	.23237	.11722
.4	1.78725	1.62045	1.55757	1.34077	.88791	.38331	.16482	.06040
.6	3.68188	1.56936	1.51905	1.35603	1.01456	.35735	.06778	-.03628
(b/b_c) = 1.15 loading								
.1	.81558	1.59345	1.48775	1.22657	.88998	.51621	.31713	.18093
.2	.91632	1.57778	1.50051	1.24209	.89108	.50304	.30171	.16865
.4	1.41938	1.54898	1.49375	1.30499	.91481	.46166	.24513	.12135
.6	3.01594	1.51580	1.46993	1.32183	1.01529	.43089	.15590	.03476
.8	10.94770	1.44589	1.40814	1.28826	1.05858	.59634	.12126	-.08487
(b/b_c) = 1.10 loading								
.1	.56887	1.49659	1.41508	1.20853	.92888	.59115	.38908	.23404
.2	.64065	1.48616	1.42440	1.21948	.92944	.58153	.37791	.22516
.4	1.00378	1.46824	1.42165	1.26457	.94520	.55017	.33586	.19020
.6	2.19802	1.45002	1.40961	1.27983	1.01618	.52122	.26413	.12202
.8	8.94496	1.41430	1.37876	1.26607	1.05126	.62700	.20060	-.00413
(b/b_c) = 1.05 loading								
.1	.29820	1.39032	1.33535	1.18874	.97157	.67337	.46802	.29231
.2	.33663	1.38512	1.34046	1.19455	.97175	.66809	.46194	.28749
.4	.53345	1.37687	1.34006	1.21883	.97959	.65033	.43854	.26813
.6	1.20278	1.36997	1.33622	1.22871	1.01727	.63112	.39583	.22819
.8	5.43663	1.35898	1.32728	1.22719	1.03845	.68071	.33960	.13732

* The loadings for η_b = 0, and for wingtip zero-slope loading with b/b_c of table 10, are the same as those in table 8.

TABLE 12. - I_{nn^*}, INDUCED DRAG INFLUENCE COEFFICIENT FOR ς=1/2, FROM APPENDIX B

n \ n*	0	1	2	3	4	5
0	0	0	0	0	0	0
1	0	.211037	0	-.023182	0	-.000442
2	-.126495	0	.107717	0	-.019769	0
3	0	-.069557	0	.058029	0	-.013710
4	-.017041	0	-.039669	0	.032101	0
5	0	-.002698	0	-.022936	0	.017975
6	.002017	0	.001243	0	-.013384	0
7	0	.001782	0	.001958	0	-.007837
8	.000806	0	.001031	0	.001766	0
9	0	.000244	0	.000516	0	.001378
10	-.000008	0	.000026	0	.000243	0
11	0	-.000049	0	-.000025	0	.000066
12	-.000037	0	-.000023	0	-.000037	0
13	0	-.000013	0	.000006	0	-.000079
14	-.000005	0	.000006	0	.000022	0
15	0	0	0	.000020	0	.000013
16	0	0	.000003	0	.000031	0
17	0	0	0	.000005	0	.000036

n \ n*	6	7	8	9
0	0	0	0	0
1	0	-.000042	0	-.000382
2	.000418	0	-.000639	0
3	0	.000550	0	-.000640
4	-.008969	0	.000549	0
5	0	-.005641	0	.000423
6	.010127	0	-.003581	0
7	0	.005505	0	-.002419
8	-.004694	0	.002362	0
9	0	-.003203	0	.000485
10	.000900	0	-.002706	0
11	0	.000371	0	-.002310
12	-.000118	0	-.000040	0
13	0	-.000337	0	.000077
14	-.000190	0	-.000506	0
15	0	-.000391	0	-

TABLE 13. - $n^*\frac{4}{\pi} D_{nn^*}$ INDUCED DRAG INFLUENCE COEFFICIENTS OF PLANAR-WING WINGLET WITH $\phi_o = 5\pi/32$, FOR EQUATIONS (172) AND (175), (DATA FROM TABLE II OF REF. 9)

γ deg	n \ n*	1	3	5	7	9	11
90	1	.03335	.00666	-.00167	-.01243	-.06192	-.10534
	3	-.00333	-.17809	-.16927	-.05646	-.02895	-.06658
	5	-.00258	-.16334	-.09138	.08085	.11343	.03307
	7	.03630	.02441	.11900	.18434	.11512	-.00789
	9	.03156	.12523	.17174	.08391	-.03334	-.07625
	11	-.02442	.06277	.04171	-.11282	-.16338	-.02769
75	1	.02254	.01464	.00887	-.00752	-.04600	-.06860
	3	-.02833	-.11801	-.09743	-.03368	-.02510	-.04331
	5	-.02362	-.10743	-.05579	.05572	.06810	.01018
	7	.02184	.01044	.07264	.11569	.06939	-.01221
	9	.01822	.08039	.10960	.04817	-.02089	-.03748
	11	-.01661	.04548	.02751	-.07520	-.09798	-.00506

TABLE 14. - T_n, WING ROOT BENDING MOMENT/LIFT INFLUENCE COEFFICIENTS OF EQUATION (171)

ϕ_o \ n	1	3	5	7	9	11
$5\pi/32$	.075139	.184765	.198455	.120903	.009690	-.066188
$\pi/4$	.285398	1/2	1/6	-1/6	-1/10	1/10

1. Report No.	2. Government Accession No.	3. Recipient's Catalog No.
NASA CR-3140		

4. Title and Subtitle	5. Report Date
Minimization Theory of Induced Drag Subject to Constraint Conditions	June 1979
	6. Performing Organization Code

7. Author(s)	8. Performing Organization Report No.
John DeYoung	
	10. Work Unit No.

9. Performing Organization Name and Address	11. Contract or Grant No.
Vought Corporation Hampton Technical Center 3221 N. Armistead Avenue Hampton, VA 23666	NAS1-13500
	13. Type of Report and Period Covered
12. Sponsoring Agency Name and Address	Contractor Report
National Aeronautics and Space Administration Washington, DC 20546	14. Sponsoring Agency Code

15. Supplementary Notes

Langley Technical Monitor: Harry H. Heyson
Topical Report

16. Abstract

Exact analytical solutions in terms of induced drag influence coefficients can be attained which define the spanwise loading with minimized induced drag, subject to specified constraint condtiions, for any nonplanar wing shape or number of wings. Closed exact solutions have been obtained for the planar wing with the constraints of lift plus wing bending moment about a given wing span station. Example applications of the theory are made to a biplane, a wing in ground effect, a cruciform wing, a V-wing, a planar-wing winglet, and linked wingtips in formation flying. For minimal induced drag the spanwise loading, relative to elliptic, is outboard for the biplane and is inboard for the wing in ground effect and for the planar-wing winglet. A spinoff of the biplane solution provides mathematically exact equations for downwash and sidewash about a planar vorticity sheet having an arbitrary loading distribution.

17. Key Words (Suggested by Author(s))	18. Distribution Statement
Induced Drag Minimization Optimum Spanwise Loading Loading Constraint Conditions Nonplanar Wings Ground Effect and Velocity Field	Unclassified - Unlimited Subject Category 02

19. Security Classif. (of this report)	20. Security Classif. (of this page)	21. No. of Pages	22. Price*
Unclassified	Unclassified	124	$6.50

*For sale by the National Technical Information Service, Springfield, Virginia 22151

NASA-Langley, 1979

END

April 16, 1981